Max-Planck-Institut für Biogeochemie

MPI-BGC Jena

TECHNICAL REPORTS 17

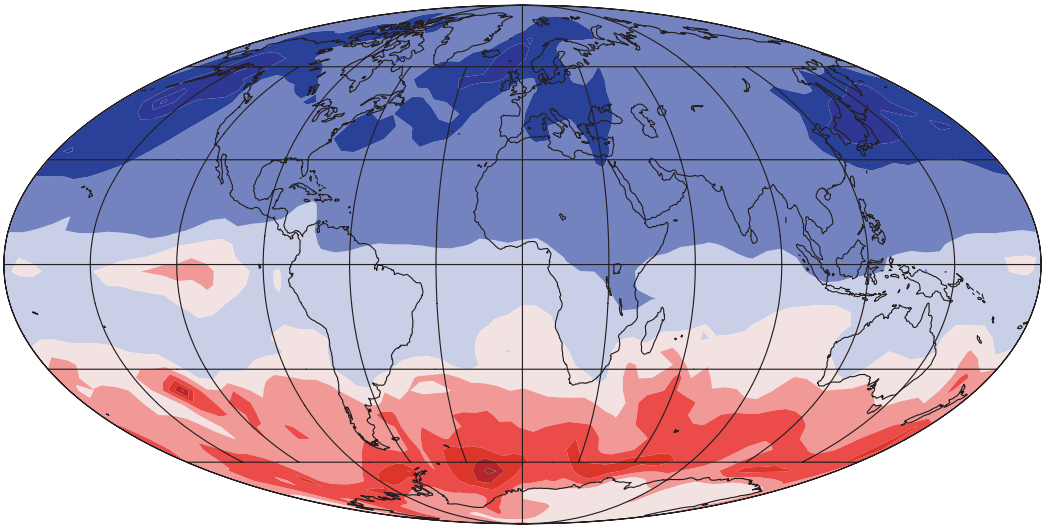

USING ATMOSHERIC POTENTIAL OXYGEN TO GAIN INSIGHT INTO CLIMATE DRIVERS OF OCEAN BIOGEOCHEMISTRY

by
Valentina Sicardi

ISSN 1615-7400

MAX-PLANCK-GESELLSCHAFT

Cover picture source

Oxygen concentration in ppm from the oceanic flux transported into the atmosphere with the TM3 model. The oceanic flux has been generated by the PISCES model for the period 1861- 2100.

Technical Reports - Max-Planck-Institut für Biogeochemie 17, 2010

Max-Planck-Institut für Biogeochemie
P.O.Box 10 01 64
07701 Jena/Germany
phone: +49 3641 576-0
fax: + 49 3641 577300
http://www.bgc-jena.mpg.de

Using Atmospheric Potential Oxygen to Gain Insight into Climate Drivers of Ocean Biogeochemistry

Dissertation

Zur Erlangung des Doktorgrades der Naturwissenschaften
im Department Geowissenschaften der Universität Hamburg

vorgelegt von

Valentina Sicardi

aus

Italien

Hamburg

Als Dissertation angenommen von
Department Geowissenschaften der Universität Hamburg

Auf Grund der Gutachten von Prof. Dr. Jochem Marotzke
und Prof. Dr. Martin Heimann

Hamburg, den 3 Dezember 2009

Prof. Dr. Jürgen Oßenbrügge
Leiter des Department Geowissenschaften

Contents

List of Figures

List of Tables

Dicette 'o pappecio 'nfacc'â noce:
Damme tiempo ....
ca te spertóso!

Acknowledgements

My immense gratitude goes to supervisors and colleagues for their support. I particularly thank Prof. Corinne Le Quéré for her invaluable advices and endless patience throughtout this project. I thank Dr. Christian Rödenbeck for his guidance and support. I am grateful to Prof. Martin Heimann for his helpful advices. I deeply thank Prof. Jochem Marotzke, chair of my Advisory Board, for his time and precious counsels. I thank Dr. Antje Weitz and Kornelia Kampman from the IMPRS for supporting so magnificently in every aspects during my doctoral studies. I thank all my friends and colleagues in Hamburg, they always made my stays in Hamburg very pleasant. I thank all my colleagues and friends at the BGC for their friendliness and helpfulness. I particularly thank Julia Steinbach for her kindness in helping me in the "discover of R". All my gratitude goes to Annett Börner for her help in editing related issues and the good stylistic suggestions she gave me, but over all, for being a very good friend. All my gratitude goes to Dr. Julia Marshall for all the time she dedicated to me. Without her support and her precious suggestions everything would have been harder. Thank you Julia! Thanks a lot to Jeremi for his kindness and Bélá for being so good and nice. I thank the Marie Curie Grant Project Greencycles for having founded part of my doctoral studies and Corinne Sacher, who provided invaluable help in the complicate EU-project bureaucracy. I am thankful to Dr. Laurent Bopp and Prof. Ralph Keeling for the data provided and the useful inputs.

There are many friends who made the past years memorable. I sincerely thank Beatriz and Emilio, Seo and Tatiana, Daniel, Catharina, Jutta, Guille and Anna, Matthias and many more, they made me see the sun during all the gray winter days. The time spent with all of you has been unforgettable and invaluable! Gracias amigos! I particularly thank my friends Enrico, Fabio and Anna who have been my reference point since I arrived in Jena, grazie ragazzi! Special thank to Danilo, for the constructive and inspiring talks we always had. I thank Gionata for being so patient with me at work and my flatmates Marco and Arianna for their patience, at home. I deeply thank my friends Jacqueline and Grit for the nice time I spent with them. Danke! I specially thank my

parents, my brother and all my friends and relatives in Italy for all the love they "transmitted" to me from such a distance. With their discrete love they gave me strength and energy to get through many difficulties. Last, but not least, I thank with all my heart Raul, who always supported me during the ups and downs of the past years. He gave me motivation and encouragment, I don't even want to image how would be my life without him. Thank you for being in my life. Moltes gràcies!

Abstract

This thesis investigates the use of atmospheric tracers to gain insight into the climatic drivers of ocean circulation and biogeochemical changes.

The results from the IPSL-CM4 coupled climate model for the period 1861-2100 have been analyzed. The fluxes generated by the climate model have been transported into the atmosphere using the TM3 atmospheric transport model to provide atmospheric tracer concentrations. We infer climate-induced changes in the ocean circulation and biogeochemistry from the changes in atmospheric tracer concentrations. To retrieve the oceanic signal from the atmospheric tracer concentrations, O_2 and CO_2 have been combined to form the Atmospheric Potential Oxygen (APO = O_2+1.1CO_2). APO removes the influence of the terrestrial biosphere and isolates the oceanic signal in the atmosphere. APO is thus influenced by the oceanic changes only. Any changes in the ocean physics will be reflected in changes in APO concentration. We explore the potential of inferring such changes from the APO observations.

Two scenarios have been considered: (a) the increasing atmospheric CO_2 leads to changes in climate and ocean physics, (b) the increasing atmospheric CO_2 does not change climate. In the first scenario the climate model projects several changes in the oceanic physics and in particular a reduction of the Atlantic Meridional Overturning Circulation by ∼70%. We explore the contribution of O_2, and CO_2 to APO and find that, O_2 dominates the APO signal on seasonal to decadal time scale, while CO_2 dominates the APO signal on longer time scale. The change in the APO interhemispheric gradient projected in the future is small and does not relate directly to the large-scale changes in the ocean circulation. The small latitudinal gradient has to be attributed to the fast mixing of the atmosphere. Changes in the amplitude of the APO seasonal cycle in the future vary between 2 to 4 ppm, depending on the location. These changes would be detectable as their amplitude is above the detection limit for the present APO measurements. Thus changes in APO seasonal cycle can

be used to detect large-scale changes in ocean physics in the future.

Even though the interest in the potential applications of APO has increased in the past years, the drivers of APO variability are still poorly understood. We investigate the APO variability to understand whether the observed APO variability is driven by the variability of the air-sea fluxes of APO or by changes in the atmospheric transport. In particular, our attention is focused on the APO interannual variability, which is not yet fully represented by the models, but is very important in order to quantify the response of the ocean to natural climate variations. Oceanic fluxes generated by a biogeochemical model have been used to carry out a sensitivity analysis combining constant and variable fluxes driven by constant and variable meteorological fields. We look at model results at 9 selected stations and compare them with the observations. The agreement between model results and observations is very good on seasonal time scales, but not on interannual time scale. This study confirms previous results, which indicate that the APO seasonality is driven by the variability of the oceanic fluxes, and further shows that the interannual variability in APO is also driven by the variability of the oceanic fluxes. A brief comparison with fluxes from another biogeochemical model confirms these results.

Chapter 1

Introduction

The Earth's climate is regulated by several complex physical, biological, and chemical processes that involve interactions among the atmosphere, the ocean, and the land. These biogeochemical processes are generally non-linear and can generate positive or negative feedbacks on the climate system.

All living organisms on Earth are composed primarily of carbon and their activities are related to carbon exchanges. For example, the biological process of photosynthesis removes carbon dioxide (CO_2) from the atmosphere and stores it on land in the form of plant biomass. Similarly, bacterial respiration decomposes the dead plant material and releases the CO_2 back into the atmosphere. These natural processes of absorption and respiration exchange CO_2 with the atmosphere and are naturally balanced. However, there is increasing evidence that human perturbations due to fossil fuel emissions, cement manufacturing and land use change have modified the carbon cycle, causing the atmospheric CO_2 concentrations to rise to levels that have never before been experienced by human beings [IPCC, 2007].

The purpose of this chapter is to review the carbon cycle and the biogeochemical processes related to the climate system. The first part of the chapter focuses on the preindustrial carbon cycle and its perturbation due to human activities. This is followed by a discussion of the oceanic carbon system. A brief overview of the ocean circulation is presented as well. Finally the use of atmospheric tracers, as a means to detect biogeochemical and physical changes

in the ocean, is discussed.

1.1 Overview of the Global Carbon Cycle

The Earth contains in total about 10^{23} grams (g) of carbon (C). The biggest amount is buried in sediments, in the form of organic compounds ($1.56 \cdot 10^{22}$ g C) and carbonates ($6.5 \cdot 10^{22}$ g C) [Schlesinger, 1997]. The sum of the total carbon on the Earth's surface is around $40 \cdot 10^{18}$ g C and the extractable fossil fuel is $4 \cdot 10^{18}$ g C. At equilibrium the ocean contains about fifty times more carbon than the atmosphere thanks to its capacity to buffer the changes in the atmospheric concentration. The major pool of carbon on land is contained in the soil, and in the sedimentary rocks. The ocean is the second largest pool of carbon (Figure 1.1).

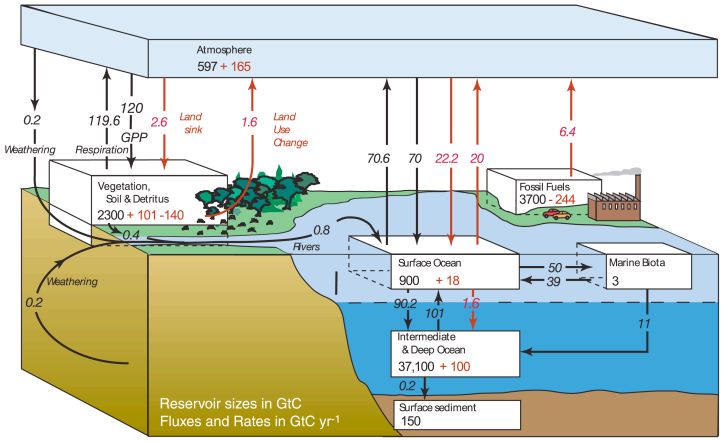

Figure 1.1— The global carbon cycle taken from the 4th IPCC Assessment Report, 2007. In the figure the carbon fluxes are shown in Gt C/yr with the natural fluxes depicted by black arrows and the anthropogenic fluxes by red arrows.

Naturally there is a continuous exchange of carbon among the different "carbon pools". For example, CO_2 is removed from the atmosphere and converted into organic matter by plants via photosynthesis, while carbon returns to the atmosphere via decomposition. The CO_2 fluxes between the land biosphere, the atmosphere, and the ocean have maintained an approximately constant

level of atmospheric CO_2 for the past 10 thousand years (ky) until the onset of the Industrial Revolution [Greenblatt and Sarmiento, 2004]. Here the focus will be on the processes that lead the ocean to be an important sink of carbon and particularly on the processes associated with climate change that can affect the ocean carbon sink.

1.2 Overview of the Ocean Carbon Cycle

The ocean plays an important part in both the organic and inorganic components of the carbon cycle. The ocean contains about fifty times more carbon than the atmosphere, but only 1% of this carbon is in the form of CO_2(g), most of the carbon is found as bicarbonate (HCO_3^-) and carbonate (CO_3^{2-}). The CO_2(g) dissolves in the ocean and reacts with water to form carbonic acid, which then dissociates into bicarbonate (HCO_3^-) and carbonate (CO_3^{2-}) ions according to:

$$CO_2 + H_2O \leftrightarrows H_2CO_3$$

$$H_2CO_3 \leftrightarrows H^+ + HCO_3^-$$

which give a combined reaction of

$$CO_2 + H_2O + CO_3^{2-} \leftrightarrows HCO_3^- + H^+ + CO_3^{2-} \leftrightarrows 2HCO_3^- \tag{1.1}$$

The sum of the CO_2, HCO_3^- and CO_3^{2-} is called Dissolved Inorganic Carbon (DIC); 91% of DIC is in the form of HCO_3^-, 8% in CO_3^{2-} and only 1% in CO_2 [Sarmiento and Gruber, 2002]. Only CO_2 is exchanged with the atmosphere.

The oceanic uptake of atmospheric CO_2 is regulated by the following processes:

- **Chemical and Physical Processes**
  The dissolution of CO_2 is highly dependent on the water's temperature and on the concentration of DIC. CO_2 is more soluble in cold waters and when the concentration of DIC is low. Cold surface waters at high latitudes absorb a large amount of CO_2 from the atmosphere. Cold and dense high latitude waters sink and transport DIC to the deep ocean, the DIC is subsequently distributed by mixing and ocean currents. The DIC transported to the deep ocean circulates with water masses around the world, where it is kept out of contact with the atmosphere for several hundred years. This physical process is known as the *Solubility Pump* [Maier-Reimer et al., 1996, Sarmiento and Gruber, 2002]. On the contrary when waters become warmer, the CO_2 is outgassed from the ocean to the atmosphere. Such outgassing occurs at equatorial regions, where the deep water rich in CO_2 upwells and CO_2 is outgassed to the atmosphere.

- **Biological Processes**

  1. *The biological pump*:
     Marine phytoplankton take up DIC and transform it into organic compounds via the process of photosynthesis. When phytoplankton die or are eaten by zooplankton and higher trophic organisms, the part of the organic carbon from dead tissues can remain in the waters as Dissolved Organic Carbon (DOC). The DOC can then be transported by currents to deeper waters. Part of the organic matter produced by the phytoplankton is remineralized back to DIC in surface waters. Finally, another fraction of the organic carbon is transformed into aggregates called Particulate Organic Carbon (POC), which sink. The carbon entrained in POC is remineralized at depth and stored in the intermediate and deep waters for decades to centuries [Denman et al., 2007]. The deep waters rich in carbon are transported back to the surface by ocean currents and vertical

mixing.

2. *The calcium carbonate pump*:
   Some marine organisms grow their shells out of calcium carbonate ($CaCO_3$), changing the surface water carbon chemistry. When $CaCO_3$ shells sink in the deep water, the concentration of CO_3^{2-} at the surface decreases, moving the equilibrium of Reaction 1.1 towards the left with a consequent release of CO_2 into the atmosphere.

1.3 Perturbation of the Carbon Cycle

It is well established that the increase of CO_2 in the atmoshere is caused by human activities [Raupach et al., 2007, Le Quéré et al., 2007, Le Quéré et al., 2009]. The perturbation of the carbon cycle is determined by two main classes of human activities: (a) fossil fuel emissions and cement production, and (b) deforestation and changes in land use. The former activities represent emissions of carbon that was stored over millions of years. These emissions have caused an increase of the atmospheric CO_2 concentration by 38% since pre-industrial times [Canadell et al., 2007]. The latter activities represent the release of carbon stored on decadal to centennial periods.

Although the anthropogenic CO_2 fluxes that perturb the natural carbon cycle are small compared to the natural turnover, they result in a significant perturbation of the natural carbon cycle. The anthropogenic perturbations of the natural carbon cycle are represented in Figure 1.1 as red arrows. The values reported are from the 4th IPCC Assessment Report, 2007 (IPCC AR4) [Denman et al., 2007]. The present level of atmospheric carbon dioxide content is about 385 ppm (in 2008), which is the highest level that the Earth's atmosphere has experienced in human history. Present (2000-2008) anthropogenic CO_2 emissions amount to 9.1 Pg C/yr, the emissions due to fossil fuel burning is around 7.6 Pg C/yr and the emissions due to land use change amount to about 1.5 Pg C/yr [Canadell et al., 2007, Le Quéré et al., 2009]. Of the annual integrated anthropogenic CO_2 emitted (i.e. the combination of fossil fuel burning and land use change) only 45% stays in the atmosphere as the Air-

borne Fraction (AF), 26% is taken up by the land biosphere, and the remaining 29% is taken up by the oceans [Canadell et al., 2007, Le Quéré et al., 2009].

Understanding the different mechanisms of CO_2 uptake by the land and ocean sinks is important when one tries to project the rise of atmospheric CO_2. Even though plants and oceans absorb the surplus greenhouse gases, the rate of CO_2 emissions may be faster than the rate of CO_2 uptake by the sinks [Le Quéré et al., 2009].

The CO_2 emitted into the atmosphere by human activities is taken up by the ocean at a rate which depends primarily on the rate of increasing atmospheric CO_2 compared with the rate of the ocean mixing. Nowadays the oceans take up $\sim$2.2 PgC/yr [Denman et al., 2007, Gruber et al., 2009]. However, in the past 20 years models and observations suggest that the rate of growth of this sink may have slowed down [Canadell et al., 2007]. Measurements show that the oceans have absorbed 29% of the total CO_2 emitted since pre-industrial times [Lee et al., 2003, Sabine et al., 2004], but at present the ocean uptake is only 15% of the potential uptake level for an atmospheric concentration of 385 ppm [Greenblatt and Sarmiento, 2004]. Possible variations in the oceans' sink efficiency due to climate change are extremely important because of the size of this sink. The feedbacks on the ocean uptake due to alteration of the climate system are discussed in the next section.

1.4 Climate Feedback on Oceanic Uptake

Climate change can affect the ocean uptake capacity through :

- Changes in CO_2 solubility:
  CO_2 solubility is a function of the temperature, therefore as the ocean's temperature increases the solubility of CO_2 decreases and consequently the uptake of the CO_2 is reduced. Ocean warming provides a good example of a potential positive feedback mechanism. As CO_2 increases in the atmosphere, climate warms and the ability of the oceans to remove CO_2 from the atmosphere decreases. Hence increasing CO_2 in the atmosphere could amplify the increase of CO_2 in the atmosphere.

- Changes in the vertical stratification:
  Increased the sea surface temperatures (SST) and increased precipitation at high latitudes lead to an increase in the ocean's surface stratification. This causes a shallower mixing layer and a reduction in the vertical exchange and transport of anthropogenic CO_2 to the deep ocean. As a consequence a reduction of anthropogenic CO_2 uptake is expected. However, changes in stratification also affect the marine biology and the natural carbon cycle. The stratification reduces the supply of DIC and nutrients, which are needed for biological activity. As the stratification increases, the biological pump tends to remove the nutrients from the surface waters, reducing DIC concentration and absorbing anthropogenic CO_2. This effect counteracts the reduction of CO_2 uptake due to the stratification [Greenblatt and Sarmiento, 2004].

- Changes in the marine productivity:
  Warming and other environmental changes (e.g. ocean acidification) can lead to further changes in marine productivity, but the direction and amplitude are not well known.

- Changes in the ocean circulation:
  On centennial time scales the ocean carbon sink may also be affected by climate-driven changes in the ocean circulation such as the slowing down of the Thermohaline Circulation [Manabe et al., 1991, Sarmiento and Le Quéré, 1996] or the enhanced upwelling caused by stratospheric ozone depletion [Le Quéré et al., 2007, Lenton et al., 2009].

- Other natural changes:
  The ocean carbon cycle can be affected by natural changes in the climate system such as the collapse of grounded ice sheets [Flower and Kennett, 1994] or the release of methane from methane hydrates in the ocean sediments [Nisbet and Chappellaz, 2009].

In addition to long term changes in climate, natural periodic oscillations in the climate system can also influence the oceanic sink capacity. For example during the El Niño period there is a reduction in the upwelling of the CO_2-rich

deep water in the equatorial Pacific, causing an increase in CO_2 uptake at the surface [Le Quéré et al., 2000, McKinley, 2004].

A deeper analysis of the feedbacks of climate change on the carbon cycle is beyond the scope of this work. Many past studies agree that a collapse of the Thermohaline Circulation will affect the CO_2 uptake drastically, but at which intensity and to what degree is still unknown [Broecker, 1997, Wood et al., 1999, Clark et al., 2002, Gregory, 2004]. Therefore due to the uncertainties in the climate models and the lack of appropriate measurements, the projection of changes in marine carbon cycle is still open to crucial questions.

1.5 Overview of the Oceanic Circulation

The main forces driving oceanic circulation are the difference in density of different water masses and the winds. The density of sea-water is controlled by its salinity and its temperature. The salinity of the surface waters is controlled mostly by the balance between evaporation and precipitation. As a result the highest salinity is found at low latitudes where evaporation is high and precipitation is low. The temperature of the oceans depends mostly on the heat exchange with the atmosphere. In general the heat is transferred from the low latitudes to the high latitudes via the winds in the atmosphere and by the currents in the ocean [Wunsch, 2002, Colling, 2004]. Our focus here is limited to the *The Thermohaline circulation* considered to be of crucial importance for the climate system [Marotzke, 2000, Thorpe et al., 2001, Rahmstorf, 2003, Wood et al., 2003]. The Thermohaline Circulation (THC) refers to the movements of waters due to density difference. The term "thermohaline" refers to a particular driving mechanisms. This circulation is sometimes called the *Meridional Overturning Circulation* (MOC), which refers to the north-south flow as function of latitude and depth [Wunsch, 2002, Bindoff et al., 2007, Rahmstorf, 2006]. This circulation is schematically represented in Figure 1.2.

Warm and salty surface waters in the western north Atlantic transport heat to the Norwegian-Greenland Sea, where it is transferred to the atmosphere.

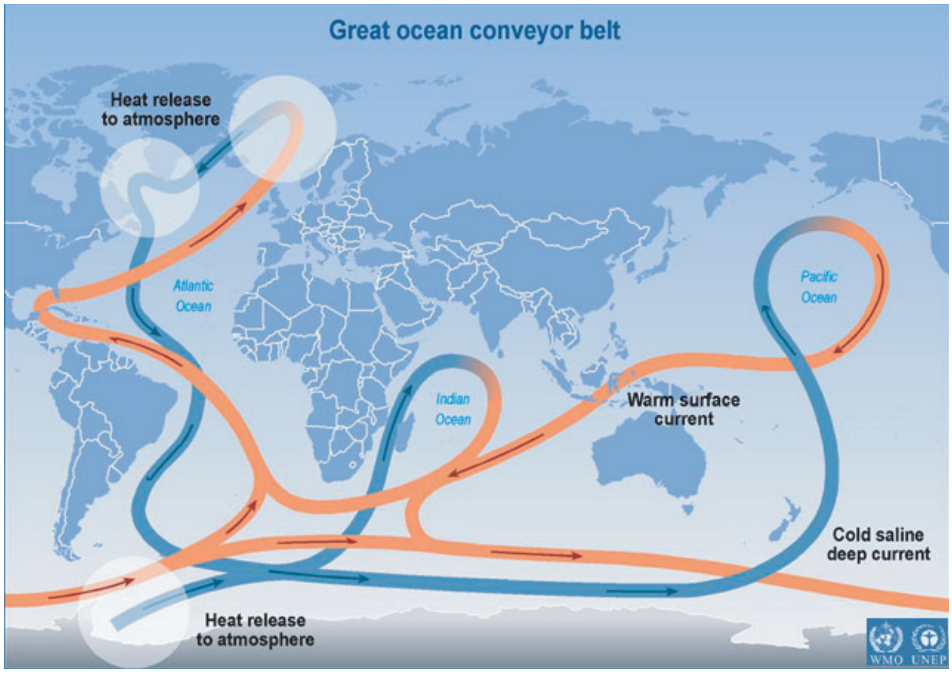

Figure 1.2— The system of the global currents, primarily showing the Thermohaline Circulation or conveyor belt that is driven by temperature and salinity differences.

This heat helps to mitigate the climate in northern Europe and this current is know as the *Gulf Stream*. As the water moves north, it cools and its density increases. This dense water sinks, forming the North Atlantic Deep Water, which travels south through the Atlantic and then in the Southern Ocean joins the Circumpolar Current. The circumpolar water flows northeast and is the source of deep water in the Indian and Pacific Oceans. From the South Pacific the deep water flows northwards along the west boundary of the Tonga Trench. The water upwells over large areas in the North Pacific and Indian Oceans. The conveyor belt is then completed by the surface flow from the Pacific to the Atlantic Ocean.

There are evidences that the THC has changed regularly in the past [Rahmstorf, 2003, Toggweiler and Russell, 2008]. The variation of the climate due to changes in the circulation has been large, abrupt and global [Denton and Hendy, 1994, Clement and Peterson, 2008]. One of the consequences of global warming will be an increase of sea surface temperature and

the alteration of the hydrological cycle, both factors will make the formation of the salty deep water, which is the main driver of the ocean circulation, more difficult. Models used by the IPCC AR4 show a reduction in the MOC by 15% to 50% in 2100 [Meehl et al., 2007].

1.6 Atmospheric Tracers

The ocean and the atmosphere are intrinsically related. It is very difficult to accurately quantify the reduction of the ocean currents due to climate change with models or direct measurements. As such, it would be important to have an indirect means to gain information about oceanic circulation. One possible way to estimate large-scale changes in ocean currents is to measure and model the changes in atmospheric tracers, this is the subject of the Chapter 3.

1.6.1 O_2 as a Tracer of Changes in the Ocean

The atmospheric reservoirs of CO_2 and O_2 are linked by the processes that involve the production and destruction of organic matter, such as photosynthesis, respiration, and combustion (Table 1.1).

On time scales of thousands of years the variability in atmospheric O_2 concentration is related to the recycling of organic matter via the reduction/oxidation reactions. The chemistry of atmospheric CO_2 is complicated by the reaction of CO_2 with seawater as described previously [Keeling, 1995, Le Quéré and Meltz, 2004]. In contrast to reduction/oxidation reactions, the acid-base reactions that involve CO_2 in the seawater do not affect the atmospheric O_2. Moreover the time scale of dissolution of CO_2 and O_2 are different: the equilibration of CO_2 with ocean waters takes about one year, while the equilbration of O_2 occurs in about one month. The carbon is exchanged slowly because most of the CO_2 contained in the ocean is in the form of carbonate and bicarbonate ions which are not exchanged across the air-sea interface. Thus,due to different requilibration time scale, the signal of the ocean photosynthesis and respiration can produce larger changes in the atmospheric O_2 than in the CO_2 [Keeling, 1995].

Table 1.1— Reactions involving CO_2 and O_2

Reactions that involve CO_2 and O_2	
Photosynthesis and respiration on land	$CO_2 + H_2O \rightleftharpoons CH_2O + O_2$
Photosynthesis and respiration in the ocean	$106CO_2+16NO_3^-+H_2PO_4^-+17\ H^+ \rightleftharpoons C_{106}H_{263}O_{110} + N_{16}P + 138O_2$
Fossil fuel burning	$CH_y+(1+\frac{y}{4})O_2 \rightleftharpoons \frac{y}{2}H_2O + CO_2$
Ocean processes	$H_2O+CO_2+CO_3^{2-} \rightleftharpoons 2HCO_3^-$

The changes in the atmospheric O_2 are usually reported as changes in the O_2/N_2 ratio of the air. This is based on the assumption that changes in the O_2/N_2 ratio will show mostly changes in the atmospheric O_2 since changes in the N_2 in the atmosphere are small and therefore atmospheric N_2 can be considered constant. The O_2/N_2 ratio is expressed as a variation with respect to a reference:

$$\partial\left(O_2/N_2\right) = \left(\frac{\left(O_2/N_2\right)_{sample}}{\left(O_2/N_2\right)_{reference}} - 1\right) \tag{1.2}$$

The result is usually multiplied by 10^6 and the resulting unit is called "per meg". In this work the unit "ppm" (parts per million) will be used to describe the concentration of both atmospheric CO_2 and O_2 (1 ppm=4.8 per meg).

In order to understand how O_2 can be used to trace changes in the ocean circulation, we will consider the variability of the atmospheric O_2 concentration. Atmospheric O_2 varies for several reasons. A brief summary is reported here, following Bender [Bender and Battle, 1999]:

1. *Combustion*: The burning of fossil fuels consumes O_2. In the past decades this has lead to a decrease of the O_2/N_2 ratio of about 4.5 ppm/yr [Bender and Battle, 1999].

2. *Land Biosphere*: The land biosphere can be a sink for CO_2 and a source of O_2 due to photosynthesis, but it can also be a source of CO_2 and a sink of O_2 due to respiration. On land the O_2 and CO_2 exchange at a fixed ratio of 1.1 (see section 1.6.2). The change in O_2 atmospheric concentration is strongly dependent on the season: in summer the rate of photosynthesis exceeds the rate of respiration, thus increasing the level of atmospheric O_2. The contrary happens during winter.

3. *Ocean Biosphere*: The annual cycle of sea surface temperature drives the seasonal cycle of oceanic productivity and air-sea O_2 fluxes. At high latitudes variation of atmospheric O_2 associated with the ocean is due primarily to net production, respiration, ventilation and other processes:

   - Net Production: the first 100 meters of the ocean are illuminated by light and, therefore, are the zones of photosynthesis and O_2 production. The photosynthesis in the upper ocean causes supersaturation of O_2 and thus a transfer of O_2 into the atmosphere.

   - Respiration and Ventilation: the O_2 is consumed by the plankton during respiration, causing the deep ocean to be undersaturated with O_2. The ocean is then mixed and ventilated. The mixing of deep water with surface water in winter at high latitudes allows the O_2-depleted water from the depth to get in contact with the O_2 rich surface waters. This mixing generates an uptake of O_2 from the atmosphere by the ocean.

4. *Ocean Thermal Effect*: The solubility of gases is temperature-dependent: there is a flux of gas to the atmosphere in summer and to the ocean in winter. O_2 is more soluble than N_2, thus the O_2/N_2 ratio increases in summer and decreases in winter.

1.6.2 Formulation of the Atmospheric Potential Oxygen

The variations of CO_2 and O_2 in the atmosphere are coupled on interannual and seasonal time scales. The variation of O_2 is mostly due to photosynthesis and respiration and it follows the alternation of seasons. On land the exchange of CO_2 and O_2 by the land biosphere happens at a fixed ratio equal to 1.1 [Keeling and J.Severinghaus, 1993, Manning and Keeling, 2006], which means that, for each mole of CO_2 absorbed by the land biosphere during photosynthesis, 1.1 moles of O_2 are released into the atmosphere.

O_2 is released by the ocean into the atmosphere at high latitudes in the spring and summer when the waters warm, the rate of net photosynthesis exceeds the rate of respiration, and when there is little ocean mixing, which prevents the O_2 depleted water to be in contact with the atmosphere. O_2 is removed from the atmosphere by the ocean in fall and winter when the respiration rate exceeds the photosynthesis rate and deep waters, undersaturated with O_2, come to the surface. The processes that regulate the O_2 and CO_2 exchange are, in the ocean, decoupled. This property has been used for partitioning the sink of CO_2 between land and ocean, based on the long term trend of atmospheric O_2 and CO_2 [Keeling et al., 1996, Bopp et al., 2002, Bender et al., 2005, Manning and Keeling, 2006].

Starting from this decoupling, it is possible to combine O_2 and CO_2 to eliminate the signal of the land in atmospheric O_2. The combination of O_2 and CO_2 formes the Atmospheric Potential Oxygen (APO) [Stephens et al., 1998]:

$$APO = O_2 + 1.1CO_2 \tag{1.3}$$

The APO has the following properties:

- it is conservative with respect to the land biosphere
- it represents only the changes in the ocean

- contributions to APO from O_2 and CO_2 are time scale dependent

We can represent the changes in atmospheric CO_2 according to:

$$\Delta CO_2 = Q^c_{foss} - Q^c_{bio} - Q^c_{ocean} \tag{1.4}$$

where Q^c_{foss} is the source of CO_2 from fossil fuel burning and cement manufacturing, Q^c_{ocean} is the uptake of CO_2 by the ocean, and Q^c_{bio} is the CO_2 sink due to photosynthesis acting on terrestrial ecosystems. Similarly, the changes in atmospheric O_2 can be represented as:

$$\Delta O_2 = -\alpha_F Q^c_{foss} + \alpha_B Q^c_{bio} + Q^o_{ocean} \tag{1.5}$$

where Q^c_{foss} is the O_2 sink due to fossil fuel burning, Q^c_{bio} is the land biotic CO_2 sink and Q^c_{ocean} is the net exchange of atmospheric O_2 with the ocean, considering the effect of both the biological and the physical pump [McKinley, 2003, Manning and Keeling, 2006]. The constant α_B represents the molar ratio for terrestrial O_2 production of biomatter and CO_2 utilization, equal to 1.1. The constant α_F is the O_2:CO_2 ratio during fossil fuel burning, equal to 1.4 [Keeling and J.Severinghaus, 1993].

The equations 1.4 and 1.5 can be combined according to the definition of APO:

$$\underbrace{\Delta O_2 + \alpha_B \Delta CO_2}_{\Delta APO} = \underbrace{(-\alpha_F + \alpha_B) Q^c_{foss}}_{fossil fuel} + \underbrace{(-\alpha_B Q^c_{ocean} + Q^o_{ocean})}_{ocean} \tag{1.6}$$

According to Equation 1.6, if we know the amount of fossil fuel emitted to the atmosphere, any variation in APO will reflect variations in the ocean gas exchange.

The alteration of ocean processes that regulate the uptake or release of O_2 by the ocean have an effect on the total uptake and release of the O_2, and therefore variations in the APO concentration at different time scales reflect changes in ocean circulation. APO allows us to eliminate the influence of the land and to infer potential changes in the ocean. The difference in APO concentrations for different time intervals or regions provides information about changes in ocean processes.

Since the first formulation of APO, it has been used in several studies: as a tracer to test oceanic models [Battle et al., 2006, Naegler et al., 2006], for partitioning the CO_2 sink between ocean and land [Manning and Keeling, 2006], and to estimate the rate of marine new production [Balkanski et al., 1999, Najjar and Keeling, 2000]. In Chapter 3, for the first time, APO is used as a potential tracer to detect large-scale changes in the ocean circulation. Although in the past decades the number of studies related to APO has increased, what drives the variability of APO is still under debate [Hamme and Keeling, 2008, Nevison, 2008]. The potential drivers of the APO interannual variability are analyzed in Chapter 4.

1.7 Thesis Objectives

This thesis looks at open issues related to the physical drivers of ocean biogeochemistry in a changing climate. The following scientific questions will be addressed:

Detection of climate induced changes in the ocean circulation from atmospheric O_2 and CO_2 measurements

- Do changes in the air-sea fluxes have an impact on atmospheric O_2 and CO_2 concentrations? Can we discern the respective contributions of O_2 and CO_2 to APO variability?

- With the projected large-scale changes in the ocean circulation, can a significant latitudinal gradient in the APO concentration be observed? Can we relate latitudinal gradient changes to changes in the ocean circulation?
- With the projected large-scale changes in the ocean circulation, does the amplitude of the APO seasonal cycle change as well? Would we be able to detect such changes?

Drivers of the APO Variability

- Is the temporal variability of oceanic fluxes reflected in the variability of the APO atmospheric concentration?
- How much of the observed APO variability is caused by variable meteorological fields?

1.8 Thesis Outline

This thesis is structured in 5 Chapters. **Chapter 1** (this chapter) is dedicated to background information and presentes the APO tracer and the uncertainty regarding its role in the Climate Sciences. The other chapters are organized as follows:

- **Chapter 2** contains technical information about the models used.
- **Chapter 3** deals with the detection of changes in the ocean circulation using APO. The idea of using APO to detect changes in the ocean circulation is introduced. The results of both a climate model and an atmospheric transport model for two different scenarios consedered are presented and discussed. A brief comparison of the model results with the measurements from selected stations is also presented in order to verify the validity of the model chosen. The spatial and temporal variability of APO and the contribution of O_2 and CO_2 to APO are analyzed. The interhemispheric variability of APO and its connection to large scale changes in the oceans, and the changes in the amplitude of the seasonal cycle as the oceanic circulation changes are also presented in this chapter.

- **Chapter 4** addresses possible drivers of APO. The models used are introduced, followed by a description of the experimental setup. The fluxes used that have different temporal variability are described. The results from the transport into the atmosphere of such fluxes with different meteorological fields are presented and discussed. A brief comparison of the results with those produced by another oceanic model is presented.

- **Chapter 5** contains the main conclusions of this work and the outlook.

Chapter 3 is in preparation for submission in a peer-reviewed journal, and as such can be read independently from the others. The results from Chapter 4 will be submitted as a paper, but they are presented here as a thesis chapter.

Chapter 2

Description of Models

Models play a fundamental role in the investigation of our research questions. To carry out our research, we use model results from state of the art geoscience models. The combinations of the models used is summarized in Figure 2.1. Validation of the models is beyond the scope of the present work, being aware of the uncertainties present in the models. Here, we give an overview of the models used for this study.

2.1 The Climate Model

The fluxes used in Chapter 3 of this thesis have been generated by the PISCES model [Aumont and Bopp, 2006] driven by the results of the climate model IPSL_CM4, "Earth System Model" [Marti et al., 2005]. This climate model is a fully coupled ocean-atmosphere general circulation model. It is composed of four modules (http://dods.ipsl.jussieu.fr/omamce/IPSLCM4/):

- LMDZ for atmospheric dynamic and physics
- ORCHIDEE for the land surface
- ORCA for the ocean dynamics
- LIM for the ice-sea interaction

There are two possible resolutions of the climate model IPSL-CM4: LMDZ 72×45×19 / ORCA 92×76×31 and LMDZ 96×72×19 / ORCA 182×149×31. The results from the latter resolution have been used for this study

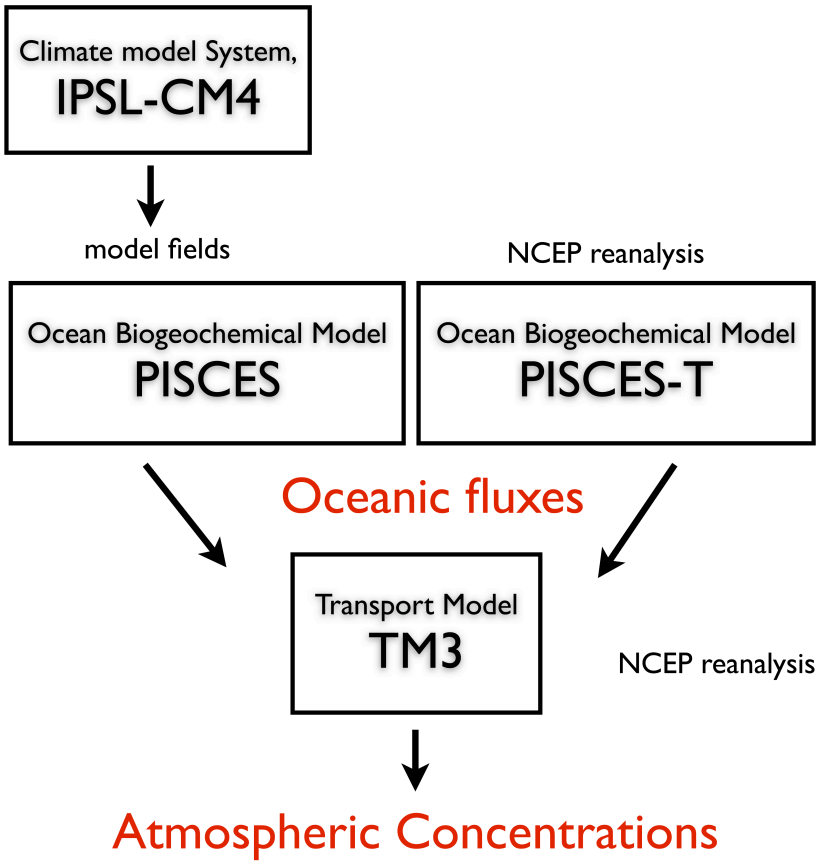

Figure 2.1— Schematization of the models with input/output used. In Chapter 3 the oceanic fluxes generated by the PISCES model (left side of this plot) are transported into the atmosphere with the TM3 model. In Chapter 4 the fluxes generated by the PISCES-T model (right side of this plot) are transported into the atmosphere with the TM3 model.

2.1.1 The Atmospheric Component LMDZ

The atmospheric component LMDZ from Laboratoire de Météorologie Dynamique is an atmospheric general circulation model, adapted to climate studies both at regional and global scales. Z indicates the possibility of zooming in on regional scales [Hourdin et al., 2006]. The dynamic part is based on a finite-difference formulation of the primitive equations of meteorology. The grid is regular in both direction and there are two resolutions available: 72×54 points for the low resolution or 96×72 points for the intermediate resolution. The vertical coordinate is based on the σ -p coordinate, in which the pressure

at the surface is given by the real pressure, but then with altitude the pressure levels follow the topography. The present version of the model is based on 19 layers.

2.1.2 The Land Surface Model ORCHIDEE

Orchidee is divided in three modules:

- module for hydrology: the hydrological model SECHIBA. This module describes the short-timescale process of energy and water exchanges between the atmosphere and the biosphere;

- module for the vegetation dynamics: it deals with the parametrization of the vegetation dynamics such as fire, light competition, tree mortality, climate criteria for introduction/elimination of plant functional types;

- module for other processes such as carbon allocation, litter decomposition, soil carbon dynamics called STOMATE.

Orchidee can be run in different configurations depending on the problem to be addressed and can be run alone or coupled with LMDZ.

2.1.3 The Oceanic Component: the OPA System

The OPA system model is a primitive equation model for both global and regional ocean circulation. It can interact with different modules of the Earth System (atmosphere, sea-ice, biogeochemistry) for different temporal and spacial resolutions. The dynamics of the ocean are described with the classical primitive equations of fluid dynamics. ORCA is the generic name given to global ocean configurations using the OPA system. The ORCA grid used for this work is the ORCA2, a curvilinear mesh used to overcome the North Pole singularity found in the geographic meshes. The grid is distorted in the Northern Hemisphere to have two poles located in the Northern Hemisphere and both are located on land [Timmermann et al., 2005].

The horizontal resolution is based on a 2 degrees Mercator mesh. The grid has a resolution of 2 ° by 2 ° on average, with a higher resolution, 0.5 °, at the equator and at the poles [Madec et al., 1998]. The vertical domain goes from the surface to a depth of 5000 meters, there are 31 vertical levels with a vertical resolution of 10 meters in the upper 100 meters. OPA also includes a 1.5-order turbulent kinetic energy model that computes vertical mixing throughtout the water column [Gaspar et al., 1990]. OPA implicitly represents the eddy-induced mixing process within the parametrization. The atmosphere and ocean models are coupled via the coupler OASIS, Ocean Atmospheric Soil Interface Software.

2.1.4 The LIM Sea-Ice Model

Louvain Ice Model (LIM) is a thermodynamic-dynamic sea-ice model designed for climate studies [Fichefet and Maqueda,]. The model is run on the same ORCA grid and is composed of three layers: one for the snow and two for the sea-ice. It computes thickness, extension, and motion of sea-ice.

2.2 The Biogeochemical Models

The field of biogeochemical models encompasses models for the behaviour and cycling of water and elements [Haag and Kaupenjohann, 2000]. The biogeochemical models offer an important means of understanding carbon dynamics [Kennedy et al., 2007]. For this study we use the biogeochemical fluxes coming from two different ocean biogeochemical models, which have the same core.

2.2.1 PISCES

The ocean biogeochemical model Pelagic Interaction Scheme for Carbon Ecosystem Study, PISCES, is derived from the Hamburg Ocean Carbon Cycle Model (HAMOCC 5) [Aumont et al., 2003]. PISCES is a biogeochemical model which simulates the marine biological productivity and describes the biogeochemical cycles of carbon and of other nutrients (P, N, Si, Fe). There are five modeled limiting nutrients for phytoplankton growth: Nitrate and

Ammonium, Phosphate, Silicate and Iron. Four living compartments are represented: two phytoplankton size-classes/groups corresponding to nanophytoplankton and diatoms, and two zooplankton size classes, microzooplankton and mesozooplankton. There are four types of dead organic particles with different sinking rate. The PISCES model also simulates dissolved inorganic carbon, total alkalinity and dissolved oxygen. The latter tracer is also used to define the regions where oxic or anoxic remineralization takes place [Aumont and Bopp, 2006]. PISCES run on the ORCA grid and therefore an appropriate integration of the data is necessary to adapt the oceanic fluxes to the transport model's grid.

2.2.2 PISCES-T

The PISCES-T model has the same core of the ocean biogeochemical model PISCES [Aumont and Bopp, 2006], but it contains additional parameterizations and equations of the biogeochemical fluxes, through mesozooplankton [Buitenhuis et al., 2006]. The main changes in PISCES-T refer to:

- the respiration rate is set to be dependent only on temperature;
- the mortality flux is a linear function of the mesozooplankton concentration;
- POC degradation is an exponential function of temperature.

Sensible and latent heat fluxes are calculated with bulk formulae, using the temperature difference between the modeled sea surface temperature and the daily air temperature from National Center for Environmental Prediction (NCEP) reanalysis [Kalnay et al., 1996]. The latent heat flux provides evaporation, the water balance is calculated at the end of every year and a water balance correction is applied over the course of the next year.

PISCES, for this study, has been forced by the meteorological conditions prescribed by the climate model IPSL_CM4. PISCES-T has been forced by daily wind and precipitation from NCEP reanalysis. Both models are coupled with the general ocean circulation model OPA and are referred to as OPA-PISCES and OPA-PISCES-T.

2.3 The Transport Model TM3

The ocean biogeochemical fluxes have been transported into the atmosphere with the transport model TM3 [Heimann and Körner, 2003]. The TM3 model a is three dimensional Eulerian transport model that solves the continuity equation based on given time-dependent meteorological fields for the surface pressure, wind velocity, air temperature and geopotential. Evaporation fluxes are also needed to calculate the transport by cumulus clouds. These forcing fields may be obtained from an atmospheric general circulation model or from weather model forecast, or from meteorological analysis, for example from NCEP. For a realistic calculation the meteorological fields have to use a time step on the order of hours.

Model Physics

The TM3 solves the continuity equation (Equation 2.1) for a variable number of tracers on a Eulerian 3-dimensional grid for the entire globe:

$$\frac{\partial}{\partial t}\rho\chi + \nabla \cdot \rho \overrightarrow{u}\chi = Q \tag{2.1}$$

Where χ represent the tracer mixing ratio (kg tracer mass per kg air mass), ρ the air density, $\overrightarrow{u}$ the wind velocity and Q the volume of the source/sink of the tracer. Denoting time-space averages over the model grid elements and model time-step by overbars and deviations from these averages with primes, we separate the horizontal and vertical directions to obtain:

$$\frac{\partial}{\partial t}\overline{\rho}\ \overline{\chi} + \nabla_h \cdot \overline{\rho}\ \overline{\overrightarrow{u_h}}\ \overline{\chi} + \frac{\partial}{\partial z}\overline{\rho}\ \overline{w}\ \overline{\chi} + \nabla_h \cdot \overline{\rho}\ \overline{\overrightarrow{u_h'}\ \chi'} + \frac{\partial}{\partial z}\overline{\rho}\ \overline{w'\chi'} = \overline{Q} \tag{2.2}$$

where w is the vertical wind velocity and the subscript h refers to horizontal vectors. The second and third term on the left hand side of Equation 2.2 represent atmospheric advection. The fourth term represent the horizontal

diffusion, which is absent in the present version of the model. The last term on the left hand side of Equation 2.2 represents the vertical convection. The model numerically solves the continuity equation in flux form and splits the transport operator in time. Advection, i.e. tracer transport by the three-dimensional air-mass fluxes resolved on the model grid, is calculated using the slopes scheme [Russell and Lerner, 1981]. In this scheme each tracer is represented within the Eulerian grid-boxes by the tracer mixing ratio. Sub-grid-scale vertical transport is parameterized in the model by two processes: vertical diffusion and cumulus cloud transport [Tiedtke, 1989, Heimann and Körner, 2003].

The model uses an equidistant latitude-longitude grid with i_m boxes in the zonal, j_m boxes in the meridional, and l_m layers in the vertical dimension. There exist four different grid versions: coarse (36×24×9), fine (72×48×19), very fine (192×96×28), extra fine (320×161×31). For all the simulations done in this work, the fine grid has been used. In the vertical levels TM3 uses hybrid coordinates. The time output can vary as well as the type of output format (NetCDF, binary, ASCII).

The output of the TM3 model is the distribution of the tracer in the atmosphere in terms of the mixing ratio. The mixing ratio of atmospheric CO_2 and other trace gases are commonly given in units of parts per million volume (ppm). In this thesis we will refer to the concentration of the gas in the atmosphere, but it should be understood that this is really a mixing ratio.

Chapter 3

Detection of changes in the ocean circulation from atmospheric measurements[1]

Abstract

Atmospheric O_2 and CO_2 concentrations can be combined to remove the signal caused by fossil fuel burning and exchanges in the terrestrial biosphere, producing a tracer called Atmospheric Potential Oxygen (APO). We discuss the potential of using APO to detect changes in the oceanic circulation in the future. We use the O_2 and CO_2 oceanic fluxes for the years 1861 to 2100 produced by a carbon-climate model forced by the A2 emissions scenario. The model projects warming of about 2°C of the sea surface, reduction of the Meridional Overturning Circulation by ∼70%, and widespread stratification of the world's oceans by 2100. These physical changes influence the air-sea O_2 and CO_2 fluxes. We transport the modeled fluxes in the atmosphere using the TM3 transport model and analyze the temporal and spatial variability of the APO concentration caused by changes in climate. We focus on the interhemispheric gradient and on the seasonal variability of APO concentration. The impact of climate change on the interhemispheric gradient of APO is too small to detect changes in the ocean circulation. However, changes in the amplitude of the

[1]This chapter corresponds in full to an article in preparation as *Detection of changes in the ocean circulation from O_2 and CO_2 atmospheric measurements* with Christian Rödenbeck, Corinne Le Quéré, Laurent Bopp, Ralph Keeling and Martin Heimann as co-authors.

APO seasonal cycle are ∼2 to 4 ppm for stations located near regions where large-scale changes in the ocean circulation occur, such as the North Atlantic. Changes in the APO seasonal cycle could thus provide an indicator to detect ocean circulation changes in the future.

3.1 Introduction

The oceans play an important role in regulating climate [Broecker, 1997], [Kuhlbrodt et al., 2007, Manabe and Stouffer, 2007]. The oceans distribute heat around the planet via the currents, and act to slow down the rate of global warming around the globe [Rahmstorf, 1997]. The ocean circulation and the vertical mixing of water masses also act to redistribute dissolved carbon between the deep and the surface water and between high and low latitudes [Sarmiento et al., 1995]. The increase of both ocean heat content and fresh water input, as a result of climate change, reduces the convective activity at high latitudes. This, in turn, decreases the sinking of the cold water and the deep water formation, weakening the ocean currents and affecting the air-sea gas exchange [Manabe and Stouffer, 2007].

The gas exchange at the air-sea interface is dependent on the solubility of the gases and is regulated by physical and biological processes that control the oxygen and carbon concentration in surface waters. Hence any changes in the oceanic physical and biological properties can affect the air-sea exchange of O_2 and CO_2 [Denman et al., 2007, Maier-Reimer et al., 1996].

Results from climate models presented in the 4th IPCC Assessment Report projected large-scale changes in the oceans' properties in response to anthropogenic forcing [Meehl et al., 2007]. In particular the model results from the 4th IPCC Assessment Report indicated a reduction of the Meridional Overturning Circulation from 15 to 50 % for a doubling atmospheric CO_2 concentration and a widespread increase in ocean stratification [Meehl et al., 2007, Friedlingstein et al., 2006].

The scientific community has expended much effort to understand and quantify changes in ocean properties induced by anthropogenic climate changes. Nevertheless, this goal is not yet fully achieved, due to the uncertainties in the model results and the lack of long-term measurements [Alley et al., 2003, Cunningham et al., 2007, Baehr et al., 2008, Bryden et al., 2009]. New methodologies are therefore required to detect large-scale changes in the oceans in the future.

We propose a new approach to infer changes in the ocean circulation using O_2 and CO_2 atmospheric observations. We base our study on the assumption that natural O_2 and CO_2 fluxes have different properties and are differently coupled for land and ocean processes [Keeling et al., 1993, Stephens et al., 1998]. On land the O_2 and CO_2 fluxes are strongly coupled. During photosynthesis and respiration the O_2 and CO_2 fluxes are exchanged at a fixed stoichiometric ratio of 1.1; during fossil fuel burning O_2 and CO_2 fluxes are exchanged at a ratio of 1.4. In the oceans, on the other hand, the situation is different and the O_2 and CO_2 fluxes are not coupled [Stephens et al., 1998]. The equilibration rate of CO_2 at the sea-air interface is much slower ($\sim$ 1 year) than the equilibration rate of O_2 ($\sim$ 1 month) and the CO_2 is involved in carbon chemistry, which does not affect the O_2 [Sarmiento and Bender, 1994, Manning and Keeling, 2006].

As a result, the combined atmospheric O_2 and CO_2 concentrations can provide information on ocean biological activity, air-sea gas exchange, and large-scale ocean circulation, that the atmospheric CO_2 concentration alone cannot discriminate [Stephens et al., 1998, Garcia and Keeling, 2001, Gruber et al., 2001, Battle et al., 2006, Rödenbeck et al., 2008]. To isolate the oceanic signal, we combine O_2 and CO_2 to form the Atmospheric Potential Oxygen (APO) in such a way that the terrestrial signals cancel out. Any variation in APO will thus contain information about the changes in biological activity, air-sea gas exchanges and large-scale ocean circulation [Stephens et al., 1998, Garcia and Keeling, 2001, Battle et al., 2006]. This work explores the potential of using the APO concentration to detect climate-induced changes in the ocean properties, in particular in the ocean circulation.

We analyze the oceanic fluxes generated by a coupled climate model for two different scenarios: one in which both climate and ocean circulation evolve as CO_2 increases, and one in which climate remains unaltered despite the increasing CO_2. We transport the oceanic fluxes projected by a coupled climate model into the atmosphere using the TM3 transport model [Heimann and Körner, 2003] and analyze the spatial and temporal variation of APO in the atmosphere in relation to changes in the oceans.

The outline of this chapter is as follows. In Section 3.2 we describe the models used, the experimental set up and the APO formulation. In Section 3.3 we present and discuss results of both the climate model and the atmospheric transport model for the two different scenarios considered. A brief comparison of the model results with the measurements from selected stations is also presented in order to verify the validity of the model chosen. We present the spatial and temporal variability of APO and the contribution of O_2 and CO_2 to APO, the interhemispheric variability of APO and its connection to large scale changes in the oceans, and the changes in the amplitude of the seasonal cycle as the oceanic circulation changes. Finally we close with conclusions and further remarks.

3.2 Methods

3.2.1 Climate model

We use the oceanic fluxes and other ocean parameters from IPSL_CM4 "Earth System Model" [Marti et al., 2005]. This climate model is a fully coupled ocean-atmosphere general circulation model. The Earth System Model is composed of an atmospheric component, an ocean component including sea-ice, and a land-surface component (http://dods.ipsl.jussieu.fr/omamce/IPSLCM4/).

The atmospheric component of the IPSL_CM4 model, LMDZ, is an atmospheric general circulation model, developed at the Laboratoire de Météorologie Dynamique. The atmospheric grid used in these sets of simula-

tions has an intermediate horizontal resolution of 3.75 ° by 2.5 ° and 19 vertical levels. The ocean component is the ocean global circulation model OPA 8.5, a primitive equation model of the ocean circulation [Madec et al., 1998]. The OPA model is interfaced with a sea ice model, LIM (Louvain Ice Model). The ocean model uses the ORCA2 grid, which has an unconventional horizontal tripolar coordinate mesh with two poles over land in the Northern Hemisphere. The grid has a resolution of 2 ° by 2 ° on average, with higher resolution, 0.5 °, at the equator and at the poles [Madec et al., 1998]. There are 31 vertical levels with 10 levels in the upper 100 meters. The atmosphere and ocean models are coupled via the coupler OASIS, Ocean Atmospheric Soil Interface Software. The monthly output from the climate model simulations force offline the ocean biogeochemical model PISCES (Pelagic Interaction Scheme for Carbon and Ecosystem Studies) [Aumont and Bopp, 2006]. The ocean biogeochemical model has multi-nutrient limitation and a plankton community structure with four Plankton Functional Groups [Bopp et al., 2003, Bopp et al., 2005]. The stratospheric ozone depletion is not considered, thus the increase in the Southern Ocean winds is underestimated [Le Quéré et al., 2007, Lenton et al., 2009].

3.2.2 Atmospheric Transport Model

We use the atmospheric transport model Tracer Model version 3 (TM3) [Heimann and Körner, 2003] to propagate the fluxes generated by the climate model described above in the atmosphere. TM3 is a 3-D Eulerian model driven offline by meteorological fields derived from NCEP (National Center for Environmental Prediction) [Kalnay et al., 1996]. We use reanalyzed meteorological fields for the year 1995 for all the years of the simulation. We assume that the use of reanalysis fields provides the best representation of the historical state of the atmosphere and avoids the impact of interannual variation in transport. The TM3 grid used here has a resolution of 4 ° by 5 ° with 19 vertical levels.

3.2.3 Experiment Setup

We look at the change of physical parameters in the oceans as projected by the climate model for the period 1861-2100. In particular we look at changes of the Atlantic Meridional Overturning Circulation (AMOC), the variation of the

Mixed Layer Depth (MLD) and heat flux, and relate them to the O_2 and CO_2 exchange across the air-sea interface. We analyze the oceanic fluxes generated by the climate model for two simulations:

(a) a coupled carbon-climate simulation where increasing atmospheric CO_2 affects climate, ocean physics and biogeochemistry, hereafter called "CO_2-climate" ;

(b) an uncoupled simulation where increasing atmospheric CO_2 is treated as a non-radiative gas and hence no climate change is present, hereafter called "CO_2-only".

In both simulations the model is forced by fossil fuel emissions from IPCC scenario A2 [IPCC-SRES, 2001]. The O_2 flux has been normalized by removing the global mean O_2 flux for 1861-1960 in order to correct the long-term drift in the model, which is an artifact of the spin up of the biogeochemical model. No corrections have been applied to the CO_2 flux, which is close to equilibrium.

We transport the oceanic O_2 and CO_2 fluxes for the entire period 1861-2100 for the CO_2-climate run and for the CO_2-only run. The O_2 and CO_2 fluxes have been interpolated from the original ORCA2 grid to the TM3 grid before being transported. In order to detect changes in the atmospheric tracer concentrations in relation to changes in the ocean circulation, we compare the results of the two runs for the entire period of simulation. We also analyse the difference between the averages over 2080-2100 and over 1990-2010 for the CO_2-climate run to better identify the changes between the future and the present conditions, globally and for 12 stations among the ones considered in this study (Figure 3.1). The model results are also compared to observations for the 1990-2006 time period for nine selected stations from the Scripps Institution of Oceanography global flask sampling network (Table 3.1) [Keeling et al., 1998, Hamme and Keeling, 2008]. In this comparison we add fossil fuel CO_2 fluxes for the years 1970-2007 [Olivier et al., 2002, EDGAR, 2006].

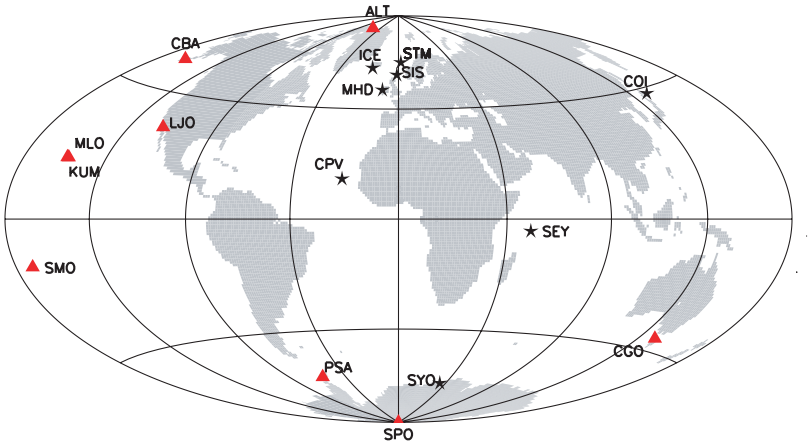

Figure 3.1— Locations of the stations considered in this study. The stations from the Scripps sampling network used to compare the model results are the in red. Alert, Canada (ALT); Cape Grim,Tasmania (CGO); Cold Bay, Alaska (CBA); Cape Oshi Ishi, Japan (COI); Cape Verde (CPV); Heimaey, Island (ICE); Kumukahi, Hawaii (KUM); La Jolla, California (LJO); Mauna Loa (MLO), Hawaii; Mace Head, Irland (MHD); Palmer Station, Antarctica (PSA); Samoa, American Samoa (SMO); Seychelles (SEY); Shetland, UK (SIS); South Pole (SPO); Station M, Norwegian Sea (STM); Syowa, Antarctica (SYO).

Table 3.1— Stations compared with model results

Station Name	*Latitude* (o)	*Longitude* (o)	*Elevation* (m asl)	*Acronym*
Alert	82.45 N	62.52 W	210	ALT
Cold Bay	55.20 N	162.72 W	25	CBA
La Jolla	32.87 N	277.25 W	15	LJO
Mauna Loa	19.53 N	155.58 W	3397	MLO
Cape Kumakai	19.52 N	154.82 W	3	KUM
Samoa	14.25 S	170.57 W	42	SMO
Cape Grim	40.68 S	144.68 E	94	CGO
Palmer Station	64.8 S	64.00 E	10	PSA
South Pole	90.0 S	24.80 W	2810	SPO

3.2.4 APO Formulation

In order to use a tracer not affected by terrestrial O_2 and CO_2 exchanges we calculate the Atmospheric Potential Oxygen using the simplified version of the formulation proposed by Stephens (1998):

$$\mathrm{APO}=\mathrm{O_2}+1.1\mathrm{CO_2} \tag{3.1}$$

For the analysis of the changes over the full simulation period, we use only the oceanic O_2 and CO_2 as computed by the models. The land contribution is eliminated by the 1.1 factor. APO thus includes only the oceanic contribution to the atmospheric concentration. When comparing model results with observations, Equation (3.1) needs to be modified to include the fossil fuel contribution:

$$APO^{Total} = \underbrace{O_2^{Ocean} + 1.1CO_2^{Ocean}}_{APO_{Ocean}} - \underbrace{0.3CO_2^{Fossilfuel}}_{APO_{Fossilfuel}} \tag{3.2}$$

Where the O_2^{Ocean} and CO_2^{Ocean} are oceanic fluxes projected by the biogeochemical model and the $CO_2^{Fossilfuel}$ are the fossil fuel fluxes taken from the Edgar database [Olivier et al., 2002]. All these fluxes are transported with the TM3. The APO^{Total} is used in this workn only for comparison with the observation.

3.3 Results and Discussion

3.3.1 Oceanic Fluxes

In the CO_2-climate run, changes in the physical properties of the oceans take place. Between 1861 and 2100, the average sea surface temperature increases by $\sim$2.4°C and the oceans warm at a rate of 0.01 °C/yr. The heat flux from the atmosphere to the oceans strongly increases from -1 to -5 W/m^2 (Figure

3.2). Negative values mean fluxes from the atmosphere to the ocean.

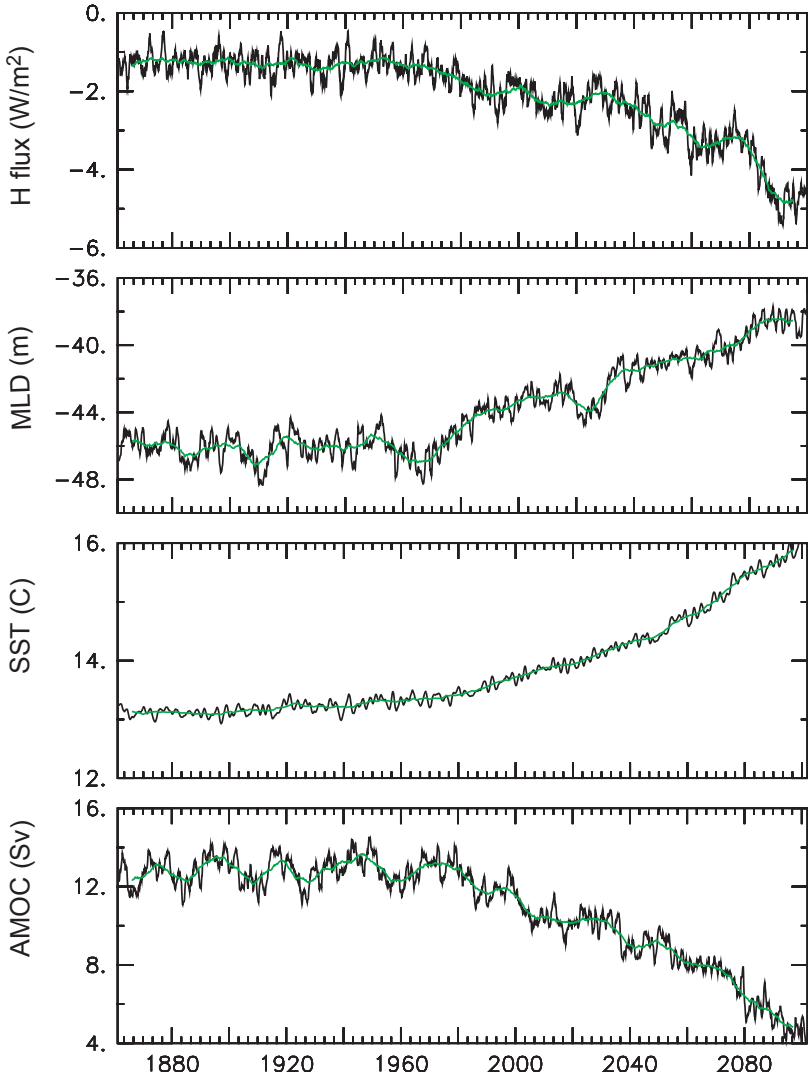

Figure 3.2— Time series of global heat flux (W/m^2), Mixed Layer Depth (m), and intensity of the Atlantic Meridional Overturning Circulation (Sverdrup, 10^6 m^3/s) for the CO_2-climate run. Negative values mean fluxes towards the ocean. The time series are deseasonalized (black line). The decadal variability (mean over 10 years) is overlayed, green line.

The vertical transport of the water masses decrease and the mean Mixed Layer Depth (MLD) becomes shallower. The mean MLD, used as measure of the vertical mixing of the water masses and of the water stratification, decreases globally by ∼20%, suggesting an increasing stratification in the future [De Boyer Montégut, 2004]. The stratification of the water mass increases particularly in winter and affects mostly the high latitudes, where the formation of intermediate and bottom waters occurs (Figure 3.3).

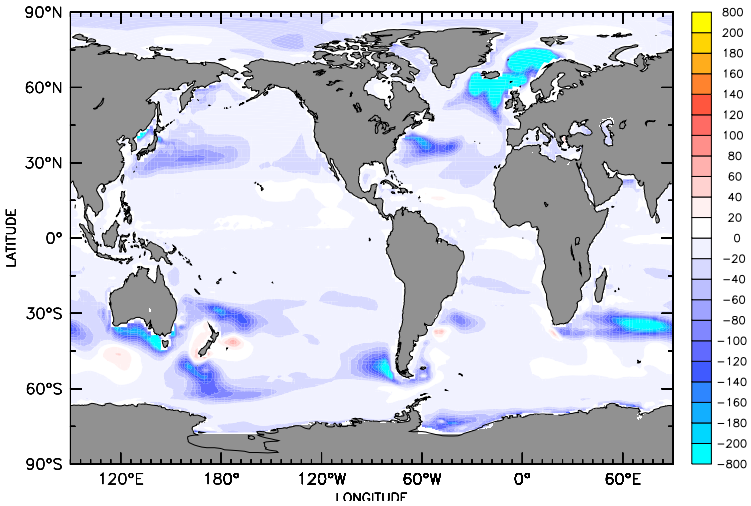

Figure 3.3— Changes in the Mixing Layer Depth in winter. The changes are computed as future MLD minus present MLD, (2080-2100 minus 1990-2010). The MLD has been calculated for the winter months in the two hemispheres (DJF and JJA) and plotted in one plot.

The deep water formation is reduced and hence the Meridional Overturning Circulation (MOC) slows down. We focus on the strength of the Atlantic Meridional Overturning Circulation (AMOC), which varies from a mean value of 14 Sv (10^6 m^3/s) at the beginning of the simulation to a mean value of 4 Sv by the end of the simulation. This is a reduction of about 70% of AMOC intensity (Figure 3.2), at the high range of the estimates presented in the IPCC 4th Assessment Report.

The changes in the ocean properties due to climate change are reflected in the air-sea gas flux dynamics [Stephens et al., 1998]. When the oceans warm,

the O_2 becomes less soluble, and when the vertical mixing and intensity of the AMOC are reduced, the O_2-depleted deep waters do not come in contact with the atmosphere. The combination of these processes causes a progressive O_2 outgassing from the ocean to the atmosphere, up to about 80 Tmol/yr by the end of the simulation period (Figure 3.4).

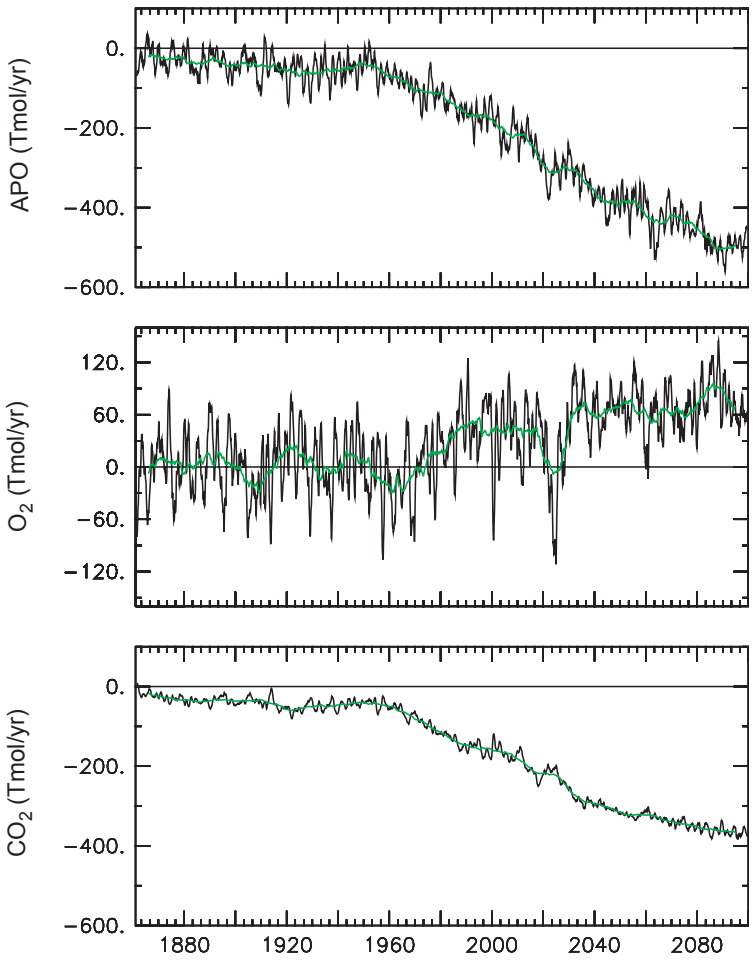

Figure 3.4— Time series of global oceanic APO, O_2 and CO_2 fluxes for the CO_2-climate run. Negative values mean fluxes towards the ocean. The time series are deseasonalized (black line). The decadal variability is overlayed (green line).

Previous studies have shown the link between climate-induced warming of the oceans and O_2 outgassing [Bopp et al., 2002, Plattner et al., 2002]. They have found that only a quarter of this outgassing is caused by thermal effects,

the remaining outgassing is due to changes in the ocean circulation. The modification of the ocean properties affects the CO_2 flux as well, but the direction of the CO_2 flux remains from the atmosphere to the ocean, due to the dominance of the response to increasing atmospheric CO_2. The APO flux follows the direction of the CO_2 flux and reaches up to about 400 Tmol/yr by the end of the simulation period (Figure 3.4).

In the CO_2-only run no changes in the physical properties of the oceans take place. The O_2 flux is in a steady state with respect to the net flux at the air-sea interface, while CO_2 is progressively taken up by the oceans in response to increasing atmospheric CO_2 (Figure 3.5).

The long-term trend in the APO flux in both runs reflects mostly the increase of ocean CO_2 uptake over longer time scale caused by increasing atmospheric CO_2. The oceans take up about 30% more APO in the CO_2-only run compared to the CO_2-climate run, due to the changes in the ocean physics present in the CO_2-climate run. The rate and the direction of the oceanic fluxes are consistent with previous studies [Bopp et al., 2002, Plattner et al., 2002, Keeling and Garcia, 2002].

3.3.2 Comparison with Measurements

APO has been used in previous studies to validate ocean carbon cycle models because it is not affected by the terrestrial signals [Stephens et al., 1998, Gruber and Keeling, 2001, Naegler et al., 2006]. A complete validation of the model is outside the scope of this study, but in order to demonstrate the reliability of the modelled APO fluxes, we compare the model results with the data from nine selected stations from the Scripps Institution of Oceanography global flask sampling network (Table 4.2). The agreement between the model and the observed APO is very good (Figure 3.6). The trend and the seasonal pattern for all the stations are well reproduced by the model, though low-latitude stations (Mauna Loa, La Jolla, and Cape Kukamai) tend to underestimate the amplitude of the seasonal cycle.

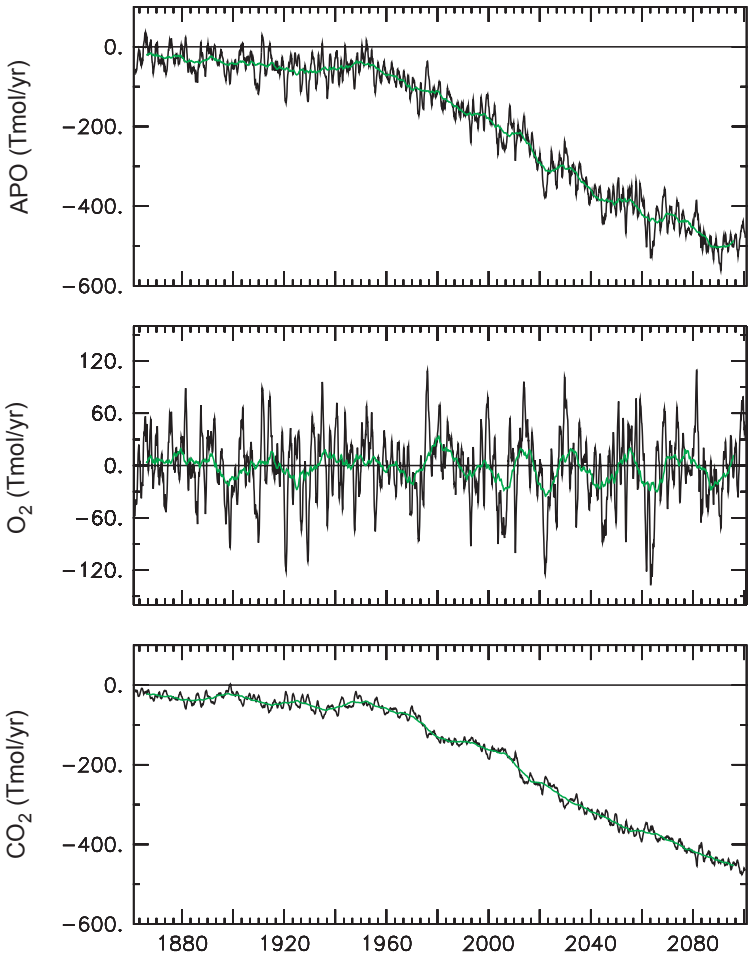

Figure 3.5— Time series of global oceanic APO, O_2, CO_2 fluxes for the CO_2-only run. Negative values mean fluxes towards the ocean. The time series are deseasonalized (black line). The decadal variability is overlayed (green line).

3.3.3 Atmospheric Concentration

Using the TM3 model, we transport the oceanic O_2 and CO_2 fluxes generated by the climate model for both CO_2-climate and CO_2-only runs. The atmospheric concentrations of O_2 and CO_2 are then combined to form the APO using Equation (3.1). The O_2, CO_2, and APO atmospheric concentrations show the same tendency as their corresponding air-sea fluxes described above (Figure 3.7).

In both the CO_2-climate and the CO_2-only runs, the atmospheric CO_2 concentration decreases due to the ocean uptake of CO_2. The difference in

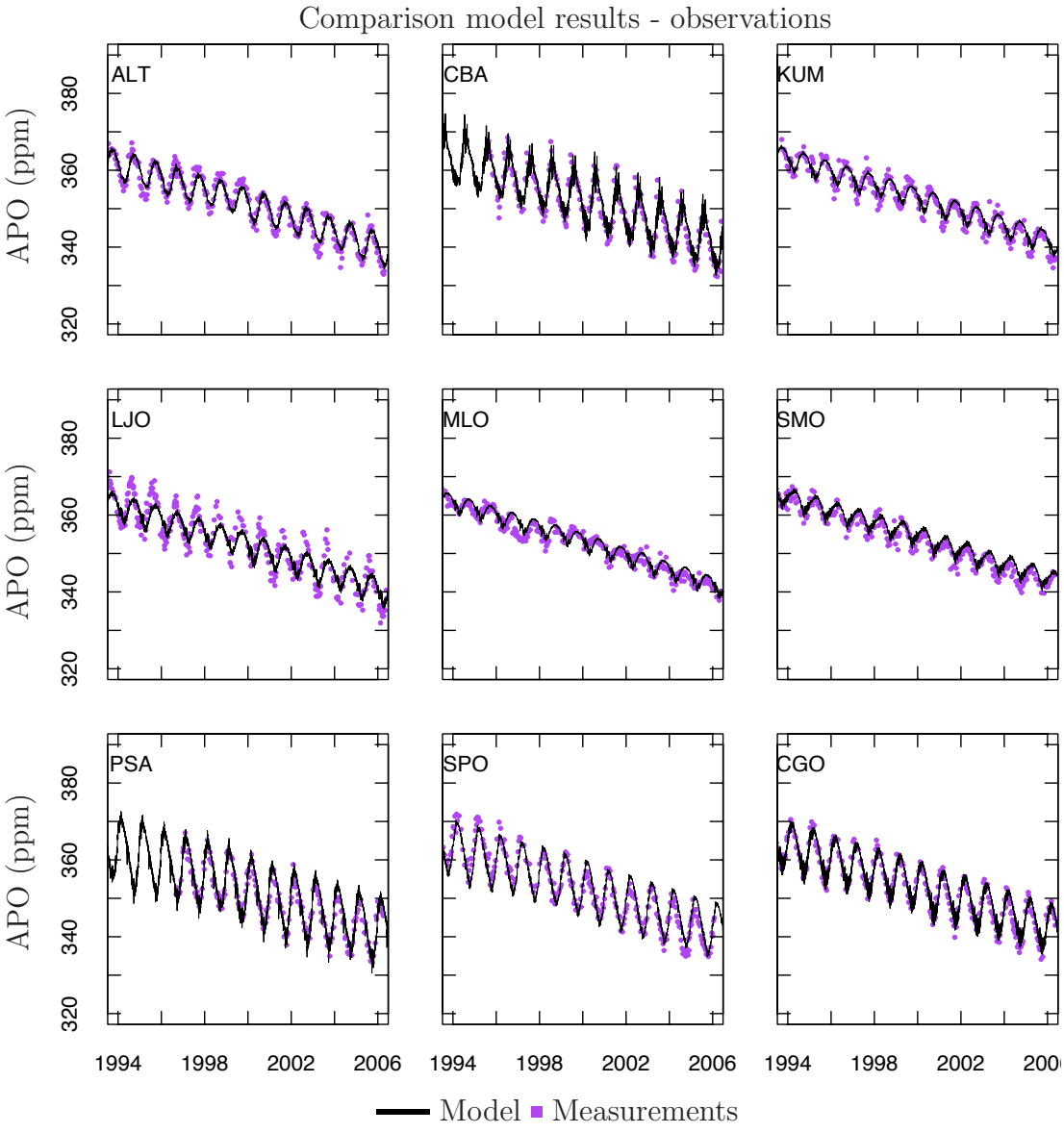

Figure 3.6— Comparison of the APO from the CO_2-climate run with the APO observed at nine selected stations from the Scripps network. The APO used here for the comparison is APO^{total}. The units are ppm and the stations are displayed in latitudinal bands. Alert, Canada(ALT); Cold Bay, Alaska (CBA); Kumukahi, Hawaii (KUM); La Jolla, California (LJO); Mauna Loa, Hawaii (MLO); Samoa, American Samoa (SMO); Palmer Station, Antarctica (PSA); South Pole (SPO); Cape Grim,Tasmania (CGO). The model results are the black solid line on top of the purple dots, which are flask measurements from the Scripps network.

CO_2 concentration between the CO_2-only and CO_2-climate runs is about 30 ppm by the end of the simulation period, which corresponds to a reduction of

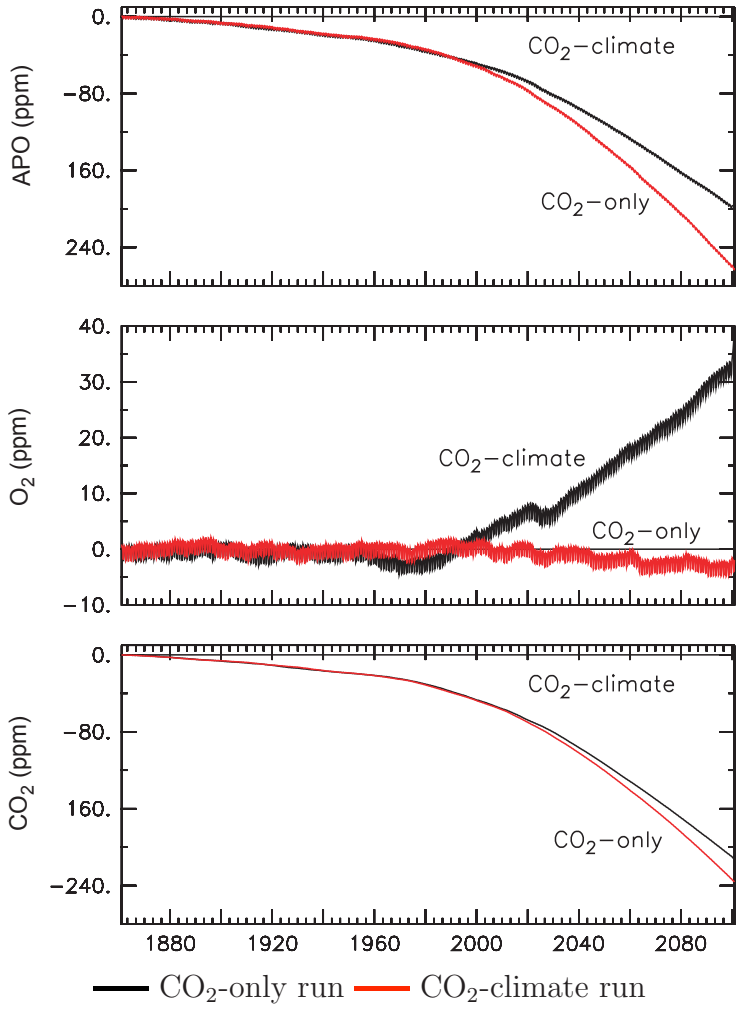

Figure 3.7— Comparison of global APO, O_2, and CO_2 concentration for the CO_2-only (black line) and CO_2-climate (red line) runs. Units are ppm.

$\sim$ 15% in the uptake of CO_2 by the ocean due to climate change. The O_2 concentration in the CO_2-climate run shows a positive long term trend. This is a response to changes in the physical conditions of the oceans including warming, stratification, and reduction of the AMOC and the associated changes in biogeochemistry. The O_2 concentration in the CO_2-only run is almost constant throughout the simulation period. The O_2 concentration in the CO_2-climate run increases up to 30 ppm by the end of the simulation. The difference of the APO concentration between the CO_2-only run and the CO_2-climate run, by the end of the simulation period, is about 60 ppm, which represents a difference

between the two runs of ∼25%.

The temporal characteristics of the tracer concentrations can be examined with a Fourier-transform based approach and visualized as a power spectrum plot or periodogram. This approach separates the contribution to the time series made by processes varying at different rates [Wilks, 2006]. The computation of the power spectra has been carried out finding the discrete-time Fourier transform of the tracers' concentrations for the period considered and taking the magnitude squared of the result. A Hanning window filter has been applied to the finite time series used in the spectrum analysis. The use of the window is important to avoid the spectral bias problems associated with the discrete Fourier transform computation [Harris, 1978].

On a weekly to seasonal time scale, the APO signal is dominated by the O_2 exchanges (Figure 3.8), primarily due to the temperature dependency of O_2 solubility, the short equilibration time scale of oceanic O_2, and to dynamic, thermal and biological processes [Garcia and Keeling, 2001, Rödenbeck et al., 2008, Nevison, 2008]. The oceanic O_2 fluxes dominate the interannual variability of the APO signal, as well. On the other hand, the APO signal is dominated by CO_2 over decadal to hundred year time scales. For very high frequencies, corresponding to processes within a short time period (for example synoptic events), it is not possible to extract information, since these frequencies are at the limit of the simulations resolution. We are able to identify the long term trend, the interannual variability, and the seasonal cycle within the periodogram (Figure 3.8).

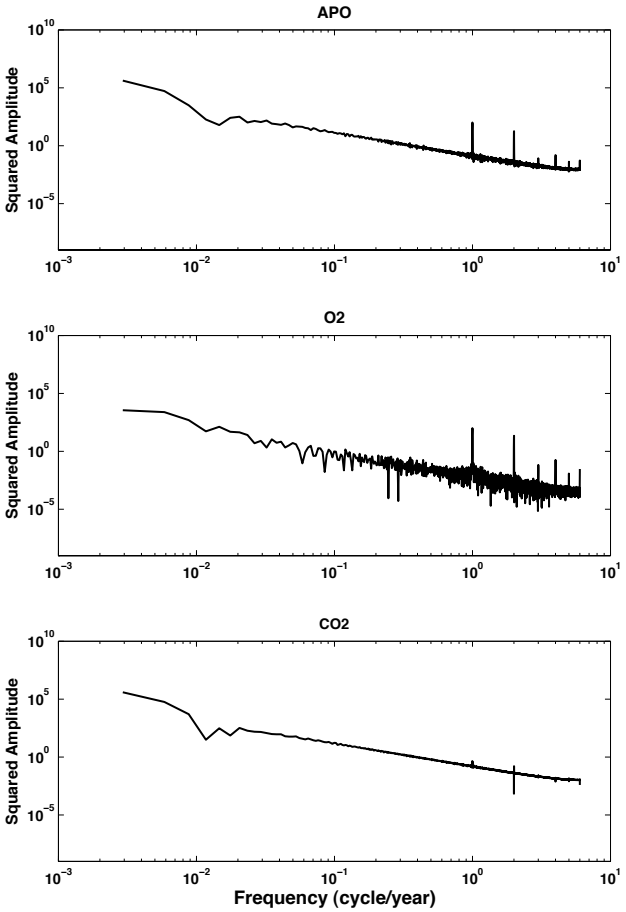

Figure 3.8— Power spectrum of the squared amplitude C^2 as function of the frequency. The axes are on a logarithmic scale.

Interhemispheric Gradient

The interhemispheric gradient of APO varies from year to year and reflects the variability of the CO_2 sources/sinks and the transport in the atmosphere [Dargaville et al., 2003]. The APO signal has a strong interhemispheric gradient, reflecting mostly the large scale oceanic processes [Stephens et al., 1998, Battle et al., 2000]. We first look at the O_2, CO_2 and APO fluxes for the CO_2-climate run for individual hemispheres to see whether the future global changes in the ocean, projected by the climate model, affect the two hemispheres differently (Figure 3.9).

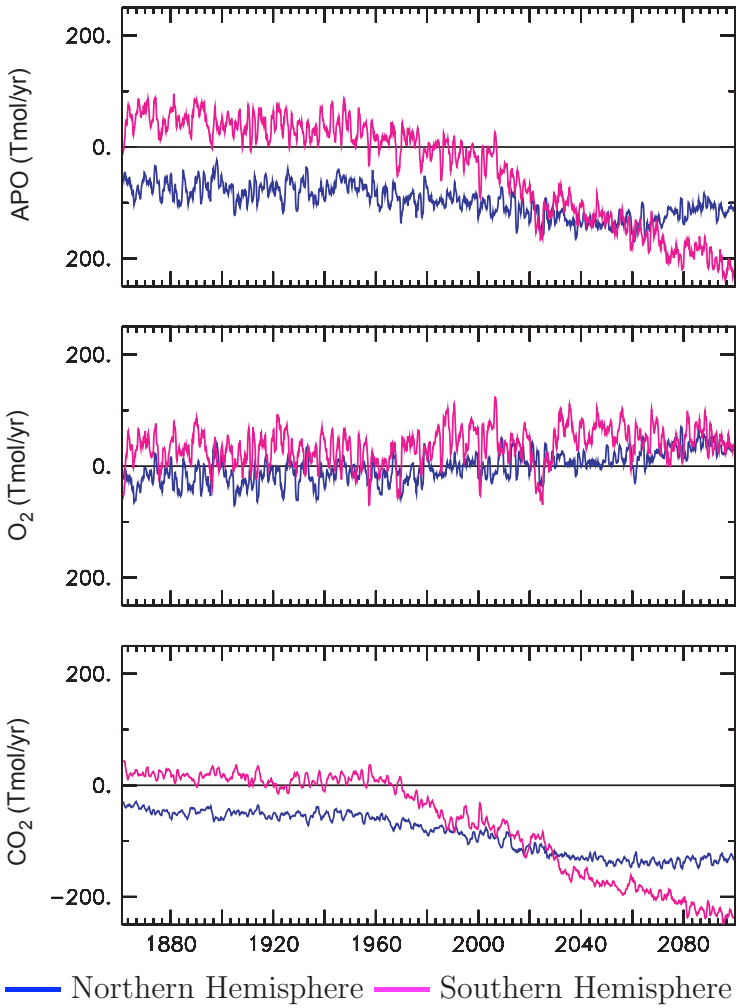

Figure 3.9— Global oceanic APO, O_2, and CO_2 fluxes from the CO_2-climate run for the two hemispheres. Negative values mean fluxes towards the ocean. Northern Hemisphere is the blue line and Southern Hemisphere is the magenta line.

By the end of the simulation perios, the Southern Hemisphere has a larger sink of CO_2 and APO than the Northern Hemisphere. This is likely due to the larger ocean surface and therefore larger uptake capacity in the Southern Hemisphere. The uptake of CO_2 in the Northern Hemisphere is reduced most by climate change because this is where the greater physical changes are visible. Both hemispheres show a source of O_2, as discussed in section 3.1.

The APO interhemispheric gradient reflects the air-sea exchanges at high and low latitudes, the transport by the currents from north to south and the redistribution in the atmosphere due to the atmospheric mixing [Naegler et al., 2006, Nevison, 2008, Tohjima et al., 2008]. Here we compute the interhemispheric gradient for the atmospheric concentrations as the difference between the mean concentration in the Northern Hemisphere and the mean concentration in the Southern Hemisphere as in Dargaville, 2003 (Figure 3.10).

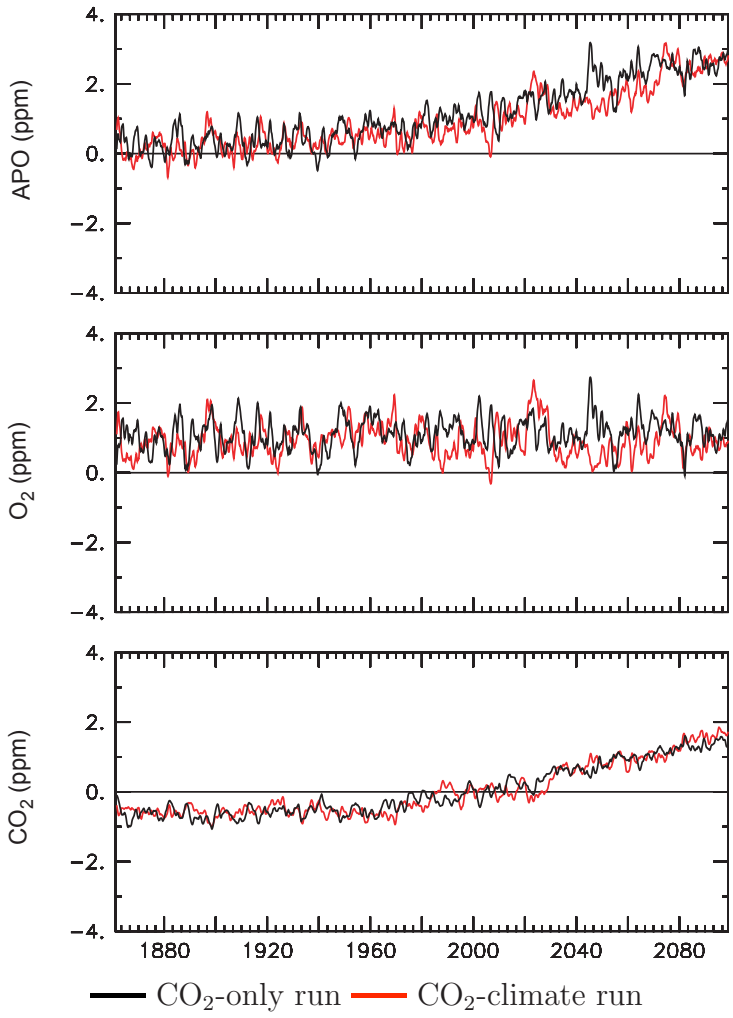

Figure 3.10— Interhemispheric gradient for the period 1861-2100. The three panels show APO, O_2, and CO_2 for the CO_2-climate run (red line) and CO_2-only run (black line).

Our results are not influenced by the way we compute the interhemispheric gradient. There are no significant differences in the interehemispheric gradient between the CO_2-climate and the CO_2-only runs (red and black curves respectively in Figure 3.10). In both runs, the interhemispheric difference is around 2 ppm for the APO and CO_2 concentrations, while for the O_2 concentration the interhemispheric difference is near 0. We attribute the lack of interhemispheric difference to the fast mixing of the atmosphere. The climate induced changes in the ocean are not visible from changes in APO interhemispheric gradient (black line Figure 3.10).

Seasonal Cycle

The processes that drive the air-sea exchanges on a seasonal time scale are thermal (warming and cooling), dynamic (mixing and stratification of the water) and biological (respiration and photosynthesis). These processes reinforce each other in the O_2 seasonal cycle, but counteract each other in the CO_2 seasonal cycle. Consequently on seasonal time scales, as seen in section 3.3.3, the APO signal is dominated by O_2 [Keeling et al., 1993]. In addition, O_2 equilibrates much faster ($\sim$ one month) than CO_2 ($\sim$ one year). If the biological or physical conditions of the ocean are altered, the seasonal air-sea exchanges will be altered as well, and the signal of changes in the ocean properties will be visible in the seasonal APO concentration.

We focus on the change in the amplitude of the APO seasonal cycle between 1990-2010 and 2080-2100. We compute the mean seasonality for O_2, CO_2, and APO and estimate the difference 2080-2100 minus 1990-2010, in the "peak to peak" amplitude of the seasonal cycle. The change in amplitude of the APO seasonal cycle allows us to highlight the areas where climate-induced changes in the ocean will occur in the future, according to the model projections.

In the CO_2-only run the amplitude of the CO_2 seasonal cycle increases with time everywhere because the summer ocean CO_2 roughly follows atmospheric CO_2 while winter CO_2 lags behind because of winter mixing. There is no change in the oceanic physics, and the greatest positive values in the difference of amplitude, about 5 ppm, are located in the areas where the bottom and

intermediate water is formed and the uptake of gases by the ocean takes place [Maier-Reimer et al., 1996]. The amplitude of the O_2 seasonal cycle decreases from 0 to -0.5 ppm, with slight positive values at the latitudes where the uptake of gases by the oceans occurs. Since the seasonality of the oceanic O_2 reflects mostly the changes of the ocean physics, when no changes in the ocean physics take place, the amplitude of the atmospheric O_2 seasonal cycle is not affected (CO_2-only run). No significant changes in the amplitude of the atmospheric APO seasonal cycle are visible in the CO_2-only run (Figure 3.11).

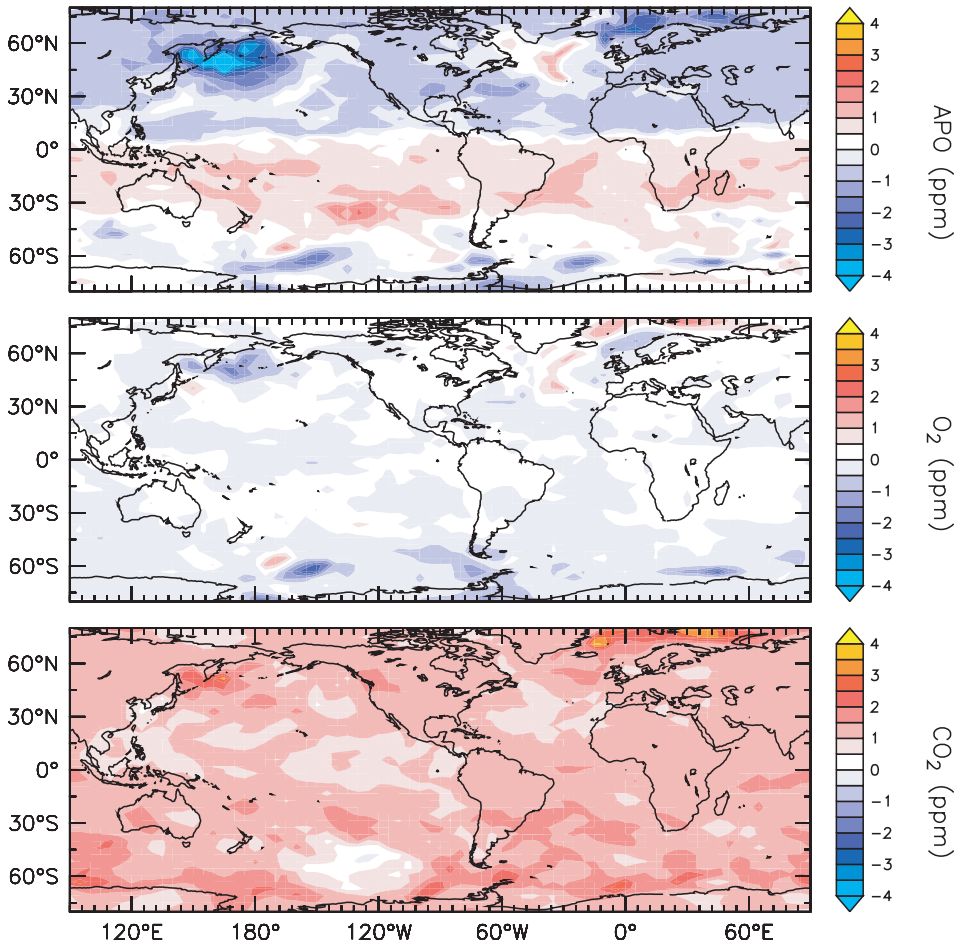

Figure 3.11— Difference in the amplitude of the seasonal cycle for atmospheric APO, O_2, and CO_2 concentrations for the period 2100-2080 minus 1990-2010 for the CO_2-only run.

In the CO_2-climate run the amplitude of the CO_2 seasonal cycle also increases nearly everywhere. The amplitude of the O_2 seasonal cycle decreases in the deep water formation regions and in regions where the MLD becomes particularly shallow due to stratification. The difference in amplitude of the APO seasonal cycle reaches more than 4 ppm in the areas where large changes in the ocean properties are present (Figure 3.12).

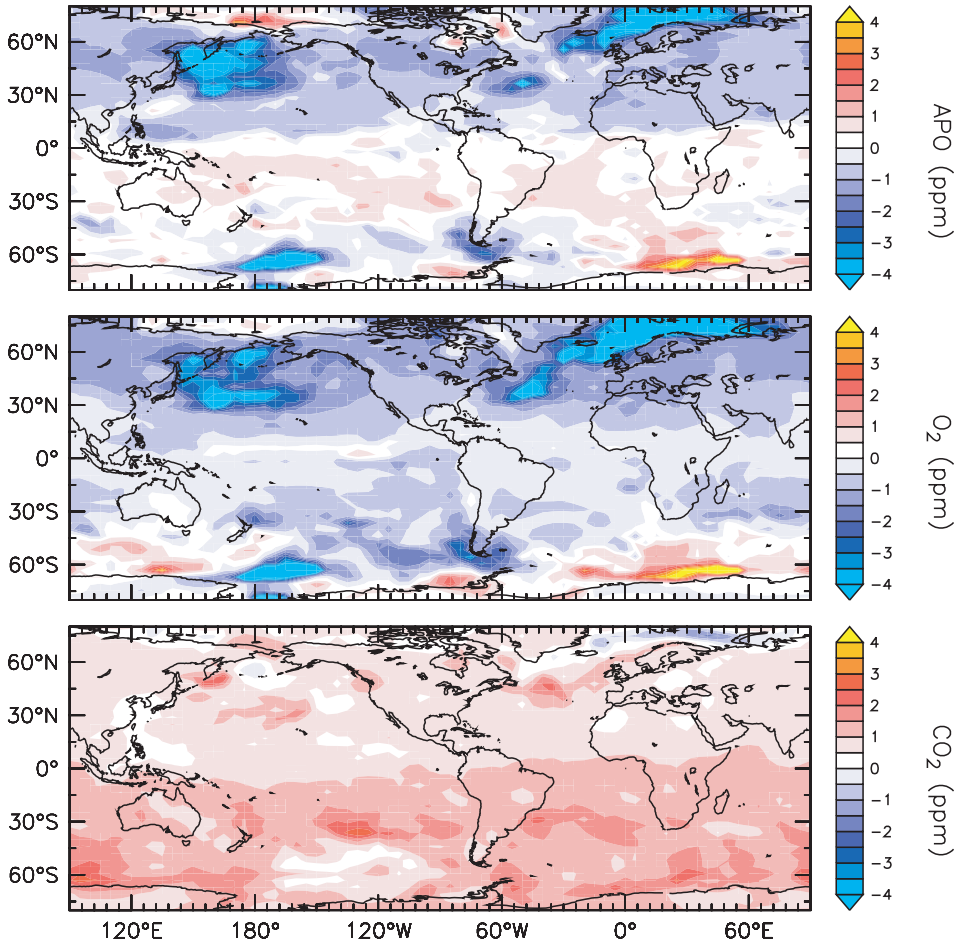

Figure 3.12— Difference in the amplitude of the seasonal cycle for atmospheric APO, O_2, and CO_2 concentrations for the period 2100-2080 minus 1990-2010 for the CO_2-climate run.

The North Atlantic is the place whre the largest changes in APO seasonal cycle take place, because of the reduction of the AMOC. The positive difference

in the amplitude of the APO and O_2 seasonal cycles around Antarctica is likely due to a local effect of sea ice melting.

We calculate the APO seasonal cycle for the locations of APO measurement stations around the world, either where they are already operative or in development (Figure 3.13). The stations that show the greater changes in seasonality in the future are located mostly at the latitudes affected by changes in the ocean. The difference in amplitude varies in the range of 2 to 4 ppm depending on the station location. Some stations also show an offset in the seasonality of about a month. We consider that the signal needed to discriminate the physical changes in the ocean is moderately above the limit of the detectability due the actual measurement techniques (from $\sim$ 1 to 2 ppm depending on the measurement techiques) [Keeling et al., 1998, Manning and Keeling, 2006].

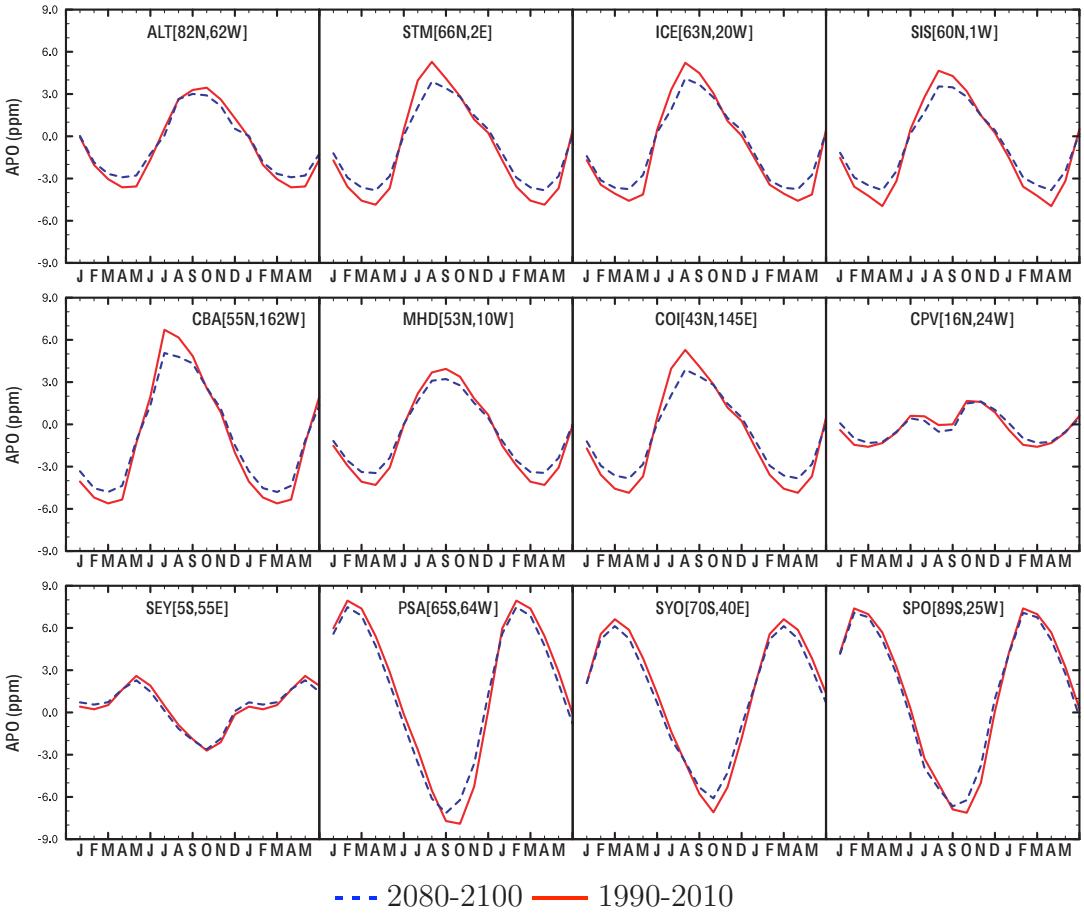

Figure 3.13— Mean seasonal cycle for APO at 12 selected stations as projected by the CO_2-climate run. Years 1990-2010 are shown with red continuous line, and years 2080-2100 are shown with blue dotted line. For a better visualization of a complete seasonal cycle 18 months are plotted. Alert, Canada (ALT); Station M, Norwegian Sea (STM); Heimaey, Island (ICE); Shetland, UK (SIS); Cold Bay, Alaska (CBA); Mace Head, Irland (MHD); Cape Oshi Ishi, Japan (COI); Cape Verde (CPV); Seychelles (SEY); Palmer Station, Antarctica (PSA); Syowa, Antarctica (SYO); South Pole (SPO).

3.4 Conclusions

We have done forward simulations with the TM3 model of oceanic fluxes of O_2 and CO_2 from a carbon-climate model to determine the potential of detecting changes in ocean properties from measuring atmospheric O_2 and CO_2. The climate model projected increasing ocean warming, stratification, and slowing down of the AMOC. All these changes have an impact on the air-sea gas exchanges.

We use the Atmospheric Potential Oxygen to isolate the oceanic from the land signal in atmospheric O_2. APO is dominated by CO_2 for the long-term trend, but by O_2 on seasonal to decadal time scales. The changes in ocean physical properties are mostly visible in seasonal changes in APO. For existing or planned stations, changes in seasonal APO amplitude around 2 to 4 ppm occurred in regions where the ocean physical changes were the largest. These changes are above the detection limit for APO measurements. Thus future changes in APO seasonal cycle could be used to detect large-scale changes in ocean physics in the future.

Our conclusions are, however, limited due to the presence of confounding effects that can also change future APO seasonal cycle:

- uncertainties related to the use of modeled oceanic fluxes; the impact on the biogeochemical fluxes depends on the amount of changes in climate as projected by the model used;

- uncertainties related to the possible changes in the atmospheric circulation in the future, not taken into account in the transport model;

- uncertainties related to the use of fossil fuel emissions.

From this study we highlight the geographical areas where the climate change signals are largest. In these areas the atmospheric O_2 and CO_2 measurements

would be most useful. The increasing of the number of stations and the improvement in the measurement technique will provide better information on the present conditions as reference for future changes. An amelioration in the global measurement network is necessary to improve the detectability of changes in the ocean properties from APO observations.

Chapter 4

Role of Atmospheric Transport in the APO Variability

4.1 Introduction

Atmospheric measurements, collected over the past 20 years, show that the increasing concentration of atmospheric CO_2 is coupled with a decreasing concentration of O_2. This trend can be used to separate the land and ocean contribution to the carbon sink, and to detect changes in the ocean [Keeling and Shertz, 1992]. The oceanic signal can be isolated combining O_2 and CO_2 to form the Atmospheric Potential Oxygen (APO = O_2+1.1CO_2) as explained in Chapter 1.

APO variations are caused by changes in both O_2 and CO_2, and as such the origin of these variations can be quite complicated to understand. On a seasonal time scale the APO signal is dominated by air-sea O_2 exchanges, while on much longer time scales the variability in CO_2 dominates the APO signal (see Chapter 3 of this thesis). The year-to-year variation in the APO concentration is one of the major features visible in the APO measurements [Hamme and Keeling, 2008], but the processes that drive this variation are not yet fully understood.

Past studies have assumed that APO interannual variations are driven by natural variations of the oceanic fluxes, depending on the geographical location

considered: in the Tropics the variations are caused by ventilation of surface O_2 due to changes in upwelling caused by El Niño Southern Oscillation, while at higher latitudes the attribution to mechanisms is less clear but at least partly due to variability in the marine biology [Rödenbeck et al., 2008]. Hamme et al (2008) analyzed the changes in APO concentration from flask measurements and attributed the variability observed, particularly at high latitudes, to changes in the ocean ventilation. Such conclusions are based on the assumption that the APO interannual variability is driven by the oceanic fluxes. Here we investigate the drivers of the APO variability using model results compared to observations.

We concentrate our study on two possible drivers of the APO variability:

1. The variability of the oceanic fluxes: changes in the APO concentration are driven by the variability of oceanic fluxes
2. The atmospheric transport: changes in the APO concentration are driven by changes in the atmospheric transport

In order to explore these possible drivers we carry out a sensitivity analysis combining different meteorological fields with the oceanic fluxes.

This chapter is organized as follows. First, the models used are introduced, followed by a description of the experimental setup. In the following section the results are presented and discussed. Finally, a brief comparison of the results with those produced by another oceanic model is presented.

4.2 Models used

A detailed description of all the models is presented in Chapter 2, and only an overview of the models used for this chapter is included here. The oceanic fluxes used in this study are generated by the ocean biogeochemistry model PISCES-T [Buitenhuis et al., 2006]. The PISCES-T model is a modified version of the ocean biogeochemistry model PISCES [Aumont and Bopp, 2006], see Chapter 2. PISCES-T contains additional parameterizations and equations

of the biogeochemical fluxes through mesozooplankton. The PISCES-T model includes O_2 and a full carbon cycle, is initialized with observations in 1948, and uses the monthly dust deposition map from [Tegen and Fung, 1995], as in [Cotrim Da Cunha et al., 2007]. The PISCES-T model is embedded in the OPA global circulation model [Madec et al., 1998] using the ORCA2 grid.

Unlike the oceanic fluxes used in Chapter 2, which are generated by the biogeochemical model PISCES driven by the monthly output of the climate model IPSL_CM4, the oceanic fluxes used in this chapter are generated by a biogeochemical model, which is not driven by climate model results, but by observed meteorological fields from NCEP reanalyses [Kalnay et al., 1996]. Therefore, the oceanic fluxes are available only for the period in which the meteorological fields exist, but the results are more suitable for comparison with the observations. The oceanic fluxes are transported into the atmosphere via the TM3 transport model [Heimann and Körner, 2003]. The TM3 transport model is a 3-D Eulerian model driven by offline meteorological fields. The resolution used for the simulations done in this chapter is 4° latitude × 5° longitude with 19 vertical levels. For more details see Chapter 2. The output of the TM3 model is the distribution of the tracer in the atmosphere in terms of mixing ratio. The mixing ratio of a gas is defined as the number of moles of gas X per mole of air. It is given in units of mol/mol (moles per mole). Here we refer to the concentration of the gas in the atmosphere as explained in Chapter 2, but it should be kept in mind that this is a mixing ratio.

4.3 Experiment Setup

The ocean biogeochemical model generates oceanic CO_2, O_2 and N_2 fluxes, that together with the fossil fuel from the Edgar database [Olivier et al., 2002, EDGAR, 2006] are transported into the atmosphere with the TM3 model. From the TM3 output, we estimate the variation in APO concentration (ΔAPO) using the following formulation [Stephens et al., 1998]:

$$\Delta(APO) = \Delta(O_2/N_2) + 1.1 \cdot \Delta(CO_2) + \frac{X^{O_2}}{X^{N_2}} \cdot \Delta(N_2) \tag{4.1}$$

with $X^{O_2} = 209460$ ppm and $X^{N_2} = 790190$ ppm. We estimate the APO concentration in ppm units rather than in the unit "per meg"[1] that is commonly used for measurements of the atmospheric oxygen, because ppm is the unit used for other trace gases in the atmosphere. Fossil fuel burning consumes O_2 decreasing APO, therefore we have to take fossil fuel into account to correct the APO modeled. We add the fossil fuel contribution from the database in order to compare the model results with measurements.

Before being transported in the atmosphere, the oceanic fluxes have been modified by the application of temporal filter to obtain fluxes with different temporal variability [Rödenbeck, 2005].

We obtain three kinds of oceanic fluxes to transport into the atmosphere (Figure 4.1):

1. Fluxes which have the full temporal variability, as generated by the ocean model. Hereafter we call these fluxes "VAR-flux";

2. Fluxes which have a constant seasonal cycle repeated for the entire simulation period. Neither long term trend nor interannual variability are present in these fluxes. Hereafter we call these fluxes "SEAS-flux";

3. Fluxes which have a constant long term mean for the entire simulation period. Neither seasonal cycle nor interannual variability are present in these fluxes. Hereafter we call these fluxes "LT-flux" (long term).

The SEAS-flux is obtained by applying a smoothing operator with cosine spectral weights that consider only the seasonal frequencies:

[1] $1/0.2095 = 4.8$ per meg is equivalent to 1 ppm, where 0.2095 is the O_2 mole fraction of air

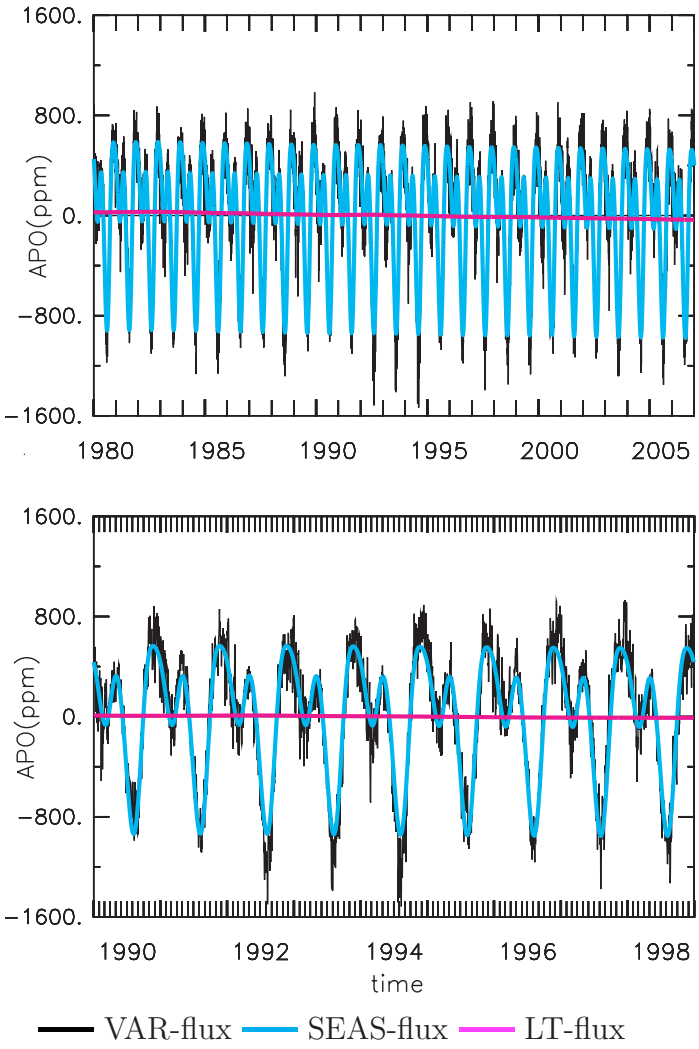

Figure 4.1— APO Fluxes from OPA-PISCES-T model. The lower panel is a zoom over the period 1990-2000, to better highlight the differences among the three fluxes.

$$W(\nu) = \begin{cases} 0 & \nu \geq \nu_c \\ \frac{1}{2}\left(1 - \cos\left(2\pi \frac{\nu}{\nu_c}\right)\right) & \nu_c > \nu > \frac{\nu_c}{2} \\ 1 & \nu \leq \frac{\nu_c}{2} \end{cases} \tag{4.2}$$

with $\nu_c = 7.0/year$.

The LT-flux is obtained by the calculation of the long term mean for the

entire period of simulation.

The transport model needs to be driven by meteorological fields. Here we use 6-hourly meteorological fields varying over the period of simulation as well as meteorological fields taken from three different fixed years, repeated for the period of simulation, all derived from the NCEP reanalyses [Kalnay et al., 1996]. In total our sensitivity analysis consist of a set of three main experiments using different fluxes in combination with four different meteorological fields, for a total of 12 simulations, as summarized in Table 4.1. The different steps done to carry out the experiments are summarized in the scheme in Figure 4.2.

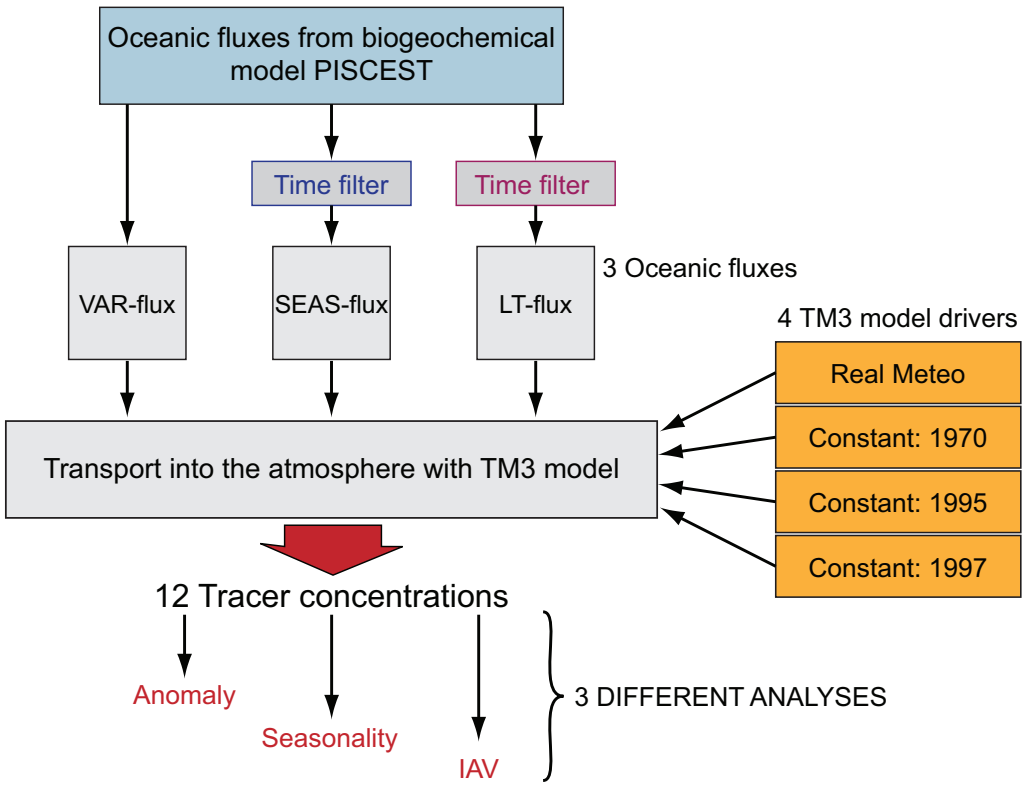

Figure 4.2— Diagram of the work-flow for the experiments done.

The presented model results are always detrended to compensate for a drift of the ocean model. Due to the spin up of the biogeochemical model, the oxygen fluxes present an initial offset, which creates an unrealistic trend in the

concentrations. We solve this problem by subtracting the linear trend from the concentrations. This solution is satisfactory for the aim of our study, but does not solve the problem as a whole. At present, further improvements to the model are ongoing.

For each of the simulations we look at the detrended concentrations, the interannual variability and the seasonal cycle (Table 4.1).

Table 4.1— Summary of the experiments done

Acronym	Description
	Fluxes
VAR-flux	Oceanic fluxes with fully variability
SEAS-flux	Oceanic fluxes only with seasonal variability
LT-flux	Oceanic fluxes without temporal variability
	Transport model drivers
Real meteo	Meteorology of actual years
1970 meteo	Repeated 1970 meteorology
1995 meteo	Repeated 1995 meteorology
1997 meteo	Repeated 1997 meteorology
	Analysis done to the concentration fields
Anomaly	Subtraction of the linear trend
Seasonality	Calculation of the seasonal cycle by applying the Gaussian filter [a]
IAV	Calculation of the Interannual Variability by applying a Gaussian filter [b]

[a] cut frequency $\nu_c = 3.0/year$ (equation 4.3)
[b] cut frequency $\nu_c = 0.5/year$ (equation 4.3)

The linear trends are calculated by a least squares fit of the APO concentration and then subtracted to look at them as anomaly records, referred to later as Anomaly; the interannual variability, referred to later as IAV and the seasonal cycle, referred to later as Seasonality are calculated through the application of frequency domain techniques, which provide more robust results even when there are gaps in the data. The interannual variability is obtained by applying a smoothing operator with Gaussian spectral weights to attenuate the higher frequencies as in Equation 4.3:

$$W(\nu) = exp\left(\frac{-\nu^2}{2\nu_c^2}\right) \tag{4.3}$$

where ν_c is the cut-off frequency for the filtering. For the IAV signal the weighting factor is chosen so as to eliminate all the variations faster than one year, that is $\nu_c = 0.5/\text{year}$. The seasonal frequencies are also eliminate by the removal of the terms $\nu = 1/year, 2/year, 3/year....$ For the calculation of the seasonality only the terms $\nu = 1/year, 2/year, 3/year...$ are taken into account. The cut-off frequency is chosen so that all the variations faster than about two months are eliminated, $\nu_c = 3.0/\text{year}$ [Rödenbeck, 2005, Rödenbeck et al., 2008].

The oceanic fluxes are transported from 1980 to 2006. We present the results only from 1990 to 2006, which is the time period during which measurements are available. We analyze the modeled concentration values taken at the same time at which the corresponding measured concentrations have been sampled, as in Rödenbeck (2008). We compare the model results with observations from nine selected stations from the Scripps Institution of Oceanography (SIO) atmospheric oxygen flask sampling network. The stations are listed in Table 4.2 and are geographically located as shown in Figure 4.3. For MLO (Mauna Loa) and SPO (South Pole), there are documented sampling problems, and the values can be considered to be significant only after 1998 [Manning and Keeling, 2006]. The measured values are always displayed on the graphs, but a complete validation of the models is beyond the scope of this work.

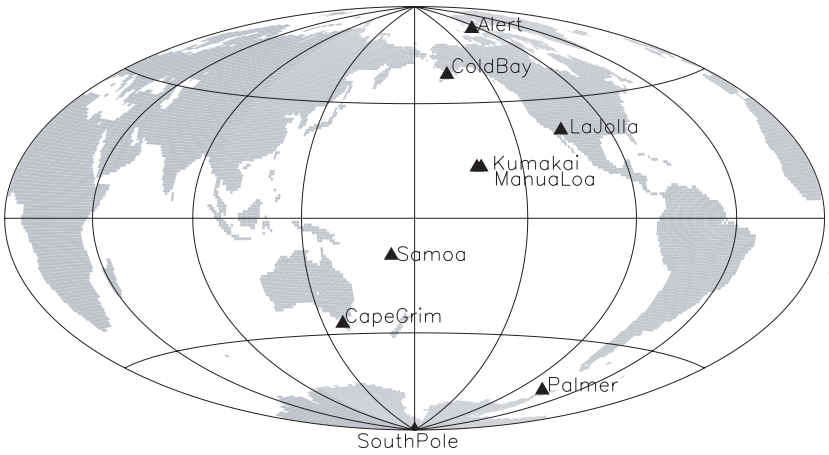

Figure 4.3— Location of the stations used in this study. All the stations are from the SIO flask sampling network.

Table 4.2— Stations from the Scripps flask sampling network

Station Name	*Latitude* (°)	*Longitude* (°)	*Elevation* (m asl)	*Acronym*
Alert	82.45 N	62.52 W	210	ALT
Cold Bay	55.20 N	162.72 W	25	CBA
La Jolla	32.87 N	277.25 W	15	LJO
Mauna Loa	19.53 N	155.58 W	3397	MLO
Cape Kumakai	19.52 N	154.82 W	3	KUM
Samoa	14.25 S	170.57 W	42	SMO
Cape Grim	40.68 S	144.68 E	94	CGO
Palmer Station	64.8 S	64.00 E	10	PSA
South Pole	-90.0 S	24.80 W	2810	SPO

The comparison of the simulations with the measurements and the comparison among the different simulations are represented with Taylor diagrams. The Taylor diagram provides a way of graphically summarizing how closely a

pattern (or a set of patterns) matches observations. The diagram summarizes correlation coefficients, root mean squared errors, and standard deviations of several models on a single plot [Taylor, 2001]. The values to compare are represented on a polar diagram in which the angle θ from the x-axis is the arccosine of the correlation coefficient R between the model and the observation. It reflects the agreement in shape and phasing. The values on the radial axis are the normalized standard deviation, calculated as ratio of the model standard deviation to the observation standard deviation. It represents the agreement in the amplitude of the variability between the model results and the observations. The distance of each symbol from the point (1,1) appearing on the diagram quantifies how closely the model's simulated pattern matches the observations.

4.4 Results

We are focusing on the variability of the APO for the past decades at interannual and seasonal time scales. To start we want to check whether the concentrations resulting from the transport of the three fluxes reflect the main temporal patterns of their corresponding oceanic fluxes. We graphically compare the three concentrations obtained (Figure 4.4) in the same way we did for the fluxes in Figure 4.1. The anomalies resulting from the transport of the three fluxes show the same variability present in the fluxes, as seen in Figure 4.1. The variability seen in the LT-flux trasnported is only due to the variability present in the meteorological fields.

4.4.1 Variable Flux

Anomaly

We transport VAR-flux as generated by the ocean biogeochemical model and look at the differences using real or constant meteorological fields (Figure 4.5). We see that all the anomalies have a predominant seasonal variability, which is well reproduced by the model. We attribute the poor agreement for La Jolla to the position of the station: this is a coastal station located at low latitudes, difficult to parametrize in the transport model. The modeled concentrations

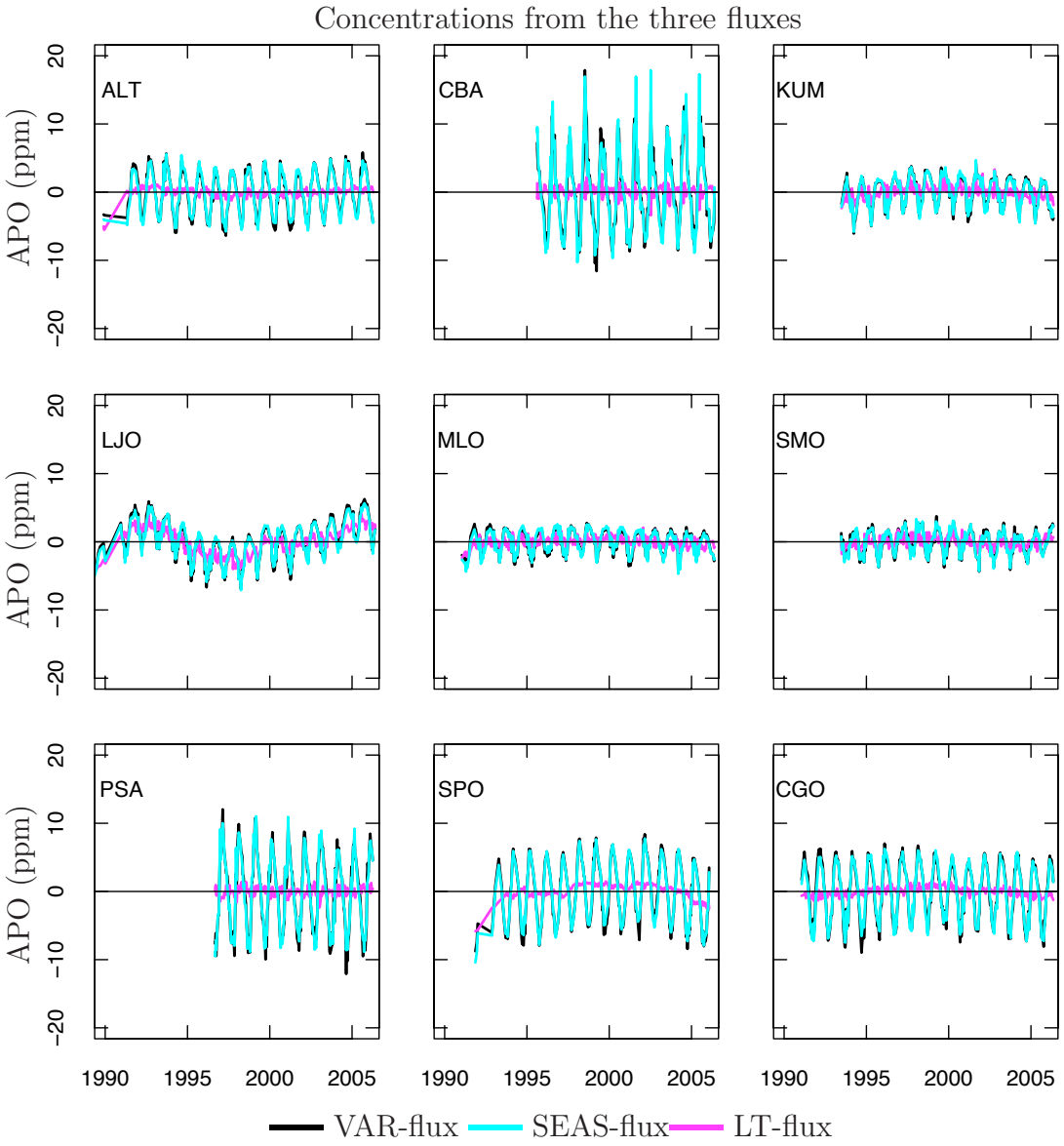

Figure 4.4— APO Concentrations resulting from the transport of three kinds of fluxes: concentration from the transport of VAR-flux in black, concentration from the transport of SEAS-flux in cyan and concentration from the transport of LT-flux in magenta, at the location of the SIO Network stations.

do not show significant differences with the measurements, at a seasonal scale independently on the meteorology used to drive the model. At interannual time scales the use of variable year-to-year or constant meteorological fields can play a more significant role.

The upper plot in Figure 4.8 shows the Taylor diagram for the anomaly concentrations for VAR-flux in combination with different meteorological fields. Most stations (symbols) have a moderately and high correlation with the observed values, confirming the ability of the models to reproduce the observed seasonal variations. The agreement is good when using both variable and constant meteorological fields. Using real meteorology, we notice for all the stations a slightly better agreement at all the stations.

Seasonality

The modeled mean seasonal cycle of APO shows good agreement with the observed seasonal cycle (Figure 4.6). The model amplitude is well represented and the agreement in phasing is very high for almost all the stations, except for La Jolla, where the model minimum is displaced by about 2 months and the amplitude of the seasonal cycle is smaller than that of the observations. The chosen filter can generate an underestimation in the amplitude of the seasonal cycle, but it allows to manage the discontinuity of the data.

Using real or constant meteorology does not influence much the seasonal variability of APO and obviously in both cases the seasonal variability of the APO is dominated by the variability of the O_2 oceanic flux [Gruber et al., 2001, Naegler et al., 2006, Battle et al., 2006, Nevison, 2008]. The location of the stations is an important factor as shown in the Taylor diagram (Figure 4.8, middle panel). We note that La Jolla, for example, has a lower correlation with the measurements than the other stations and the agreement in the amplitude is poorer as well. The high correlations for all the stations show that the models reproduce well the seasonal cycle.

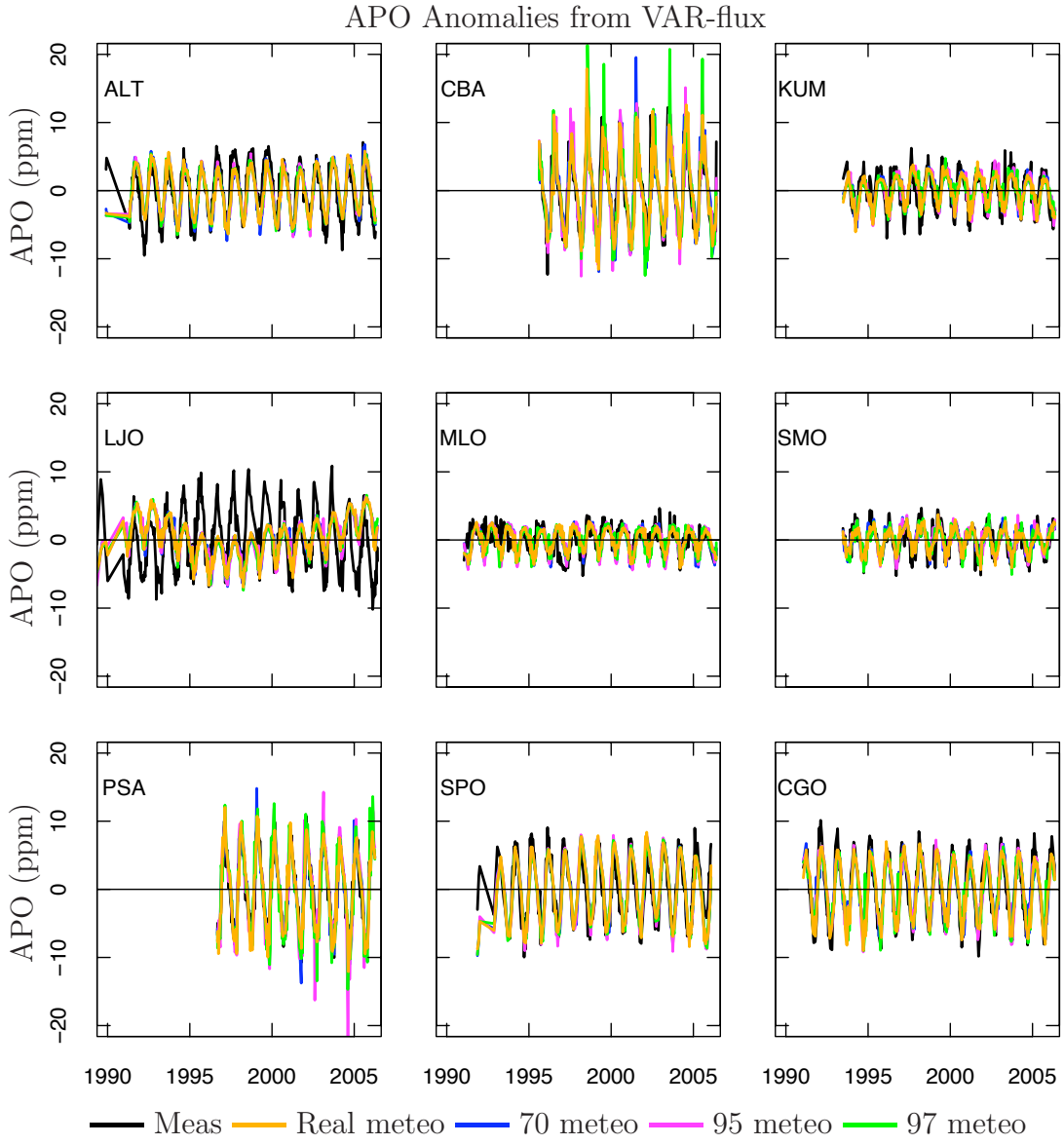

Figure 4.5— APO Anomalies resulting from the transport of VAR-flux with different meteorological fields. The stations are displayed in latitudinal bands from North to South.

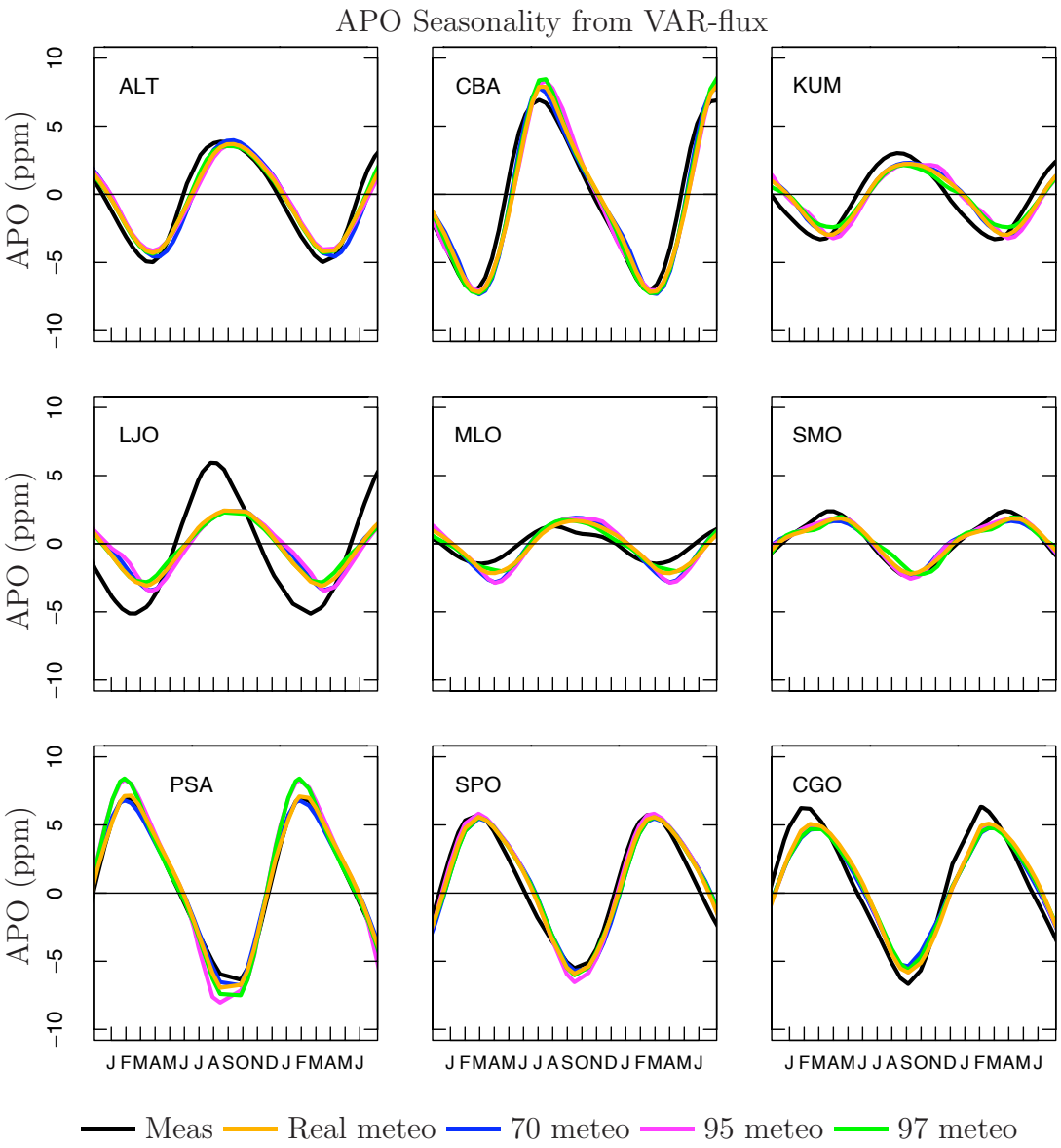

Figure 4.6— APO Seasonality resulting from the transport of VAR-flux with different meteorological fields. For a better visualization of the complete seasonal cycle, 18 months are plotted.

Interannual Variability

Measurements show a strong increase of APO concentration at the end of the 1990's and a strong decrease at the beginning of the 2000's for the stations in the Northern Hemisphere (ALT, CBA, LJO, MLO, KUM) (Figure 4.7). This phenomenon has been explained by Hamme (2008) as a result of a ventilation event. In this event first a decrease, then an increase of the winds in the Northern Hemisphere causes first an out-flux and then a sudden influx of APO. This event can indicate that the APO interannual variability is mostly driven by the oceanic fluxes.

The model results for IAV only partially agree with the observations. The amplitude of the event is underestimated, and for some stations entirely absent (Figure 4.7). The use of constant rather than variable meteorological fields does not influence the results. None of the runs seem to better represent the observed variability. These results indicate that the atmospheric transport contributes to the variability of the APO, but is likely not the main source of the variability. They also highlight the poor representation of the interannual variability by both ocean and transport models. These results are confirmed by the Taylor diagram in Figure 4.8, lower panel. The IAVs modeled for all the stations have low correlation with the measurements (-0.05 to 0.5), independent of the stations location. The amplitude of the IAV is also underestimated by about a factor of two.

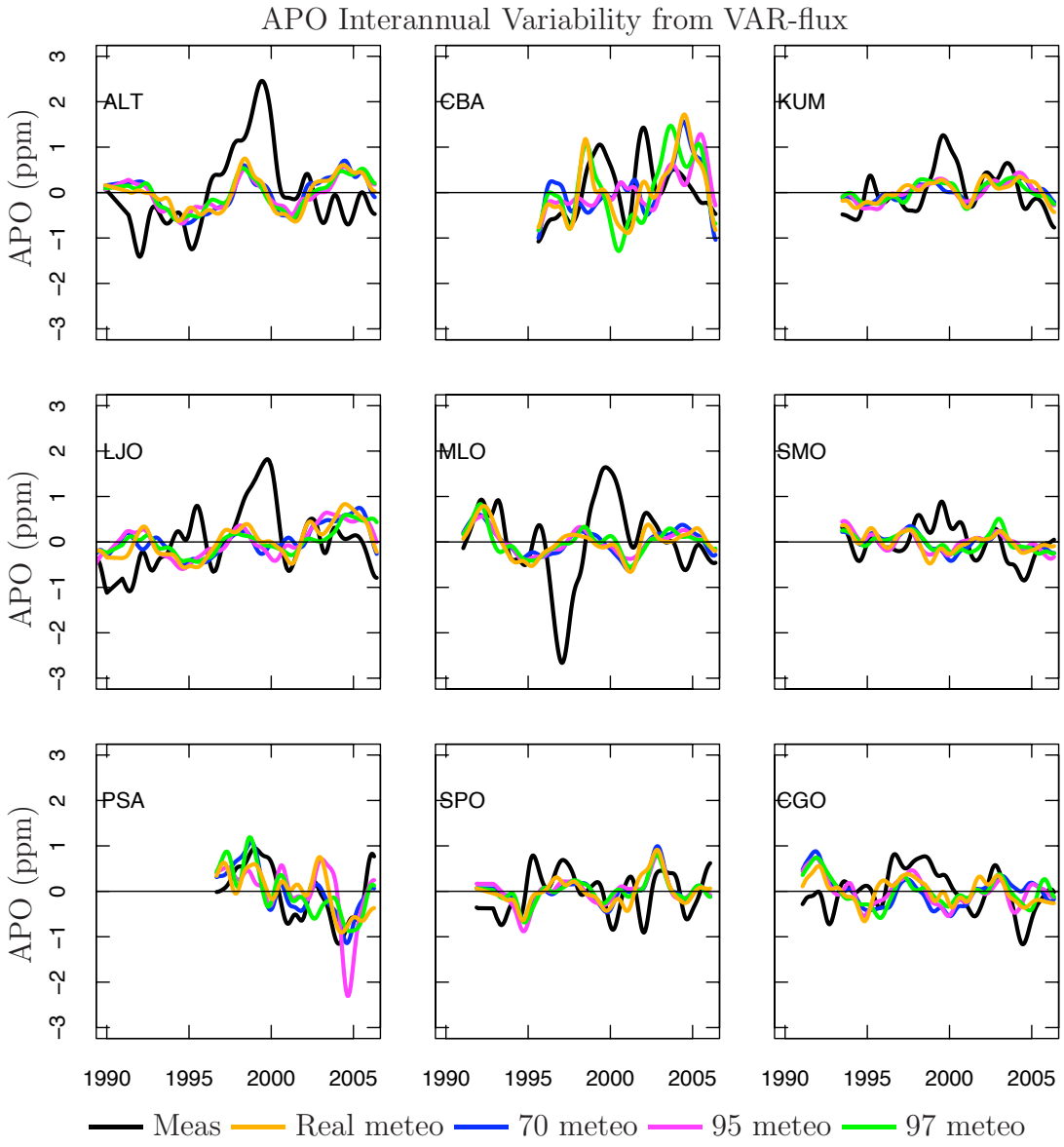

Figure 4.7— APO Interannual Variability resulting from the transport of VAR-flux with different meteorological fields.

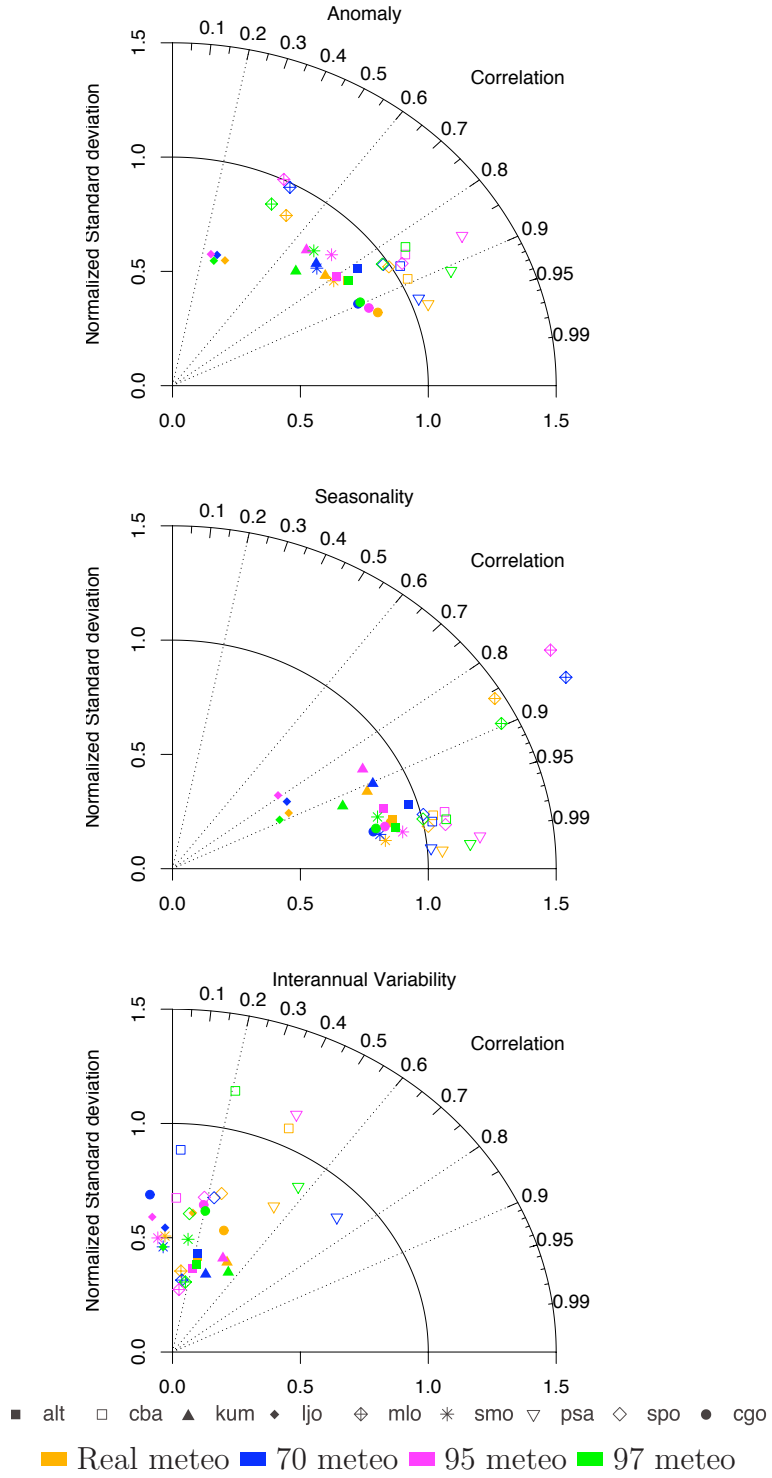

Figure 4.8—

Taylor diagrams for the anomalies, seasonality and IAV resulting from the transport of VAR-flux with different meteorological fields.

4.4.2 Modified fluxes

We transport into the atmosphere the modified fluxes generated as described above: the SEAS-flux, which has a constant seasonal cycle, but no interannual variability, and the LT-flux, which has neither seasonality nor interannual variability. This experiment aims to understand the role of the atmospheric transport in the APO variability. By the comparison of the results from the transport of constant fluxes with the ones from variable fluxes, we are able to infer the drivers of observed APO variability.

SEAS-flux: Anomaly, Seasonality, IAV

The transport of SEAS-flux allows us to identify the role of real or constant meteorological fields in the transport and its influence on the APO variability observed. The anomalies and the seasonal cycles resulting from the transport of SEAS-flux are very similar to the anomalies and the seasonality resulting from the transport of VAR-flux. The main feature present in both fluxes, VAR-flux and SEAS-flux, is the seasonal cycle, the only difference between the two fluxes is that in the latter flux the same seasonal cycle is repeated. The anomalies reflect mostly the variability of the transported flux and the use of real or constant meteorology does not influence the resulting variability (Figure 4.9 and Figure 4.10). For La Jolla, the same mismatch between model and observations is occurring.

The Taylor diagrams for these two cases (upper and middle panels of Figure 4.12) show good agreement with the observations for all the stations. The seasonality of La Jolla is well represented by the model in shape (high correlation), but the distance of the station from the observations shows the poor agreement in the amplitude. The position of Mauna Loa (high error) represents the known problem with the data of this station, as mentioned in section 4.3. The transported flux contains only the seasonal variability and therefore there is no year-to-year change from the transport of SEAS-flux (Figure 4.11). The only variability present is due to the driving winds, but the use of variable or constant winds do not affect much the results. The variability of two stations, Cold Bay and Palmer Station, seem to be driven

by the meteorology, but the low correlations observed in the Taylor diagram (Figure 4.12, bottom panel) do not confirm it.

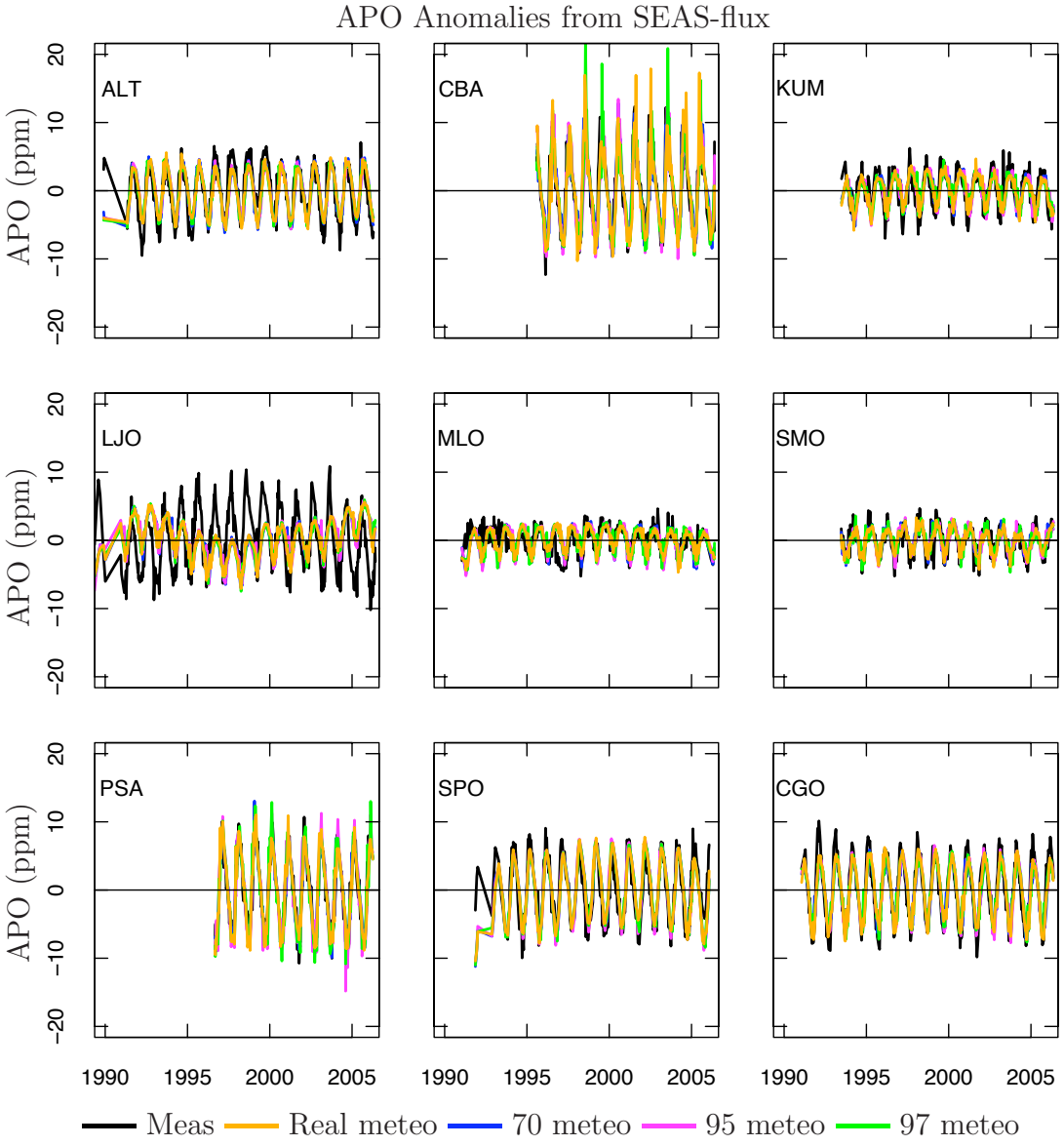

Figure 4.9— APO Anomalies resulting from the transport of SEAS-flux with different meteorological fields.

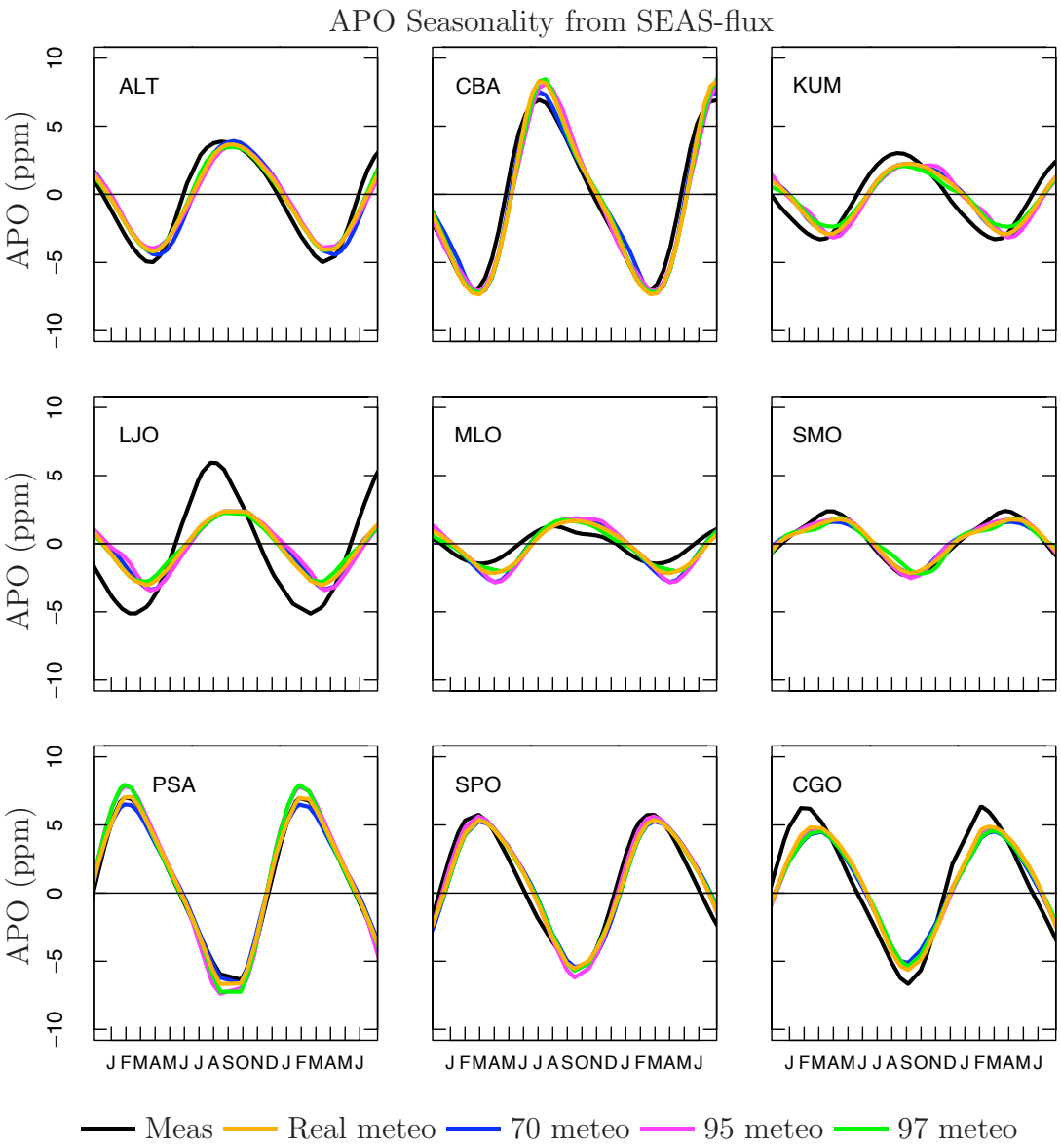

Figure 4.10— APO Seasonality resulting from the transport of SEAS-flux with different meteorological fields. For a better visualization of the complete seasonal cycle, 18 months are plotted.

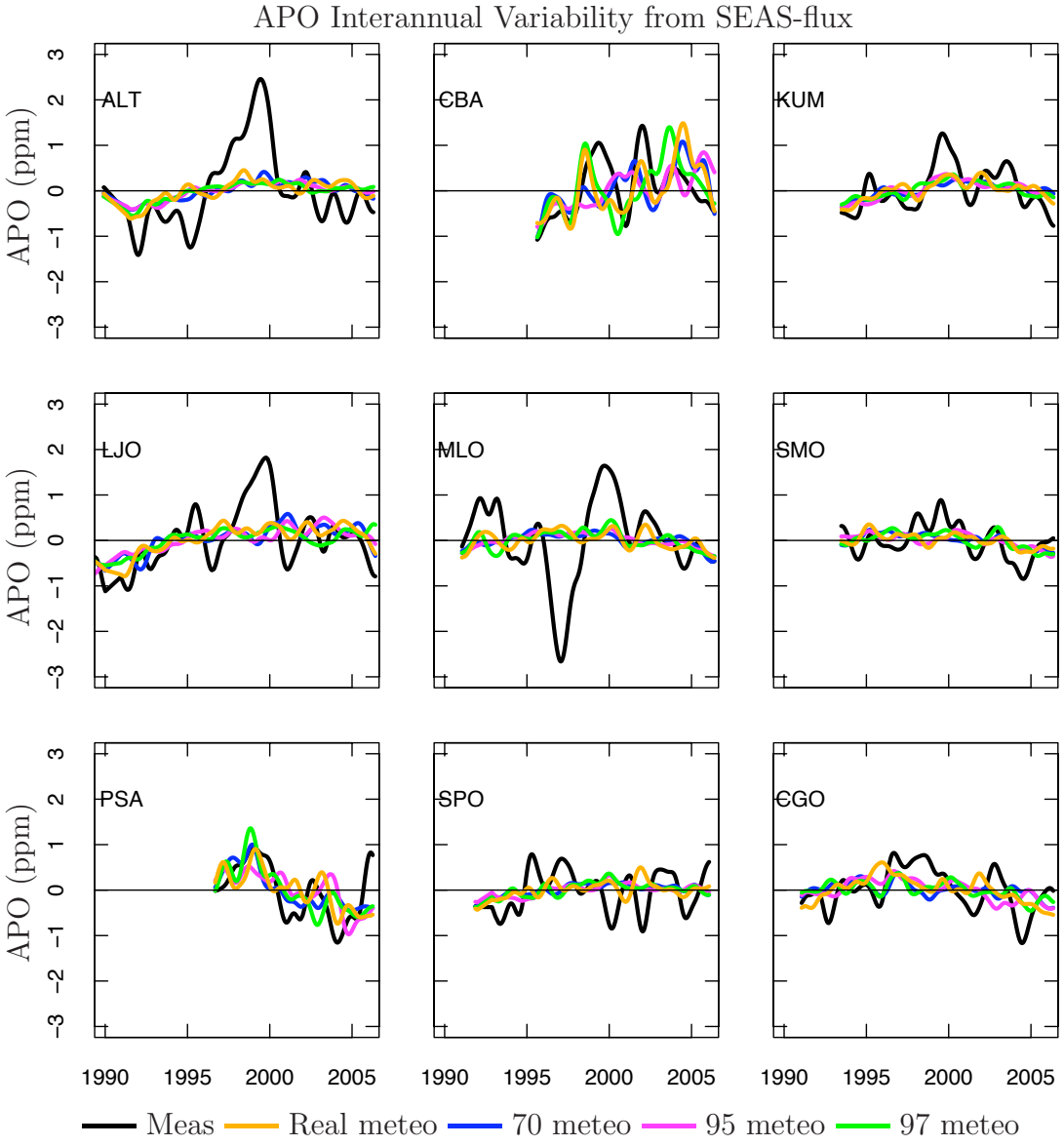

Figure 4.11— APO Interannual Variability resulting from the transport of SEAS-flux with different meteorological fields.

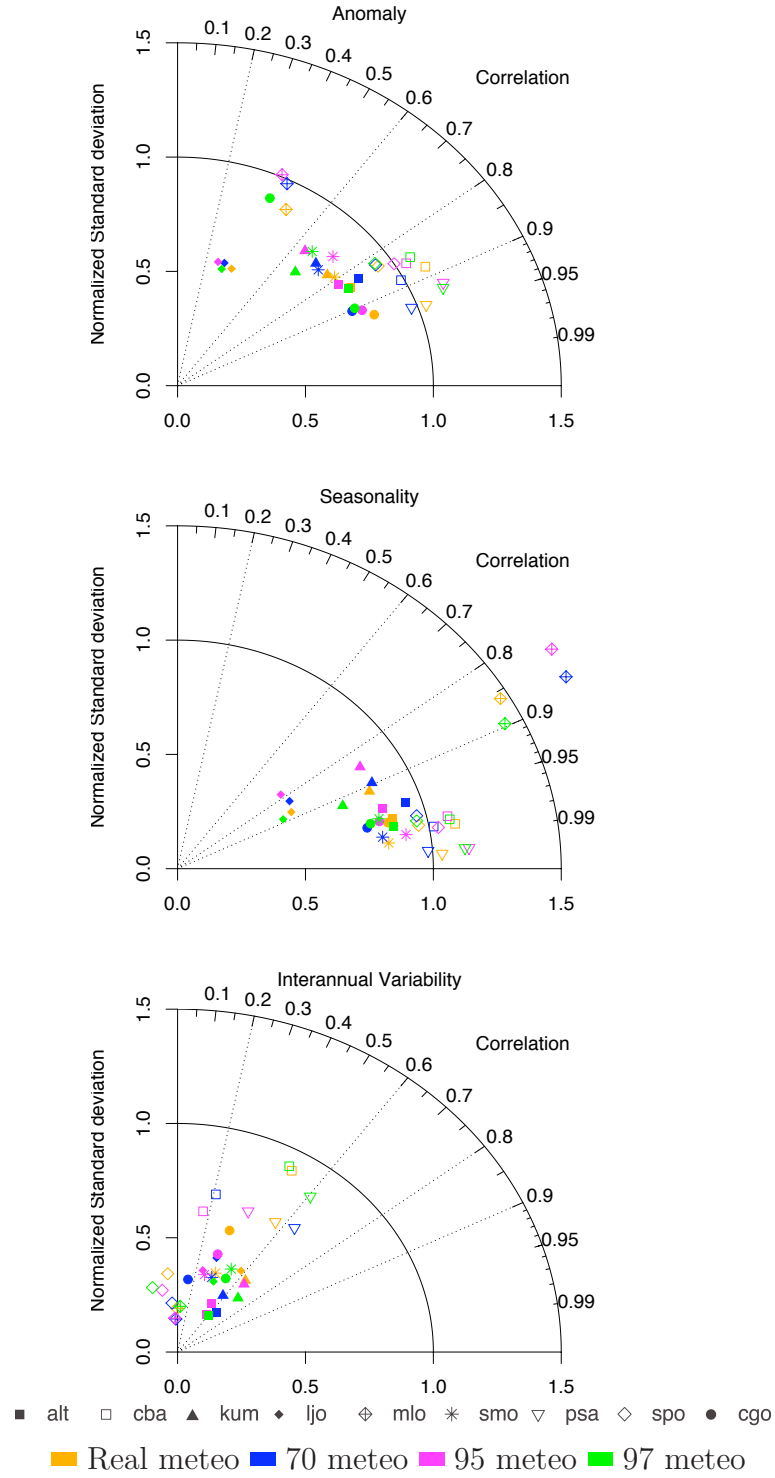

Figure 4.12—

Taylor diagrams for the anomalies, seasonality and interannual variability from the transport of SEAS-flux with different meteorological fields.

Long Term flux: Anomaly, Seasonality, IAV

The transport in the atmosphere of LT-flux gives information about the role of the atmospheric transport on the variability observed. The anomalies obtained from the transport of LT-flux show small interannual variability and no seasonal cycle, both for variable and constant meteorological fields (Figure 4.13). The small variability present in the anomalies is only due to the variability of the driving winds.

Figure 4.14 shows the seasonality resulting from the transport of LT-flux. For all the stations the seasonality is small or totally absent. Again, the small variability visible is only due to the seasonal variability of the driving meteorological fields. It is worth noting that for some stations the variability of the meteorological fields seems to create greater variability than for other stations in the model results. This effect is to be attributed to the locations of those particular stations, but in all cases it is small compared to the observed variability.

Figure 4.15 represents the APO interannual variability resulting from the transport of LT-flux. We observe a small year-to-year variability due to the variability of the meteorological fields. It is important to point out that the IAV resulting from the transport with variable meteorological fields (orange curve in Figure 4.15), shows larger variability than the IAV from transport with constant meteorological fields winds. This reflects the year to year variations of the real, variable meteorological fields. Nevertheless the variation in the concentration due to the use of variable meteorological fields is far too small with respect to the observed interannual variability to be considered the driver of such variability.

The Taylor diagrams for the anomalies, seasonality and interannual variability for the transport of LT-flux, show low correlations between the model results and the observations for all the stations for all three cases (Figure 4.16). This result highlights what was already pointed out from the time series: the variability in the flux influences the observed IAV, while the use of different meteorological fields is not the main driver even though they do

influence the APO IAV.

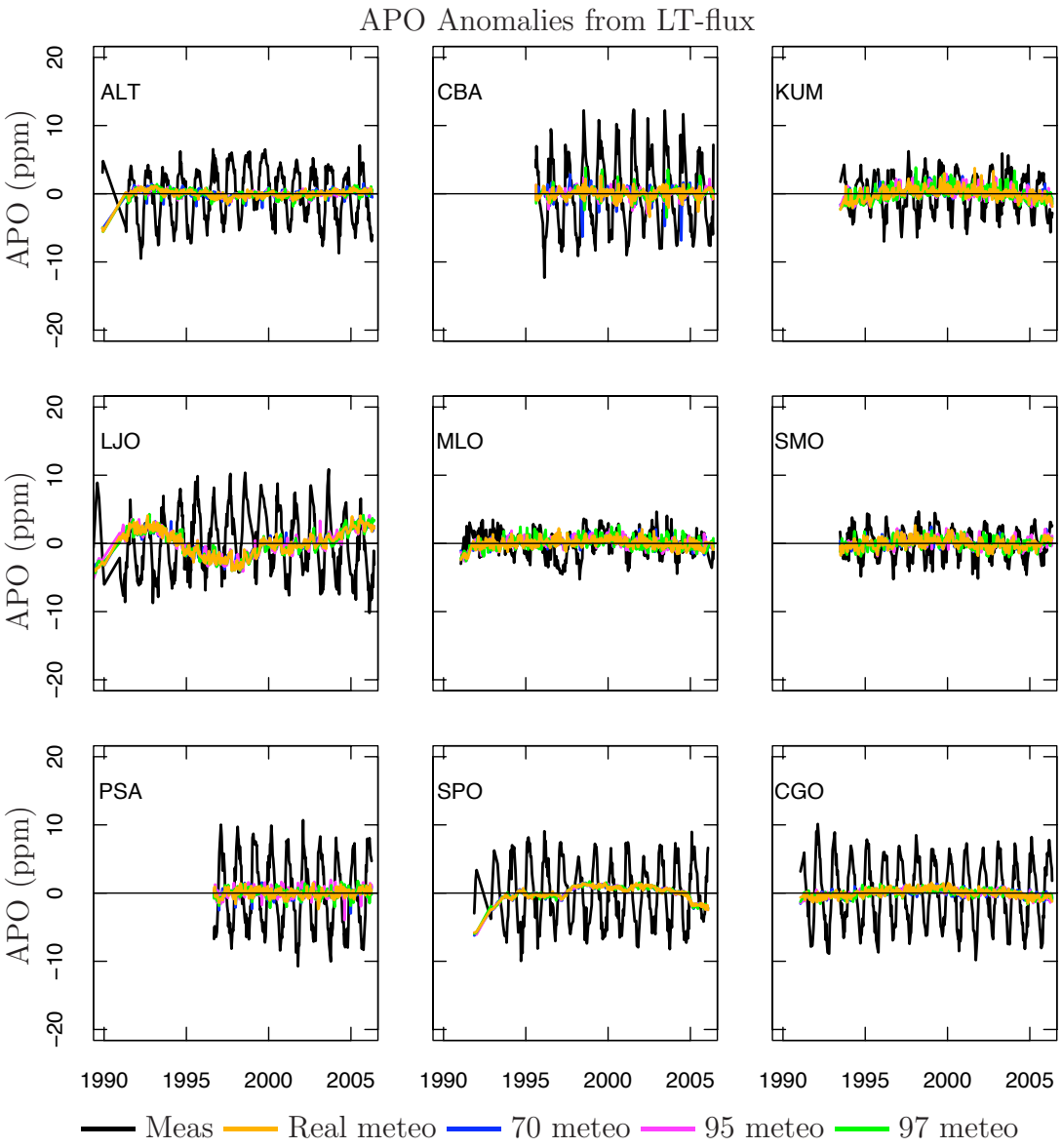

Figure 4.13— APO Anomalies from the transport of LT-flux with different meteorological fields.

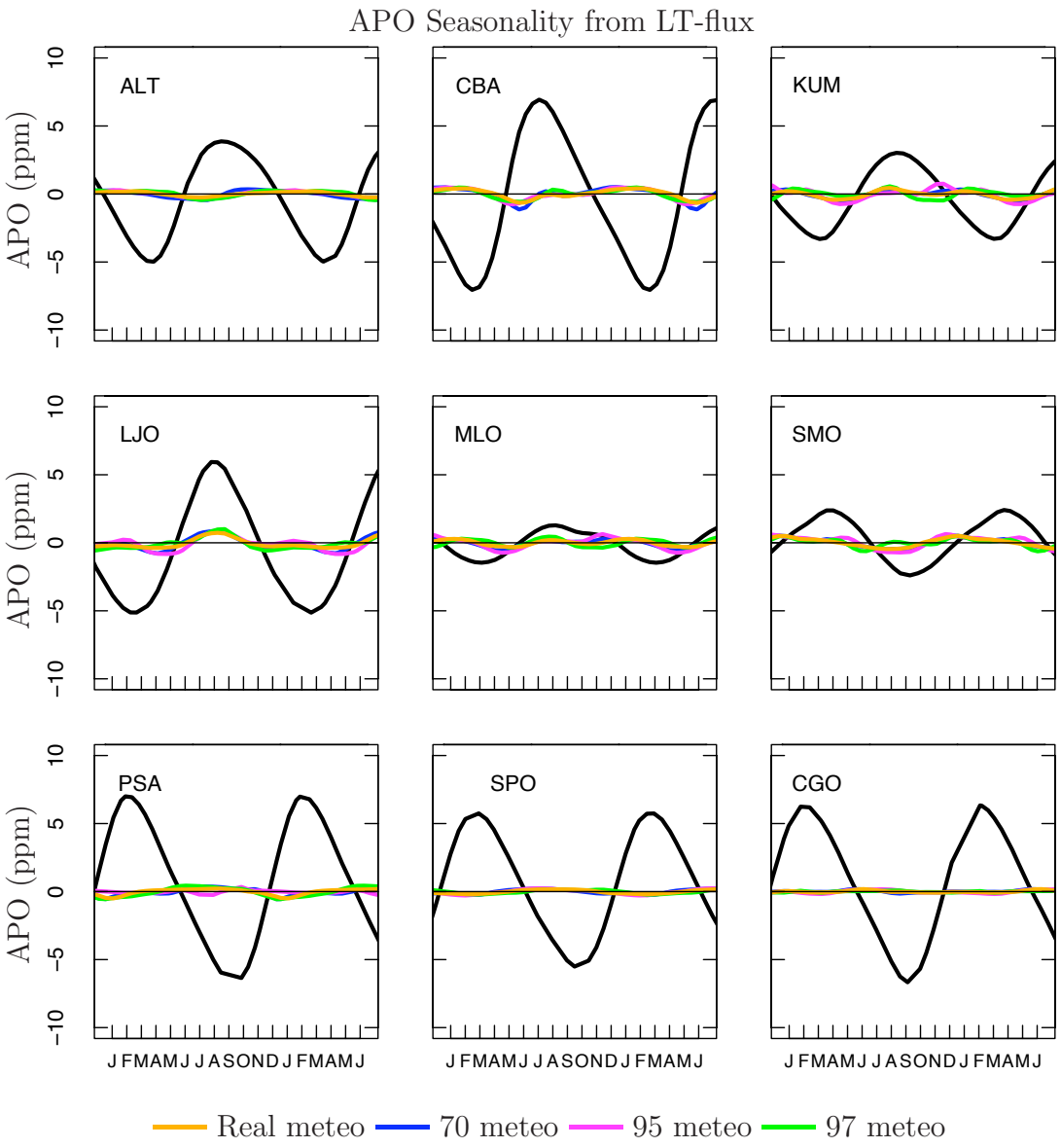

Figure 4.14— APO Seasonality resulting from the transport of LT-flux with different meteorological fields. For a better visualization of the complete seasonal cycle, 18 months are plotted.

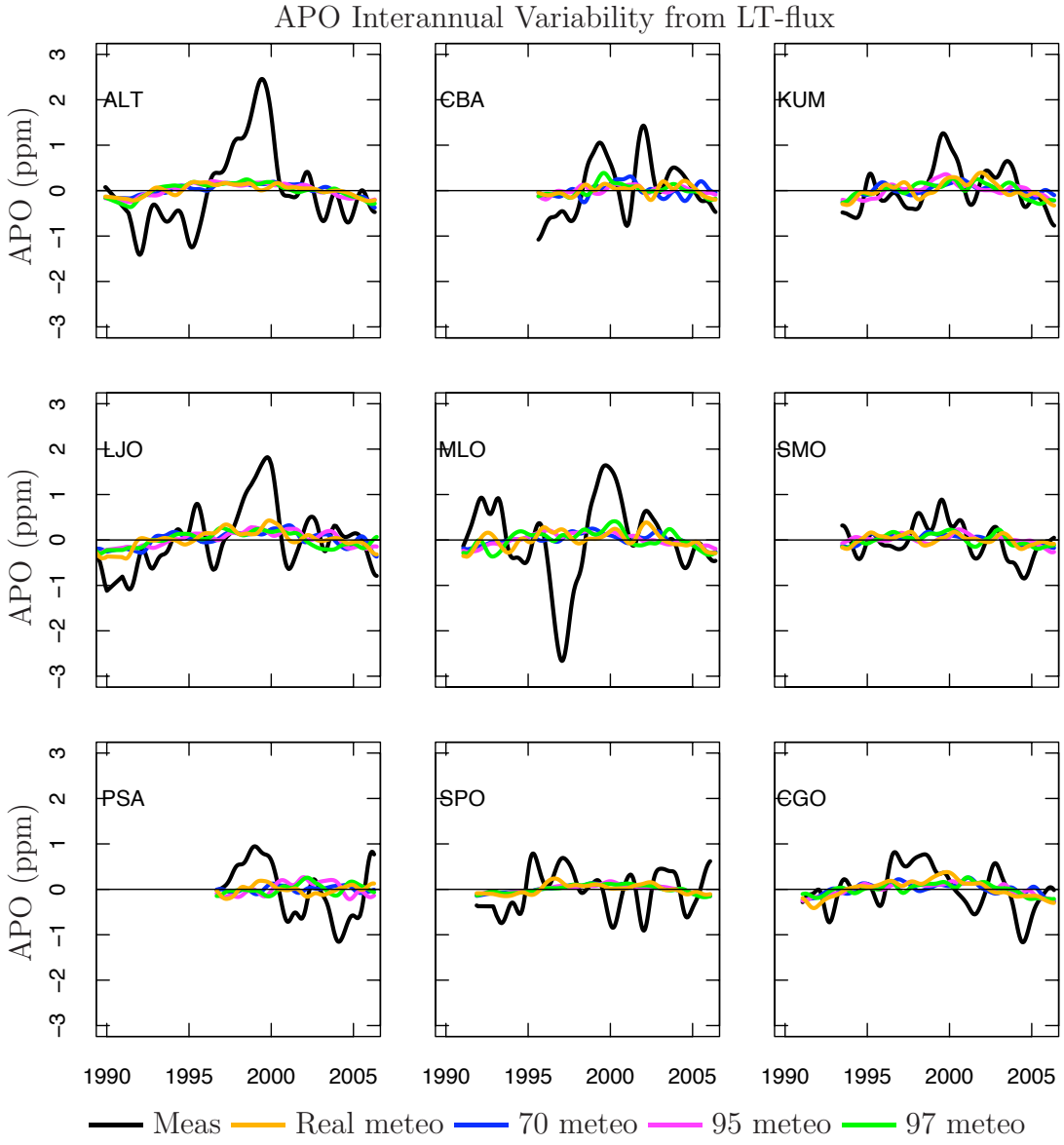

Figure 4.15— APO Interannual Variability resulting from the transport of LT-flux with different meteorological fields.

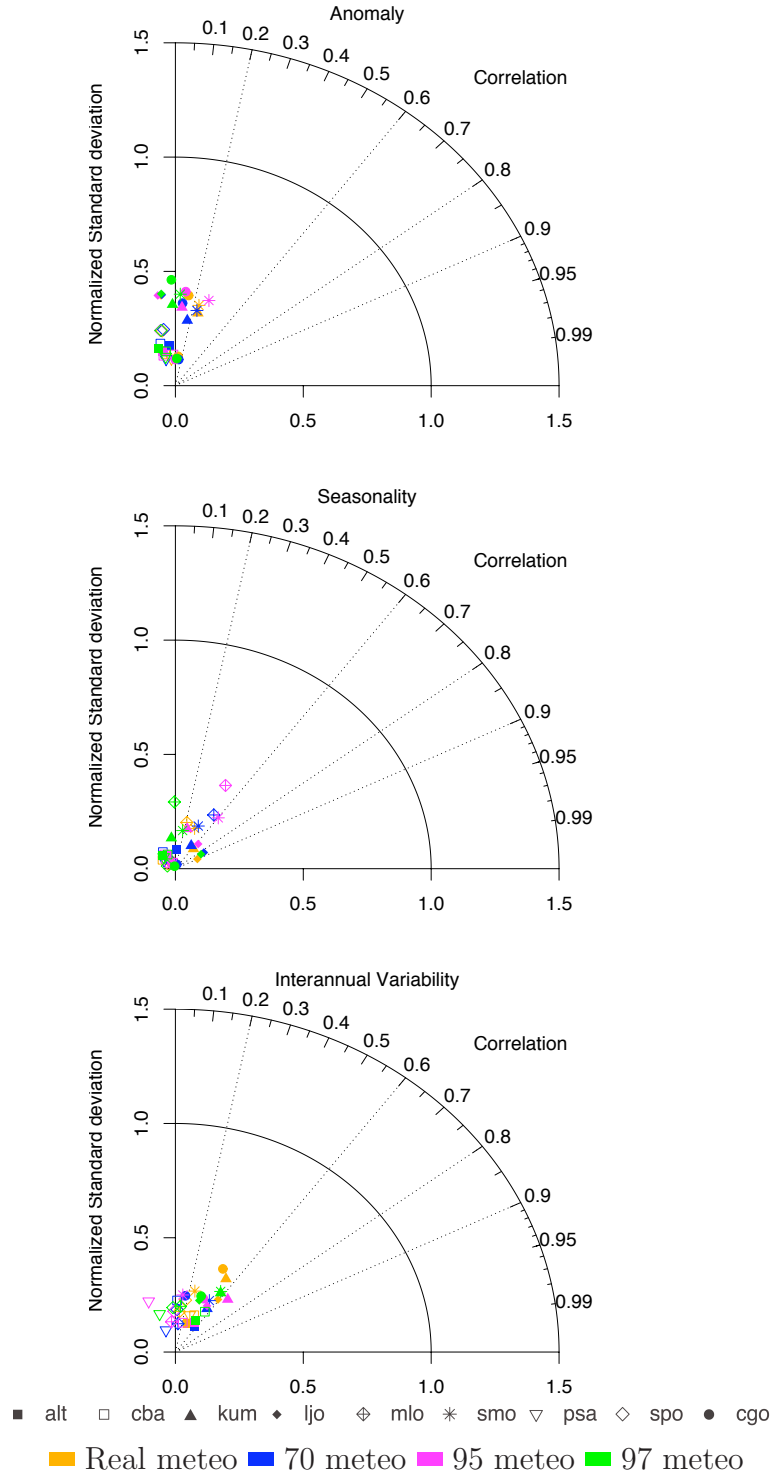

Figure 4.16—

Taylor diagrams for the anomalies, seasonality and interannual variability from the transport of LT-flux with different meteorological fields.

4.4.3 Comparison of Two Cases

From the results shown we have seen that the use of real or constant meteorological fields does not influence the APO seasonality and that the APO variability is mostly driven by the oceanic fluxes. However, to give strength to these results we compare the analyzed cases in one Taylor diagram. We compare the anomalies and the IAV for cases in which either the flux or the meteorological fields have limited temporal variability as summarized in Table 4.3. We will refer to the comparison of the anomalies as "Comparison 1" and to the comparison of the IAV as to "Comparison 2". By comparing the anomalies resulting from the transport of VAR-flux (fully

Table 4.3— Summary of the comparisons done

Fluxes	Meteo
	Comparison 1 (Anomaly)
VAR-flux	Real meteo
VAR-flux	1995 meteo
LT-flux	Real meteo
	Comparison 2 (IAV)
VAR-flux	Real meteo
VAR-flux	1995 meteo
SEAS-flux	Real meteo

variable flux) with LT-flux (flux without variability) we can identify whether the observed APO variability reflects the variability of the fluxes or the effect of the transport. By comparing the IAV from VAR-flux with the IAV from SEAS-flux (flux without interannual variability) we can identify the main drivers of the observed IAV. In both comparisons the VAR-flux is transported with variable and constant meteorological fields in order to highlight the role of variable meteorological fields in the transport.

In the Taylor diagram in Figure 4.17 the anomalies for Comparison 1 are shown. The correlations for the anomalies from the transport of VAR-flux vary from about 0.95 to 0.5 for both the variable (green symbols) and constant (blue symbols) winds. The dominant feature in VAR-flux is the seasonality, therefore, from the similarity of the anomalies from the transport of VAR-flux with constant and variable meteorological fields (blue and green symbols in Figure 4.17) we deduce that at a seasonal time scale the variability of the APO is driven by the variability of the oceanic fluxes. The use of variable or constant meteorological fields has only a small influence on the APO variability. This result is valid independently of the location of the stations. However, when VAR-flux is transported with variable meteorological fields, for all the stations, the agreement with the observations is slightly better than when the constant meteorological fields are used.

The variability contained in the transported fluxes is reflected in the anomalies of the APO. When the flux does not contain temporal variability, i.e. LT-flux, the corresponding anomalies contain only the variability due to the meteorological patterns. The good agreement between the model results and the observations at a seasonal time scale, gives strength to the validity of applying repeated constant meteorological fields for the transport of fluxes over long periods, for example in climate runs as done in Chapter 3 of this thesis. Moreover, it highlights the ability of the models to reproduce the observed seasonality.

From Comparison 2 (Figure 4.18) we want to identify the drivers of the interannual variability. The correlations between modeled results and measurements are low, for all the stations. This poor agreement of the modeled IAV with the observed IAV values reveals that the interannual variability we measure is due to the variability of the fluxes, as previously mentioned. Although the transport is important, it does not represent the principal driver. The correlations in the VAR-flux with real meteorology are generally higher (0.2 to 0.6) at high latitude stations (PSA, CBA, SPO, CGO) than at lower latitudinal stations (LJO, MLO). The lowest correlations between the model results and the measured value suggest that the modelled fluxes do not re-

produce well the interannual variability in the observed processes. For LJO, this could be because of the coastal nature of the station. The fact that the model correlates much better with KUM (r=0.35) than with MLO, two stations located at the same place but at different elevations, suggest that the atmospheric transport may be at fault. However, for MLO we have to consider the presence of known problems in the measurements, as mentioned before.

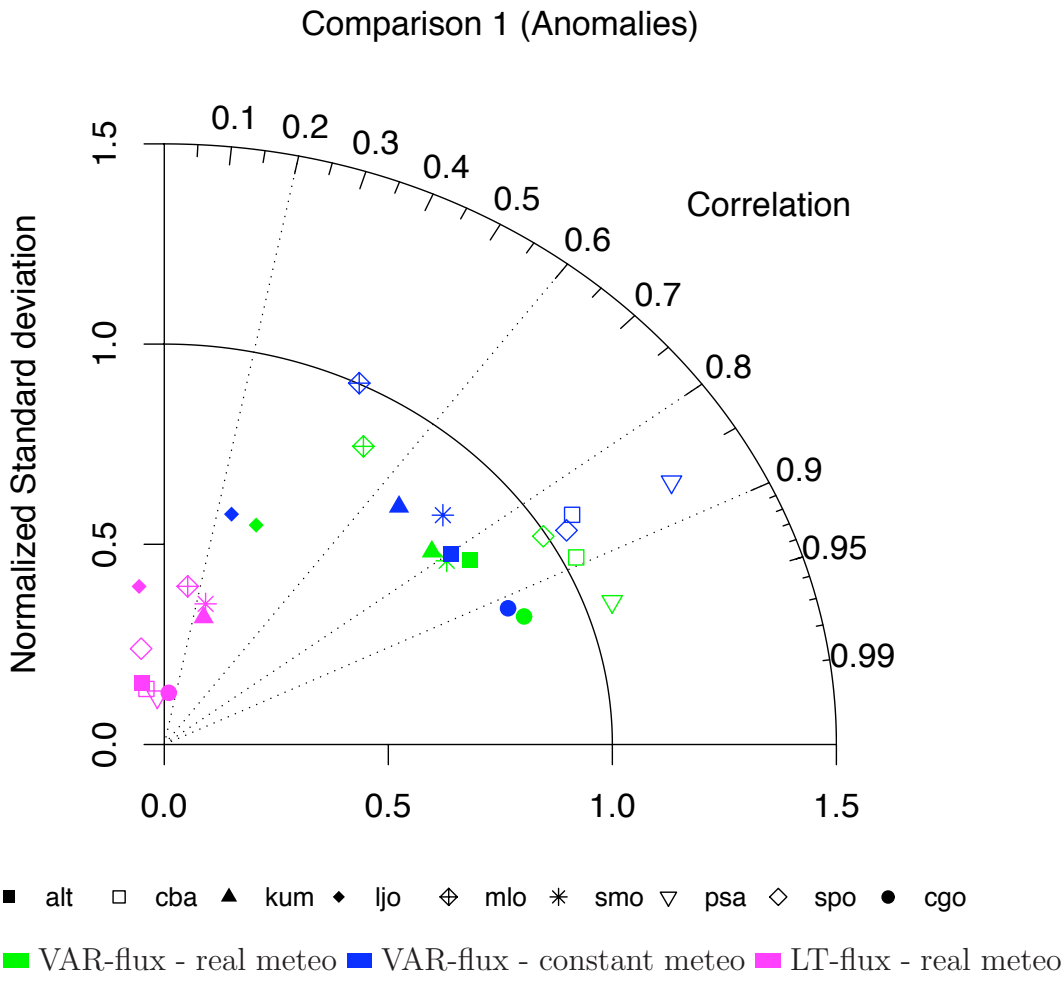

Figure 4.17— Taylor diagram summarising the comparison of the APO anomalies resulting from the transport of VAR-flux with variable and constant meteorology and APO anomalies resulting from the transport of LT-flux with real meteorological fields.

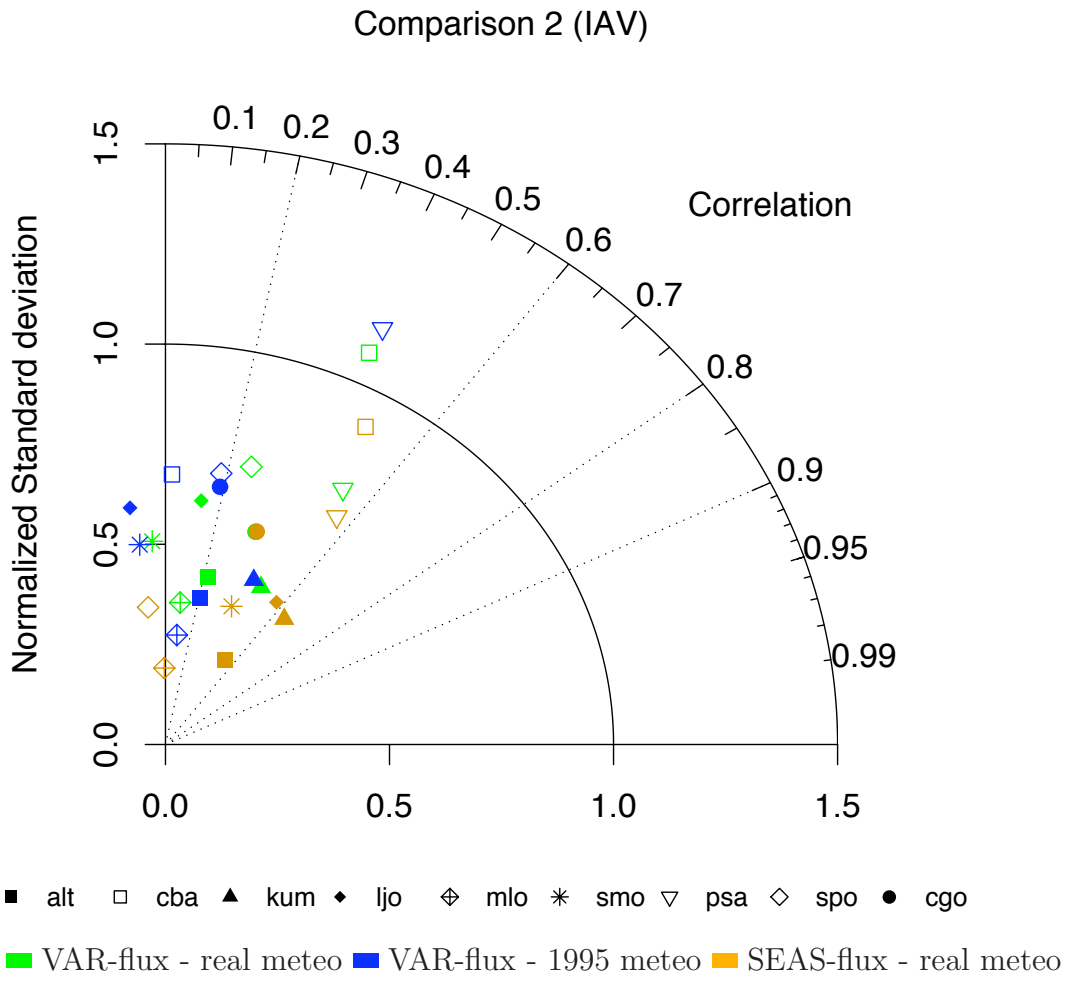

Figure 4.18— Taylor diagram summarising the comparison of the APO IAV resulting from the transport of VAR-flux with variable and constant meteorology and the APO IAV resulting from the transport of SEAS-flux with real meteorological fields.

4.5 Brief Comparison with Other Oceanic Fluxes

We present a brief study done with the fluxes from another ocean biogeochemical model that helps to reinforce our finding. A complete and detailed model comparison has not been possible due to the limited time period over which the oceanic fluxes from the second model are available. We apply the same approach used for the OPA-PISCES-T fluxes to the fluxes from the biogeochemical model based on the MITgcm (Massachusetts Institute of Technology global circulation model) [Marshall et al., 1997]. The resolution of the physical model is 1° longitude by a variable resolution from 0.3° to 1° in latitude. The biogeochemical model is forced with 10 days-average meteorological fields from the physical model which is forced with 12 hourly winds and heat and freshwater fluxes from NCEP reanalysis [McKinley et al., 2002, McKinley, 2003].

The available oceanic fluxes from the MIT model go only from 1990 to 1998. We apply the same filters as for the OPA-PISCES-T fluxes to obtain three fluxes with different temporal variability, here called VAR-flux-MIT, SEAS-flux-MIT and LT-flux-MIT (Figure 4.19). The fluxes are transported into the atmosphere with the TM3, using the same resolution as before, driven by variable and constant meteorological fields (same steps illustrated in Figure 4.2). We look at the anomalies, seasonality and interannual variability resulting from the three fluxes for three stations from the SIO network. The stations chosen for this study are the ones that have data within the period of the MIT fluxes and represent different latitudinal regions.

Despite the limited temporal availability of the MIT-fluxes, we can graphically check whether the concentrations obtained by the transport with different meteorologies confirm our previous results. We look at the anomalies (Figure 4.20), the seasonality (Figure 4.21), and the interannual variability (Figure 4.22), calculated using the same method and filters as for the OPA-PISCES-T run. In all the analyses the linear trend has been subtracted, both for the measurements and model results. To obtain seasonality and interannual variability both measurements and model results have been filtered. Because the

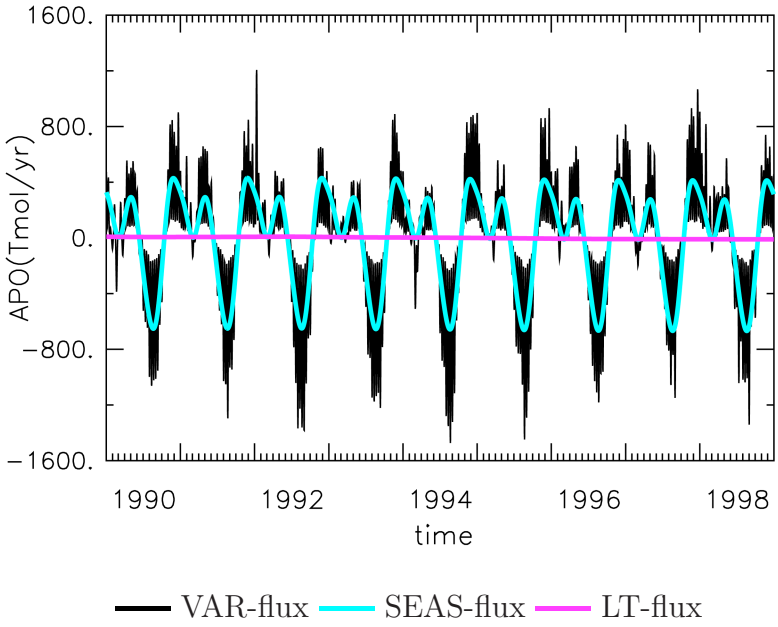

Figure 4.19— APO oceanic fluxes from the MIT model.

time-period of comparison is different, the variability in the measurements is slightly smaller than the variability estimated with the longer time period and compared to the OPA-PISCES-T results, even if the observations themselves are identical. In Figure 4.22 the IAVs of the measurements are shown both for the period 1990-1998 (full black line) and for the period 1990-2006 used to compare the OPA-PISCES-T results (dashed gray curve). The variability of the observations used to compare the MIT-fluxes (black line) appears damped due to the smaller period considered, but does not affect our comparison of the role of variable versus constant meteorology.

The concentration fields show the same patterns of their corresponding fluxes (Figure 4.20). As in the previous experiment the use of constant or variable meteorological fields does not influence much the seasonal variability of APO (Figure 4.21). The results confirm that the interannual variability of the APO is driven by the variability of the oceanic fluxes (Figure 4.22).

The similarity of these results based on fluxes from an independent biogeochemical model, with the other results, lend weight to the previous conclusions.

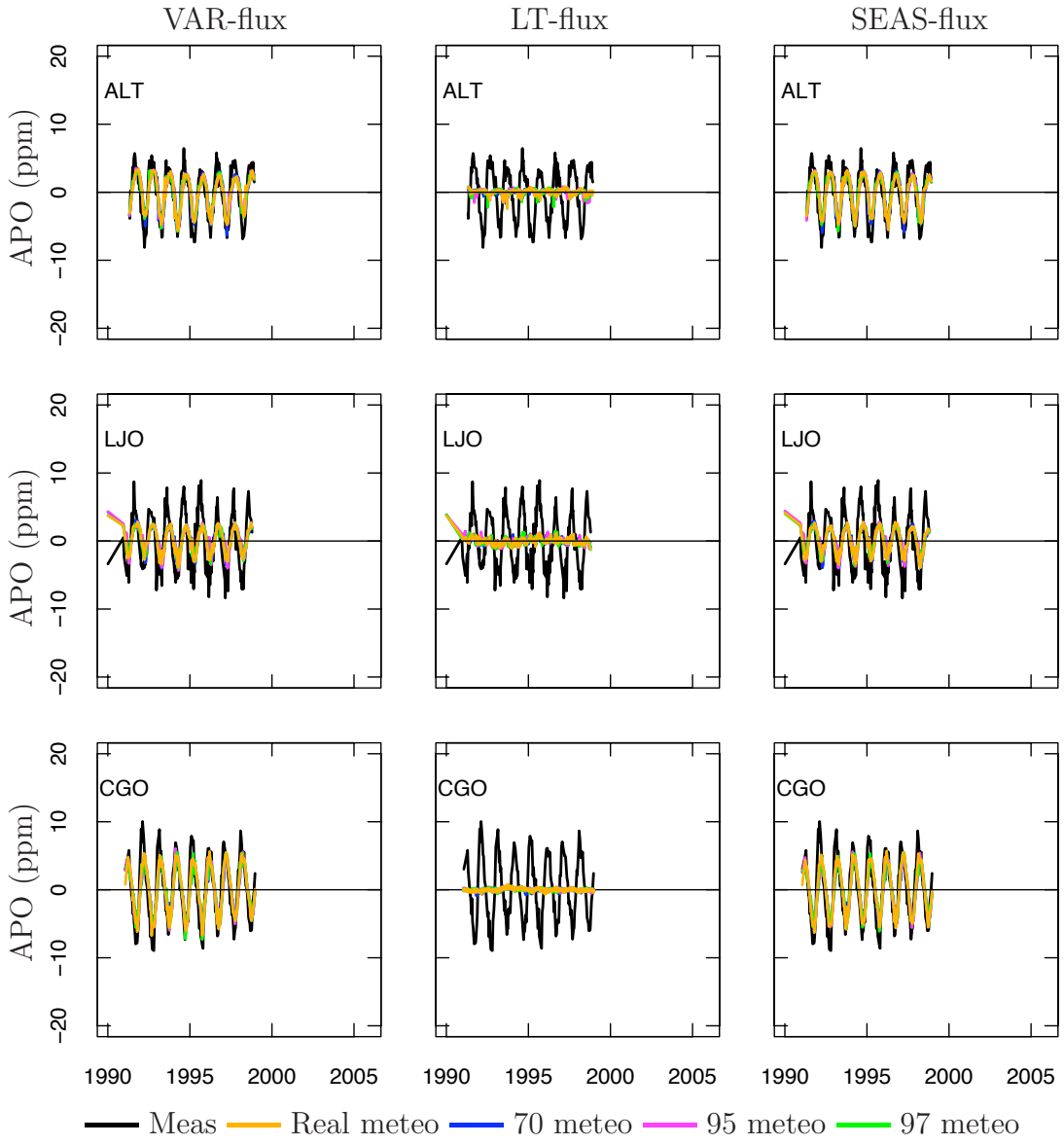

Figure 4.20— APO Anomalies resulting from the transport of the three MIT- fluxes with different meteorological fields. The stations are displayed in latitudinal bands.

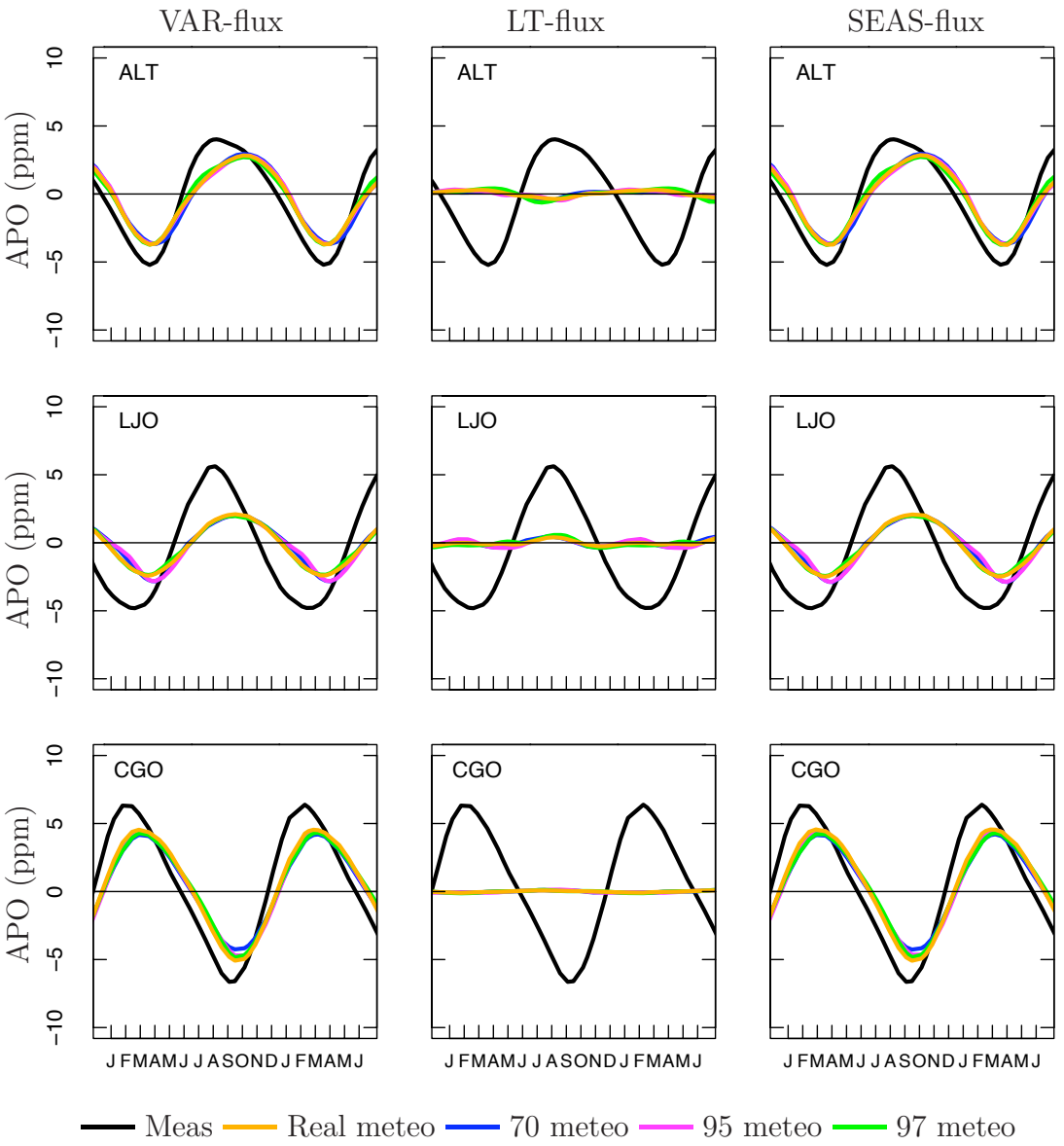

Figure 4.21— APO Seasonality resulting from the transport of the three MIT- fluxes with different meteorological fields. The stations are displayed in latitudinal bands. For a better visualization of the complete seasonal cycle, 18 months are plotted.

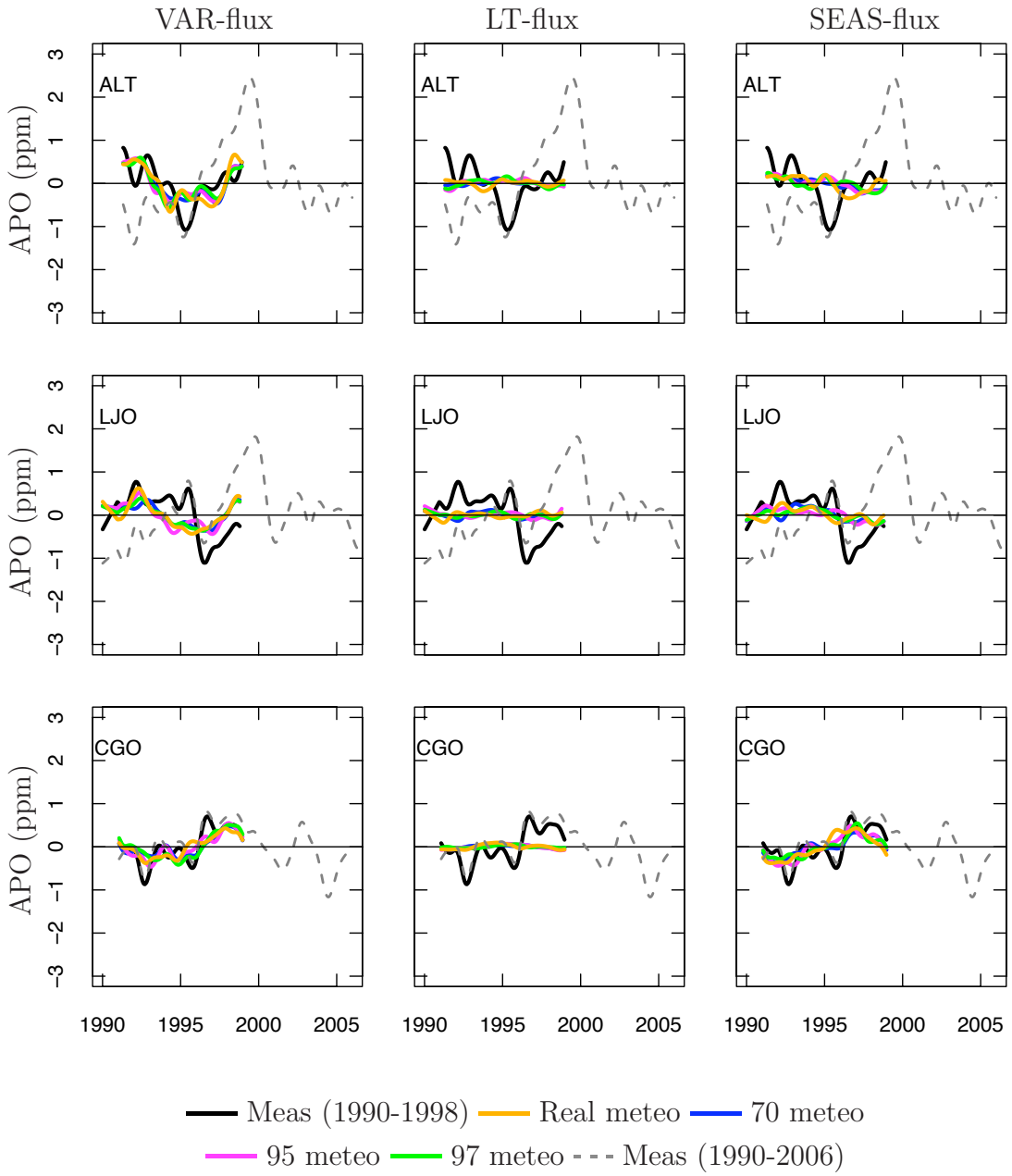

Figure 4.22— APO Interannual Variability from the transport of the three MIT-fluxes with different meteorological fields. The stations are displayed in latitudinal bands.

4.6 Conclusions

Ocean biogeochemical fluxes from a biogeochemical model have been transported into the atmosphere to investigate the possible drivers of the Atmospheric Potential Oxygen. We carry out a sensitivity analysis with a set of 12 experiments to understand the observed APO variability. Two possible processes can influence the APO variability: the oceanic fluxes and the atmospheric transport. We have modified the biogeochemical ocean fluxes generated by the OPA-PISCES-T model to create fluxes with limited temporal variability: one with only seasonal cycle (SEAS-flux) and one without any temporal variability (LT-flux). These fluxes together with with fully variable fluxes (VAR-flux) have been transported into the atmosphere with the TM3 model driven by variable and constant meteorological fields. From this study we reach the following conclusions:

- the use of variable meteorological fields does not improve the agreement of the model results with the measurements significantly at a seasonal time scale;
- the seasonality of the APO is driven by the variability of the oceanic fluxes;
- the interannual variability of APO reflects the variability of the oceanic flux; the atmospheric transport contributes partially to this variability, but it is not the main driver.

These results are important for several reasons:

- they confirm the validity of other studies, which based their results on the assumption that APO variability is driven by oceanic fluxes;
- they justify the use of constant meteorological fields in long term climate simulations, as we did in Chapter 3, since no significant improvements occur when the variable meteorological fields are used;
- they support other techniques, such as inverse modeling, which derive the biogeochemical fluxes starting from observed concentrations.

It is worth mentioning that there is a chance that the actual transport models do not properly represent the changes in the atmospheric transport from year to year. Should this be the case, the variability of the atmospheric tracer could be more influenced by the transport than is shown here. A comparison of several transport models would be useful in order to more specifically address this issue.

Chapter 5

Conclusions and Outlook

5.1 Main Conclusions

In the introduction to this thesis we highlighted a set of research questions. We conclude this thesis by briefly answering these questions while summarising the main conclusions of each chapters, and by giving an outlook on the possible future development of the results presented.

Detection of climate-induced changes in the ocean circulation from atmospheric O_2 and CO_2 measurements
The results of the climate model IPSL-CM4 used in this study show several changes in the ocean physics for the period 1861-2100 due to increasing atmospheric CO_2 concentration. Two different scenarios have been taken into account and compared: the first scenario, called CO_2-only, assumes that despite the atmospheric CO_2 increase there are no effects on the ocean circulation; the second scenario, called CO_2-climate, allows the oceans physical properties to change with increasing atmospheric CO_2. In particular, the model, for the CO_2-climate scenario, projects a reduction of the Atlantic Meridional Overturning Circulation (AMOC) by about 70% of its intensity, widespread stratification of the ocean, an increase of the Sea Surface Temperature by $\sim$2.4°C, and an increase of the heat flux entering the ocean from 1 to 5 W/m^2. These physical changes have, in turn, an impact on the biogeochemical fluxes. The model results project an O_2 out-flux from the ocean up to 80 Tmol/yr due to the combined effects of increasing temperature and a reduction of the ocean

circulation, and a reduction in the ocean CO_2 uptake capacity by up to 15% by the end of the simulation period. When no ocean physical changes occur (CO_2-only scenario), CO_2 is taken up by the oceans in response to increasing atmospheric CO_2, but the O_2 flux stays at constant levels for the whole simulation period. Thus changes in the ocean circulation do particularly affect the oceanic O_2 flux.

Do changes in the air-sea fluxes have an impact on atmospheric O_2 and CO_2 concentrations? Can we discern the respective contributions of O_2 and CO_2 to APO variability?

To explore the impact of changes in ocean circulation and biogeochemical fluxes on the atmospheric tracer concentrations due to the, the air-sea fluxes, for the two scenarios considered, have been transported into the atmosphere with the transport model TM3. To detect the signal of changes in the ocean physics in the atmosphere, the atmospheric O_2 and CO_2 concentrations have been combined to create the Atmospheric Potential Oxygen (APO=O_2 + 1.1CO_2), which removes the influence of the terrestrial biosphere and is influenced by the ocean only. The changes in atmospheric O_2, CO_2 and APO concentrations reflect the same tendency as the oceanic fluxes: an increase of O_2 coming from the ocean, a decrease of the CO_2 uptake capacity of the ocean, and a decrease of APO concentrations. The temporal contributions of O_2 and CO_2 to APO was discriminated by spectral analysis. On a seasonal time scale, O_2 dominates the APO signal, while on longer time scales, CO_2 dominates the APO signal.

With the projected large-scale changes in the ocean circulation, can a significant latitudinal gradient in the APO concentration be observed? Can we relate latitudinal gradient changes to changes in the ocean circulation?

The analysis of the APO interhemispheric gradient highlights the areas where the uptake and release of gases by the ocean occur: uptake of APO at high latitudes where the dense cold waters sink and absorb gas from the atmosphere, release of APO into the atmosphere at low latitudes, where the warm waters in contact with the atmosphere release gas. Changes in the ocean circulation should therefore be visible in the interhemispheric signal. Our results show that

changes in the APO interhemispheric gradient are too small to discriminate changes in the ocean circulation from atmospheric measurements. The small signal observed is likely due the fast mixing of the atmosphere.

With the projected large-scale changes in the ocean circulation, does the amplitude of the APO seasonal cycle change as well? Would we be able to detect such changes?

The simultaneous action of thermal, biological, and dynamic processes drive the air-sea exchanges of gases. Since on a seasonal time scale the APO is dominated by O_2, if the physical conditions of the ocean are altered, the seasonal air-sea exchanges will be altered as well, and the signal of changes in the ocean will be visible in the seasonal APO concentration. Thus one way to detect those changes is to look at the difference in the amplitude of the APO seasonal cycle. For the CO_2-climate scenario, the difference in amplitude of the APO seasonal cycle between the years 2080-2100 and 1990-2010 (taken as future minus present conditions) is in the range of 2 to 4 ppm. The areas that show greater changes in seasonality in the future are located mostly at latitudes where the AMOC is reduced and the Mixing Layer Depth has become shallower. There is no significant difference in the amplitude of the APO seasonal cycle if the oceanic properties do not change (CO_2-only scenario). Therefore we relate the seasonal variations in APO to changes in the ocean circulation. The magnitude of changes found is greater than the limit of the measurement precision and would therefore be detectable by atmospheric measurements. This study highlights that the density and frequency of the present observations are insufficient, and more measurements sites around the world would be desirable to improve the detectability of changes in ocean properties from atmospheric APO observations.

Drivers of the APO variability

The oceanic fluxes from the biogeochemical model PISCES-T have been used and modified by the application of temporal filters to obtain fluxes with different temporal characteristics. The analysis has focused on three kinds of fluxes: (a) fully variable fluxes as generated by the model, (b) fluxes whose only variability is a repeated seasonal cycle, and (c) constant fluxes. These fluxes have been transported into the atmosphere with the TM3 transport model. The transport model has been driven by four different meteorological fields: (1) meteorological fields that vary interannually according to the simulation period; (2) constant meteorological fields for the year 1970, (3) for the year 1995; (4) for the year 1997, repeated for the simulation period. We then have a sensitivity analysis composed of a set of 12 model experiments to detect drivers that can determine the APO variability as observed in the past decades. Our attention is focused on two possible main drivers: (1) the variability of the oceanic fluxes and (2) the variability in the atmospheric transport.

Is the temporal variability of oceanic fluxes reflected in the variability of the APO atmospheric concentration?
The temporal variations of the atmospheric concentrations can be examined by driving the oceanic fluxes into the atmosphere with constant and variable meteorological fields and looking at their detrended, seasonal and interannual concentrations for the nine selected stations. We find that, in general, the variability observed in the concentrations is related to the kind of flux used. When the fluxes transported do not contain variability, the corresponding atmospheric concentrations show only the variability due to the driving winds. The variability present in the meteorological fields does influence the concentration, but is not the main driver. This conclusion is valid for both the seasonal and the interannual variability. Nevertheless it is important to point out that the interannual variability is not well represented by the models, in particular for coastal stations.

How much of the observed APO variability is caused by variable meteorological fields?
The agreement between the model results and the observations at seasonal time scale is very good for all the stations considered. The greatest agreement between observations and model results exists when variable fluxes and real meteorological fields are used. To further explore this result we analyze the Taylor diagrams for all the cases considered. The correlations found between observations and model results (both detrended), when variable fluxes are transported, is between 0.95 and 0.6, with significance at 99%. Similar conclusions are reached when analysing the seasonal cycle for the variable fluxes with the Taylor diagram. Transporting the flux with no variability into the atmosphere, the correlations between model results and observations are very low and not significant for all the stations: if no temporal variability is present in the fluxes, the concentration fields simulated show a variability different from the real variability. Thus the use of variable meteorological fields or constant meteorological fields at a seasonal time scale does not influence the concentrations patterns, rather what shapes the concentrations is the variability of the fluxes. However over smaller time scales the local meteorological patterns could influence more significantly the APO variability.

5.2 Outlook

The agreement between model results and the measurements at different time scales confirms the effectiveness of APO to test climate models [Naegler et al., 2006]. However it is important to mention that it remains difficult to establish a strong relationship between the signal detected by the models and changes in the ocean circulation because of the sparsity of the measurements and of the convolution of different driving processes. The density and frequency of the observations are insufficient to detect the projected changes in APO in many areas of the world. It is therefore essential to increase the number and the spatial density of atmospheric observations. The results from Chapter 3 can be a starting point to carry out an optimization strategy to identify the best locations for new stations. More measurements and improvements in the measurement technique could reduce the uncertain-

ties and therefore increase the detectability of APO variations. A further step of this study would be to set up an experiment in which the transport model is driven by the meteorological fields as projected by the climate model. In this way the potential future changes in the atmospheric circulation would also be taken into account. Although this is a possible limitation of this study, results on interannual time scales suggest that most of the expected changes in APO would be due to changes in air-sea gas fluxes (Chapter 3).

The results of Chapter 4 although identify the APO drivers, they do not answer one pending question: Is the representation of the atmospheric transport by the transport model realistic? A comparison exercise using several oceanic fluxes transported by different transport models would be useful to answer this question.

Bibliography

[Alley et al., 2003] Alley, R., Marotzke, J., Nordhaus, W., and Overpeck, J. (2003). Abrupt climate change. *Science*, 299(5615):2005–2010.

[Aumont and Bopp, 2006] Aumont, O. and Bopp, L. (2006). Globalizing results from ocean in situ iron fertilization studies. *Global Biogeochem. Cycles*, 20(2):2017.

[Aumont et al., 2003] Aumont, O., Maier-Reimer, E., Blain, S., and Monfray, P. (2003). An ecosystem model of the global ocean including fe, si, p colimitations. *Global Biogeochem. Cycles*, 17(2):1060.

[Baehr et al., 2008] Baehr, J., Keller, K., and Marotzke, J. (2008). Detecting potential changes in the meridional overturning circulation at 26N in the Atlantic. *Climatic Change*, 91(1):11–27.

[Balkanski et al., 1999] Balkanski, Y., Monfray, P., Battle, M., and Heimann, M. (1999). Ocean primary production derived from satellite data: An evaluation with atmospheric oxygen measurements. *Global Biogeochem. Cycles*, 13(2):257–271.

[Battle et al., 2000] Battle, M., Bender, M., Tans, P., White, J., Ellis, J., Conway, T., and Francey, R. (2000). Global carbon sinks and their variability inferred from atmospheric O_2 and $\delta^{13}C$. *Science*, 287(5462):2467–2470.

[Battle et al., 2006] Battle, M., Fletcher, S. M., Bender, M. L., Keeling, R. F., Manning, A. C., Gruber, N., Tans, P. P., Hendricks, M. B., Ho, D. T., Simonds, C., Mika, R., and Paplawsky, B. (2006). Atmospheric potential oxygen: New observations and their implications for some atmospheric and oceanic models. *Global Biogeochem. Cycles*, 20(1):GB1010.

[Bender and Battle, 1999] Bender, M. and Battle, M. (1999). Carbon cycle studies based on the distribution of O_2 in air. *Tellus B*, 51B:165–169.

[Bender et al., 2005] Bender, M., Ho, D., Hendricks, M., Mika, R., Battle, M., Tans, P., Conway, T., Sturtevant, B., and Cassar, N. (2005). Atmospheric O_2/N_2 changes, 1993-2002: Implications for the partitioning of fossil fuel CO_2 sequestration. *Global Biogeochem. Cycles*, 19(4):GB4017.

[Bindoff et al., 2007] Bindoff, N. L., Willebrand, J., Artale, V., Cazenave, A., Gregory, J., Gulev, S., Hanawa, K., Le Quéré, C., Levitus, S., Nojiri, Y., C.K. Shum, L. T., and Unnikrishna, A. (2007). Observations: oceanic climate and sea level - Chapter 5 In The Physical Science Basis. Contribution of Working group 1 to the Fourth Assessment Report of the Intergovernmental Panel on Climate Change. *Fourth Assessment Report of the Intergovernmental Panel on Climate Change*. Cambridge University Press.

[Bopp et al., 2005] Bopp, L., Aumont, O., Cadule, P., Alvain, S., and Gehlen, M. (2005). Response of diatoms distribution to global warming and potential implications: A global model study. *Geophys Res Lett*, 32(19):L19606.

[Bopp et al., 2003] Bopp, L., Kohfeld, K., Le Quéré, C., and Aumont, O. (2003). Dust impact on marine biota and atmospheric CO_2 during glacial periods. *Paleoceanography*, 18(2):1046.

[Bopp et al., 2002] Bopp, L., Le Quéré, C., Heimann, M., Manning, A., and Monfray, P. (2002). Climate-induced oceanic oxygen fluxes: Implications for the contemporary carbon budget. *Global Biogeochem. Cycles*, 16(2):GB1022.

[Broecker, 1997] Broecker, W. (1997). Thermohaline circulation, the achilles heel of our climate system: Will man-made CO_2 upset the current balance? *Science*, 278(5343):1582–1588.

[Bryden et al., 2009] Bryden, H. L., Mujahid, A., Cunningham, S. A., and Kanzow, T. (2009). Adjustment of the basin-scale circulation at 26 deg n to variations in gulf stream, deep western boundary current and ekman transports as observed by the rapid array. *Ocean Science*, 5(4):421–433.

[Buitenhuis et al., 2006] Buitenhuis, E., Le Quéré, C., Aumont, O., Beaugrand, G., Bunker, A., Hirst, A., Ikeda, T., O'Brien, T., Piontkovski, S., and Straile, D. (2006). Biogeochemical fluxes through mesozooplankton. *Global Biogeochem. Cycles*, 20(2):GB2003.

[Canadell et al., 2007] Canadell, J. G., Le Quéré, C., Raupach, M. R., Field, C. B., Buitenhuis, E. T., Ciais, P., Conway, T. J., Gillett, N. P., Houghton, R. A., and Marland, G. (2007). Contributions to accelerating atmospheric CO_2 growth from economic activity, carbon intensity, and efficiency of natural sinks. *P Natl Acad Sci Usa*, 104(47):18866–18870.

[Clark et al., 2002] Clark, P., Pisias, N., Stocker, T., and Weaver, A. (2002). The role of the thermohaline circulation in abrupt climate change. *Nature*, 415(6874):863–869.

[Clement and Peterson, 2008] Clement, A. C. and Peterson, L. C. (2008). Mechanisms of abrupt climate change of the last glacial period. *Rev Geophys*, 46(4):RG4002.

[Colling, 2004] Colling, A. B. (2004). Ocean Circulation. The Open University. Volume 3.

[Cotrim Da Cunha et al., 2007] Cotrim Da Cunha, L., Buitenhuis, E. T., Le Quéré, C., Giraud, X., and Ludwig, W. (2007). Potential impact of changes in river nutrient supply on global ocean biogeochemistry. *Global Biogeochem. Cycles*, 21(4):GB4007.

[Cunningham et al., 2007] Cunningham, S. A., Kanzow, T., Rayner, D., Baringer, M. O., Johns, W. E., Marotzke, J., Longworth, H. R., Grant, E. M., Hirschi, J. J. M., Beal, L. M., Meinen, C. S., and Bryden, H. L. (2007). Temporal variability of the atlantic meridional overturning circulation at 26.5 degrees n. *Science*, 317(5840):935–938.

[Dargaville et al., 2003] Dargaville, R., Doney, S., and Fung, I. (2003). Interannual variability in the interhemispheric atmospheric CO_2 gradient: contributions from transport and the seasonal rectifier. *Tellus B*, 55(2):711–722.

[De Boyer Montégut, 2004] De Boyer Montégut, C. (2004). Mixed layer depth over the global ocean: An examination of profile data and a profile-based climatology. *J. Geophys. Res.*, 109(C12):C12003.

[Denman et al., 2007] Denman, K. L., G., B., A., C., P., C., P.M., C., Dickinson, R.E., Hauglustaine, Heinze, D., C., E., H., D., J., U., L., S., R., da Silva P.L., S.C., W., and Zhang, X. (2007). Coupling between changes in the climate system and biogeochemistry - Chapter 7. In The Physical Science Basis. Contribution of Working group 1 to the Fourth Assessment Report of the Intergovernmental Panel on Climate Change. *Fourth Assessment Report of the Intergovernmental Panel on Climate Change*. Cambridge University Press.

[Denton and Hendy, 1994] Denton, G. H. and Hendy, C. H. (1994). Younger Dryas Age Advance of Franz Josef Glacier in the Southern Alps of New Zealand. *Science*, 264(5164):1434–1437.

[EDGAR, 2006] EDGAR, D. E. (2006). Edgar 3.2 database emissions: http://www.mnp.nl/edgar/index/.

[Fichefet and Maqueda,] Fichefet, T. and Maqueda, M. A. M. Sensitivity of a global sea ice model to the treatment of ice thermodynamics and dynamics. *J. Geophys. Res.*, 102:12609–12646.

[Flower and Kennett, 1994] Flower, B. and Kennett, J. (1994). The middle miocene climatic transition - east antarctic ice-sheet development, deep-ocean circulation and global carbon cycling. *Palaeogeogr Palaeocl*, 108(3-4):537–555.

[Friedlingstein et al., 2006] Friedlingstein, P., Cox, P., Betts, R., and et al., L. B. (2006). Climate–carbon cycle feedback analysis: Results from the c4mip model intercomparison. *J Climate*, 19:3337–3353.

[Garcia and Keeling, 2001] Garcia, H. and Keeling, R. (2001). On the global oxygen anomaly and air-sea flux. *J Geophys Res-Oceans*, 106(C12):31155–31166.

[Gaspar et al., 1990] Gaspar, P., Yves, G., and Jean-Michel, L. (1990). A simple eddy kinetic energy model for simulations of the oceanic vertical mixing: Tests at station papa and long-term upper ocean study site. *Journal Geophysical Research - Oceans*, 95(C9):16179–16193.

[Greenblatt and Sarmiento, 2004] Greenblatt, G. B. and Sarmiento, J. (2004). *The Global Carbon Cycle: integrating humans, climate and the natural world. Chapter 13*, volume 62 of *Scope*. Island Press.

[Gregory, 2004] Gregory, J. M. (2004). Simulated and observed decadal variability in ocean heat content. *Geophys Res Lett*, 31(15):L15312.

[Gruber et al., 2001] Gruber, N., Gloor, M., Fan, S., and Sarmiento, J. (2001). Air-sea flux of oxygen estimated from bulk data: Implications for the marine and atmospheric oxygen cycles. *Global Biogeochem. Cycles*, 15(4):783–803.

[Gruber et al., 2009] Gruber, N., Gloor, M., Fletcher, S. E. M., Doney, S. C., Dutkiewicz, S., Follows, M. J., Gerber, M., Jacobson, A. R., Joos, F., Lindsay, K., Menemenlis, D., Mouchet, A., Müller, S. A., Sarmiento, J. L., and Takahashi, T. (2009). Oceanic sources, sinks, and transport of atmospheric CO_2. *Global Biogeochem. Cycles*, 23(1):GB1005.

[Gruber and Keeling, 2001] Gruber, N. and Keeling, C. (2001). An improved estimate of the isotopic air-sea disequilibrium of CO_2: Implications for the oceanic uptake of anthropogenic CO_2. *Geophys Res Lett*, 28(3):555–558.

[Haag and Kaupenjohann, 2000] Haag, D. and Kaupenjohann, M. (2000). Ibiogeochemical models in the environmental sciences. the dynamical system paradigm and the role of simulation modeling. *Internatioal Journal of Philosophy of Chemistry*, 6(2):117 – 142.

[Hamme and Keeling, 2008] Hamme, R. C. and Keeling, R. F. (2008). Ocean ventilation as a driver of interannual variability in atmospheric potential oxygen. *Tellus B*, 60(5):706–717.

[Harris, 1978] Harris, F. (1978). On the use of windows for harmonic analysis with the discrete fourier transform. *Proceedings of the IEEE*, 66(1):51–83.

[Heimann and Körner, 2003] Heimann, M. and Körner, S. (2003). *The Global Atmospheric Transport Model TM3: Model Description and User Manual*.

[Hourdin et al., 2006] Hourdin, F., Musat, I., Bony, S., Braconnot, P., Codron, F., Dufresne, J.-L., Fairhead, L., Filiberti, M.-A., Friedlingstein, P., Grandpeix, J.-Y., Krinner, G., Levan, P., Li, Z.-X., and Lott, F. (2006). The lmdz4 general circulation model: climate performance and sensitivity to parametrized physics with emphasis on tropical convection. *Climate Dynamics*, 27(7-8):787–813.

[IPCC, 2007] IPCC (2007). *Intergovernamental Panel on Climate Change. Fourth Assessment Report: Climate Change 2007: Working Group I Report: The Physical Science Basis*. Geneva: IPCC.

[IPCC-SRES, 2001] IPCC-SRES (2001). Intergovernamental panel on climate change. special report on emissions scenario.

[Kalnay et al., 1996] Kalnay, E., Kanamitsu, M., Kistler, R., Collins, W., Deaven, D., Gandin, L., Iredell, M., Saha, S., White, G., Woollen, J., Zhu, Y., Chelliah, M., Ebisuzaki, W., Higgins, W., Janowiak, J., Mo, K., Ropelewski, C., Wang, J., Leetmaa, A., Reynolds, R., Jenne, R., and Joseph, D. (1996). The ncep/ncar 40-year reanalysis project. *B Am Meteorol Soc*, 77(3):437–471.

[Keeling, 1995] Keeling, R. (1995). The atmospheric oxygen cycle - the oxygen isotopes of atmospheric CO_2 and O_2 and the O_2/N_2 ratio. *Rev Geophys*, 33:1253–1262.

[Keeling and Garcia, 2002] Keeling, R. and Garcia, H. (2002). The change in oceanic O_2 inventory associated with recent global warming. *P Natl Acad Sci Usa*, 99(12):7848–7853.

[Keeling and J.Severinghaus, 1993] Keeling, R. and J.Severinghaus (1993). Atmospheric oxygen measurements and the carbon cycle. *Proceedings of the 1993 Global Change Institute, The Carbon Cycle*, pages 135–140.

[Keeling et al., 1993] Keeling, R., Najjar, R., Bender, M., and Tans, P. (1993). What atmospheric oxygen measurements can tell us about the global carbon-cycle. *Global Biogeochem. Cycles*, 7(1):37–67.

[Keeling et al., 1996] Keeling, R., Piper, S., and Heimann, M. (1996). Global and hemispheric CO_2 sinks deduced from changes in atmospheric O_2 concentration. *Nature*, 381(6579):218–221.

[Keeling and Shertz, 1992] Keeling, R. and Shertz, S. (1992). Seasonal and interannual variations in atmospheric oxygen and implications for the global carbon-cycle. *Nature*, 358(6389):723–727.

[Keeling et al., 1998] Keeling, R., Stephens, B., Najjar, R., Doney, S., Archer, D., and Heimann, M. (1998). Seasonal variations in the atmospheric O_2/N_2 ratio in relation to the kinetics of air-sea gas exchange. *Global Biogeochem. Cycles*, 12(1):141–163.

[Kennedy et al., 2007] Kennedy, R., Turner, D., Cohen, W., and Guzy, M. (2007). A method to efficiently apply a biogeochemical model to a landscape. *Landscape Ecology*, 21:213 – 224.

[Kuhlbrodt et al., 2007] Kuhlbrodt, T., Griesel, A., Montoya, M., Levermann, A., Hofmann, M., and Rahmstorf, S. (2007). On the driving processes of the atlantic meridional overturning circulation. *Rev Geophys*, 45(2):RG2001.

[Lee et al., 2003] Lee, K., Choi, S., Park, G., Wanninkhof, R., PENG, T., Key, R., Sabine, C., Feely, R., Bullister, J., Millero, F., and Kozyr, A. (2003). An updated anthropogenic CO_2 inventory in the atlantic ocean. *Global Biogeochem. Cycles*, 17(4):1116.

[Lenton et al., 2009] Lenton, A., Codron, F., Bopp, L., Metzl, N., Cadule, P., Tagliabue, A., and Sommer, J. L. (2009). Stratospheric ozone depletion reduces ocean carbon uptake and enhances ocean acidification. *Geophys Res Lett*, 36(12):L12606.

[Le Quéré and Meltz, 2004] Le Quéré, C. and Meltz, N. (2004). *The Global Carbon Cycle: integrating humans, climate and the natural world. Chapter 12*, volume 62 of *Scope*. Island Press.

[Le Quéré et al., 2000] Le Quéré, C., Orr, J., Monfray, P., Aumont, O., and Madec, G. (2000). Interannual variability of the oceanic sink of CO_2 from 1979 through 1997. *Global Biogeochem. Cycles*, 14(4):1247–1265.

[Le Quéré et al., 2009] Le Quéré, C., Raupach, M. R., Canadell, J. G., and et al., G. M. (2009). Trends in the sources and sinks of carbon dioxide. *Nature Geosciences*, advance online publication:–. 10.1038/ngeo689.

[Le Quéré et al., 2007] Le Quéré, C., Rödenbeck, C., Buitenhuis, E. T., Conway, T. J., Langenfelds, R., Gomez, A., Labuschagne, C., Ramonet, M., Nakazawa, T., Metzl, N., Gillett, N., and Heimann, M. (2007). Saturation of the southern ocean CO_2 sink due to recent climate change. *Science*, 316(5832):1735–1738.

[Madec et al., 1998] Madec, G, P, D., M, I., and C, L. (1998). Opa 8.1 ocean general circulation model reference manual. *Reference Manual*, N11:91.

[Maier-Reimer et al., 1996] Maier-Reimer, E., Mikolajewicz, U., and Winguth, A. (1996). Future ocean uptake of CO_2 interaction between ocean circulation and biology. *Climate Dynamics*, 12:711–721.

[Manabe et al., 1991] Manabe, S., Stouffer, R., Spelman, M., and Bryan, K. (1991). Transient responses of a coupled ocean atmosphere model to gradual changes of atmospheric CO_2 .1. annual mean response. *J Climate*, 4(8):785–818.

[Manabe and Stouffer, 2007] Manabe, S. and Stouffer, R. J. (2007). Role of ocean in global warming. *J Meteorol Soc Jpn*, 85B:385–403.

[Manning and Keeling, 2006] Manning, A. and Keeling, R. (2006). Global oceanic and land biotic carbon sinks from the Scripps atmospheric oxygen flask sampling network. *Tellus B*, 58B:95–116.

[Marotzke, 2000] Marotzke, J. (2000). Abrupt climate change and thermohaline circulation: Mechanisms and predictability. *P Natl Acad Sci Usa*, 97(4):1347–1350.

[Marshall et al., 1997] Marshall, J., Hill, C., Perelman, L., and Adcroft, A. (1997). Hydrostatic, quasi-hydrostatic, and nonhydrostatic ocean modeling. *J. Geophys. Res.*, 102(C3):5733–5752.

[Marti et al., 2005] Marti, O., Braconnot, P., Bellier, J., R., B., Bony, S., P, B., Cadule, P., A, C., S, D., Dufresne, J., Fairhead, L., Filiberti, M.-A.,

Fichefet, T., Friedlingstein, P., Grandpeix, J.-Y., Hourdin, F., Krinner, G., C, L., Musat, I., and C, T. (2005). The new IPSL Climate System Model: IPSL-CM4. *User's manual*.

[McKinley et al., 2002] McKinley, G., Follows, M., and Marshall, J. (2002). Interannual variability of the air-sea flux of oxygen in the north atlantic. *Geophys Res Lett*, 27(18):2933–2936.

[McKinley, 2003] McKinley, G. A. (2003). Interannual variability of air-sea O_2 fluxes and the determination of CO_2 sinks using atmospheric O_2/N_2. *Geophys Res Lett*, 30(3):1101.

[McKinley, 2004] McKinley, G. A. (2004). Pacific dominance to global air-sea CO_2 flux variability: A novel atmospheric inversion agrees with ocean models. *Geophys Res Lett*, 31(22):4.

[Meehl et al., 2007] Meehl, G. A., F.Stocker, T., D.Collins, W., P.Friedlingstein, Gaye, A., J.M.Gregory, A.Kithoh, R.Knutti, J.M.Murphy, A.Noda, S.C.B.Raper, I.G.Watterson, A.J.Weacer, and Zhao, Z. (2007). Global climate projections - Chapter 10 In The Physical Science Basis. Contribution of Working group 1 to the Fourth Assessment Report of the Intergovernmental Panel on Climate Change. *Fourth Assessment Report of the Intergovernmental Panel on Climate Change*. Cambridge University Press.

[Naegler et al., 2006] Naegler, T., Ciais, P., Orr, J. C., Aumont, O., and Rödenbeck, C. (2006). On evaluating ocean models with atmospheric potential oxygen. *Tellus B*, 59(1):138–156.

[Najjar and Keeling, 2000] Najjar, R. and Keeling, R. (2000). Mean annual cycle of the air-sea oxygen flux: A global view. *Global Biogeochem. Cycles*, 14(2):573–584.

[Nevison, 2008] Nevison, C. (2008). Impact of variable air-sea O_2 and CO_2 fluxes on Atmospheric Potential Oxygen (APO) and land-ocean carbon sink partitioning. *Biogeosciences*, 5(5):875–889.

[Nisbet and Chappellaz, 2009] Nisbet, E. G. and Chappellaz, J. (2009). Atmospheric science. shifting gear, quickly. *Science*, 324(5926):477–4788.

[Olivier et al., 2002] Olivier, Berdowski, J. J. M., Peters, J., Bakker, J., Visschedijk, A. J. H., and Bloos, J. P. J. (2002). Applications of edgar including description of EDGAR 3.2:reference database with trend data for 1970-1995. RIVM report 773301001(NRP report 410200051).

[Plattner et al., 2002] Plattner, G., Joos, F., and Stocker, T. (2002). Revision of the global carbon budget due to changing air-sea oxygen fluxes. *Global Biogeochem. Cycles*, 16(4):1096.

[Rahmstorf, 1997] Rahmstorf, S. (1997). Risk of sea-change in the Atlantic. *Nature*, 388(6645).

[Rahmstorf, 2003] Rahmstorf, S. (2003). The current climate. *Nature*, 421(6924):699–699.

[Rahmstorf, 2006] Rahmstorf, S. (2006). Thermohaline ocean circulation. *Encyclopedia of Quaternary Sciences*.

[Raupach et al., 2007] Raupach, M. R., Marland, G., Ciais, P., Le Quéré, C., Canadell, J. G., Klepper, G., and Field, C. B. (2007). Global and regional drivers of accelerating CO_2 emissions. *P Natl Acad Sci Usa*, 104(24):10288–93.

[Rödenbeck, 2005] Rödenbeck, C. (2005). Estimating CO_2 sources and sinks from atmospheric mixing ratio measurement using a global inversion of atmosheric transport. Technical report.

[Rödenbeck et al., 2008] Rödenbeck, C., Le Quéré, C., Heimann, M., and Keeling, R. (2008). Interannual variability in oceanic biogeochemical processes inferred by inversion of atmospheric O_2/N_2 and CO_2 data. *Tellus B*, 60B:685–705.

[Russell and Lerner, 1981] Russell, G. L. and Lerner, J. A. (1981). A new finite-differencing scheme for the tracer transport equation. *Journal of Applied Meteorology*, 20(12):1483–1498.

[Sabine et al., 2004] Sabine, C., Feely, R., Gruber, N., Key, R., Lee, K., Bullister, J., Wanninkhof, R., Wong, C., Wallace, D., Tilbrook, B., Millero, F.,

PENG, T., Kozyr, A., Ono, T., and Rios, A. (2004). The oceanic sink for anthropogenic CO_2. *Science*, 305(5682):367–371.

[Sarmiento and Bender, 1994] Sarmiento, J. and Bender, M. (1994). Carbon biogeochemistry and climate change. *Photosynthesis Research*, 39:209–234.

[Sarmiento and Gruber, 2002] Sarmiento, J. and Gruber, N. (2002). Sinks for anthropogenic carbon. *Physics Today*, 55(8):30–36.

[Sarmiento and Le Quéré, 1996] Sarmiento, J. and Le Quéré, C. (1996). Oceanic carbon dioxide uptake in a model of century-scale global warming. *Science*, 274(5291):1346–1350.

[Sarmiento et al., 1995] Sarmiento, J., Murnane, R., and Le Quéré, C. (1995). Air-sea CO_2 transfer and the carbon budget of the north-atlantic. *Philos T Roy Soc B*, 348(1324):211–219.

[Schlesinger, 1997] Schlesinger (1997). *Biogeochemistry: an analysis of global change*. Academc press, second edition.

[Stephens et al., 1998] Stephens, B., Keeling, R., Heimann, M., Six, K., Murnane, R., and Caldeira, K. (1998). Testing global ocean carbon cycle models using measurements of atmospheric O_2 and CO_2 concentration. *Global Biogeochem. Cycles*, 12(2):213–230.

[Taylor, 2001] Taylor, K. E. (2001). Summarizing multiple aspects of model performance in a single diagram. *J. Geophys. Res.*, 106(D7):7183–7192.

[Tegen and Fung, 1995] Tegen, I. and Fung, I. (1995). Contribution to the atmospheric mineral aerosol load from land-surface modification. *J Geophys Res-Atmos*, 100(D9):18707–18726.

[Thorpe et al., 2001] Thorpe, R., Gregory, J., Johns, T., Wood, R., and Mitchell, J. (2001). Mechanisms determining the atlantic thermohaline circulation response to greenhouse gas forcing in a non-flux-adjusted coupled climate model. *J Climate*, 14(14):3102–3116.

[Tiedtke, 1989] Tiedtke, M. (1989). A comprehensive mass flux scheme for cumulus parameterization in large-scale models. *Monthly Weather Review*, 117(8):1779–1800.

[Timmermann et al., 2005] Timmermann, R., Goosse, H., Madec, G., and Fichefet, T. (2005). On the representation of high latitude processes in the orca-lim global coupled sea ice–ocean model. *Ocean Modelling*, 8:175–201.

[Toggweiler and Russell, 2008] Toggweiler, J. R. and Russell, J. (2008). Ocean circulation in a warming climate. *Nature*, 451(7176):286–288.

[Tohjima et al., 2008] Tohjima, Y., Mukai, H., Nojiri, Y., Yamagishi, H., and Machida, T. (2008). Atmospheric O_2/N_2 measurements at two japanese sites: estimation of global oceanic and land biotic carbon sinks and analysis of the variations in Atmospheric Potential Oxygen (APO). *Tellus B*, 60(2):213–225.

[Wilks, 2006] Wilks, D. S. (2006). *Statistical Methods in the Atmospheric Sciences - An Introduction*, volume 91 of *International Geophysics Series*. Academic Press, second edition.

[Wood et al., 1999] Wood, R., Keen, A., Mitchell, J., and Gregory, J. (1999). Changing spatial structure of the thermohaline circulation in response to atmospheric CO_2 forcing in a climate model. *Nature*, 399(6752):572–575.

[Wood et al., 2003] Wood, R., Vellinga, M., and Thorpe, R. (2003). Global warming and thermohaline circulation stability. *Philos T Roy Soc A*, 361(1810):1961–1974.

[Wunsch, 2002] Wunsch, C. (2002). What is the thermohaline circulation? *Science*, 298(5596):1179–1180.